Supporting Information

Immobilized Prolinamide-Catalyzed Highly Enantioselective Aldol Reactions in Continuous-Flow Systems: Effect of Water for Catalyst Lifetime and Application to Synthesis of Chiral Fenpentadiol Analogue

Caizhen Yue, Yasuhiro Yamashita* and Shū Kobayashi*

Department of Chemistry, School of Science, The University of Tokyo, Bunkyo-ku, Tokyo, 113-0033, Japan

Corresponding Authors:
Shū Kobayashi: *shu_kobayashi@chem.s.u-tokyo.ac.jp*
Yasuhiro Yamashita: *yyamashita@chem.s.u-tokyo.ac.jp*

Table of Contents

Supporting experiments
Synthesis of PS-Pro catalysts (Schemes S1-3)

Scheme S1 Synthesis of **PS-Pro 1**

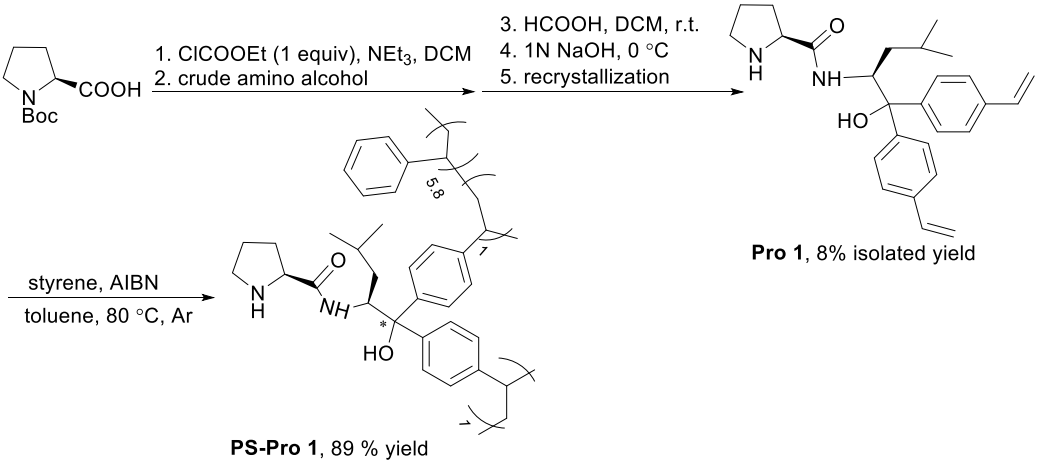

Firstly, we chose the copolymerization strategy of a catalyst monomer and styrene previously developed by our group.[1] The polystyrene part in **PS-Pro 1** was installed far from the catalyst active site, which might have small steric hindrance and retain the similar catalytic reactivity with the homogeneous catalysis. The monomer **Pro 1** derived from commercially available L-Proline and L-Leucine was synthetized in one pot procedure according to the previous reported route.[2] The low isolated yield suffered from the undesired polymerization problem in the acid treatment step. The final polymerization step could give an almost quantitative yield. The catalyst loading in the **PS-Pro 1** was identified by the nitrogen value in elemental analysis. Unexpected formed diastereomers in the polymerization step led to the decrease of the enantioselectivity albeit with the high catalytic reactivity. (Scheme S1)

Scheme S2 Synthesis of **PS-Pro 2**

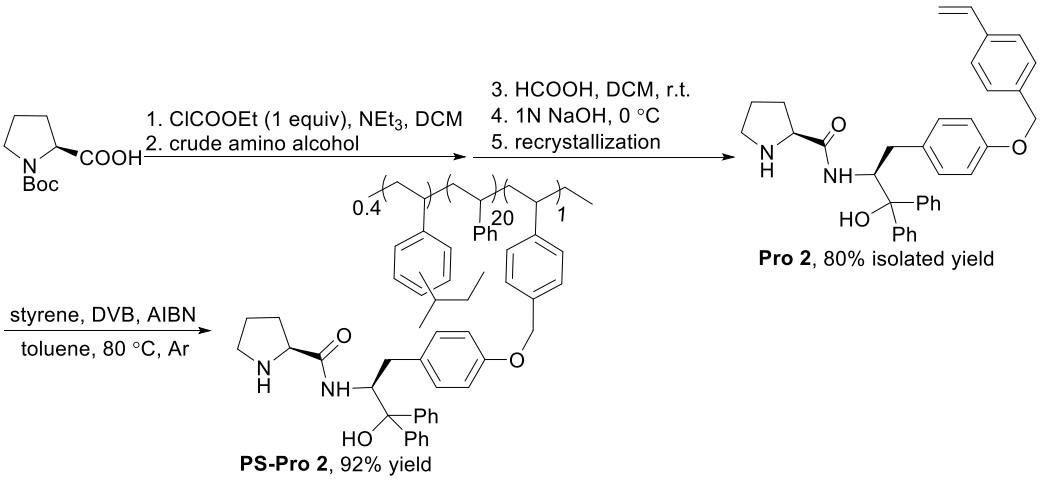

Next, we moved to the synthesis of **PS-Pro 2** derived from commercially available L-Proline and L-Tyrosine. The monomer **Pro 2** was synthetized in one pot procedure according to the previous reported route.[2] The next polymerization could successfully give the desired **PS-Pro 2** in a quantitative yield. The catalyst loading in the **PS-Pro 2** was identified by the nitrogen value in elemental analysis. The examination in the batch system showed lower catalytic reactivity and enantioselectivity than the homogeneous example. The decrease in reactivity and enantiocontrol might come from the change of an isopropyl group to a phenyl group. (Scheme S2)

Finally, **PS-Pro 3** was chosen as our best catalyst due to the highest enantioselectivity. However, the catalyst reactivity slightly decreased compared with the homogeneous example. This drop of catalytic ability might arise from the increased steric hindrance or loss of active sites in the

polymerization step. The monomer **Pro 3** was synthetized in one pot procedure according to the previous reported route.[2,3] The **Pro 3** was successfully obtained in 97% isolated yield. The catalyst loading in the **PS-Pro 3** was identified by the nitrogen value in elemental analysis. (Scheme S3)

Scheme S3 Synthesis of **PS-Pro 3**

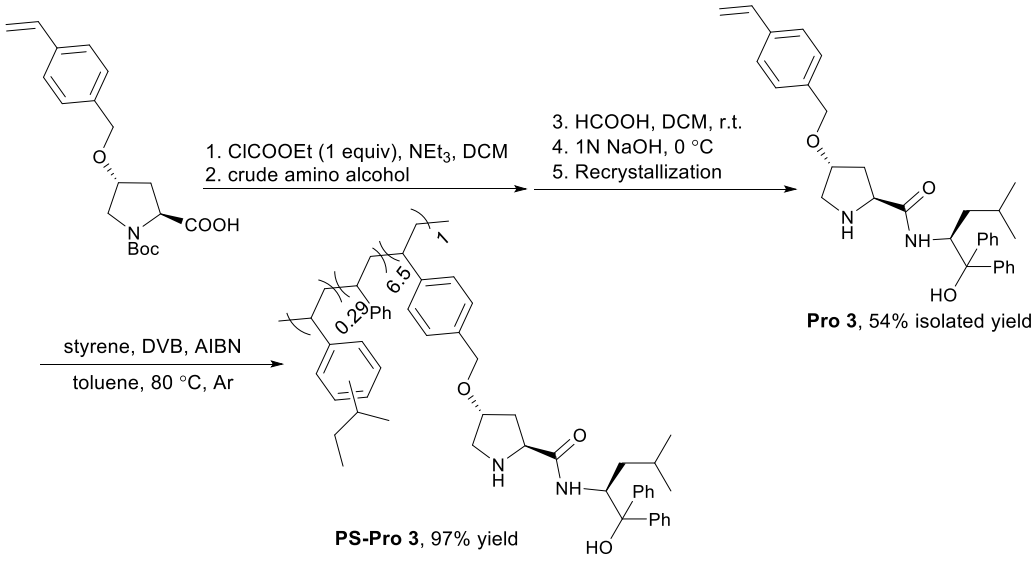

Additional condition screenings in a heterogeneous batch system (Tables S1-3)

Table S1 Effect of solvents and solid additives

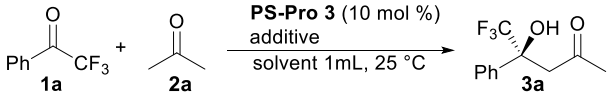

Entry	Solvent	Additive	Time (h)	Yield (%)[b]	Ee (%)[c]
1	acetone		6.5	85	87
2[a]	acetone/toluene		12	89	74
3[a]	acetone/DCM		14	93	55
4[a]	acetone/$CHCl_3$		20	57	ND
5[a]	acetone/CH_3CN		11	97	82
6	**acetone**	**celite[d]**	**6.5**	**89**	**88**
7	acetone	sea sand[e]	6.5	93	86

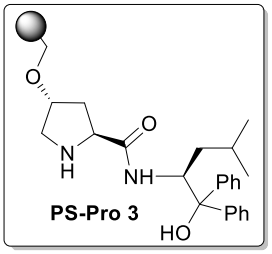

[a] Reaction conditions: **1a** (0.2 mmol), **PS-Pro 3** (0.02 mmol) in dry solvent (1.0 mL) under air at RT. V/V (acetone/other solvent) = 0.17. [b] Isolated yield. [c] Determined by HPLC. [d] Celite 13 mg. [e] Sea sand 13 mg.

As shown in the Table S1, solvent screenings failed to give the better results than entry 1. And sea sand and celite (entries 6 and 7) in the heterogeneous batch were examined and almost the same result with entry 1 was obtained. We chose celite as a solid support in a flow reactor to dilute the **PS-Pro 3** and avoid undesired side reactions.

As shown in the Table S2, acid additive screenings (entries 2-6) failed to give the better results than entry 1. As we documented in the main text, this aldol reaction was reversible, and sensitive to the acid additives. The acid additives accelerated the target reaction and also simultaneously promoted the undesired reverse reaction leading to decreased enantioselectivity.

The effect of phenol derivatives (Table S3) was further tried to achieve high efficiency. However, similar racemization to Table S1 was observed.

The catalyst reuse experiment was conducted and it was found that the reactivity could be totally recovered at the second run. (Table S4) But the next third run gave only 47% isolated yield. It was not difficult to say that some of the polymer **PS-Pro 3** deactivated at this moment. Within this process, a sequential washing method (HCOOH 2 h, 1M NaOH 1 h, H_2O, MeOH, THF, DCM, Vacuum) was employed. (Scheme S4)

Table S2 Effect of acid additives

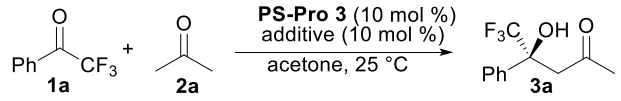

Entry	Additive	Time (h)	Yield (%)[b]	Ee (%)[c]
1		**6.5**	**85**	**87**
2[a]	AcOH	2	73	55
3[a]	PhCOOH	2	59	53
4[a]	4-NO_2PhCOOH	2	79	42
5[a]	4-NO_2Phenol	3	81	63
6[a]	TFA	12	ND	ND

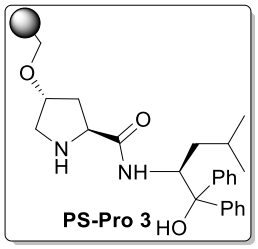

[a] Reaction conditions: **1a** (0.2 mmol), **PS-Pro 3** (0.02 mmol) and additive (0.02 mmol) in dry acetone (1.0 mL) under air at RT. [b] Isolated yield. [c] Determined by HPLC.

Table S3 Effect of phenol derivatives as additives

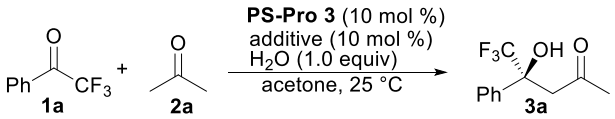

Entry	Additive/Pka	Time (h)	Yield (%)[b]	Ee (%)[c]
1		**6.5**	**84**	**86**
2[a]	2,6-diertbutylphenol /16.8	6	88	79
3[a]	2,6-ditertbutyl-4-bromophenol/16	5	85	82
4[a]	2,6-ditertbutyl-4-nitrophenol/10.8	2	89	82

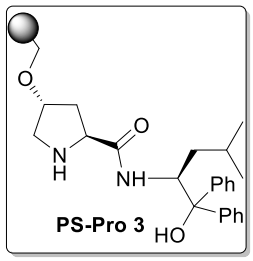

[a] Reaction conditions: **1a** (0.2 mmol), **PS-Pro 3** (0.02 mmol), 1.0 equiv H_2O and additive (0.02 mmol) in dry acetone (1.0 mL) under air at RT. [b] Isolated yield. [c] Determined by HPLC.

Catalyst recovery and reuse in a heterogeneous batch system (Tables S4-S5 and Scheme S4)

Table S4 Catalyst recovery and reuse within limited reaction time

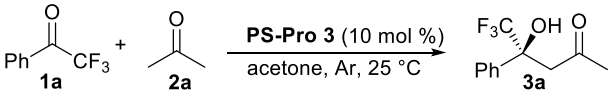

Run	Time (h)	Yield (%)[b]	Ee (%)[c]	TON	TOF (h^{-1})
1[a]	8 h	84	89	8.4	1.05
2[a]	8 h	14[e]	nd	1.4	0.18
2[a,d]	8 h	86	90	8.6	1.08
3[a,d]	8 h	47	89	4.7	0.59

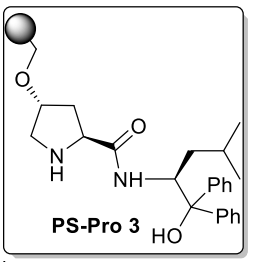

[a] Reaction conditions: **1a** (0.2 mmol), **PS-Pro 3** (0.02 mmol) in dry acetone (0.5 mL) under argon at RT. [b] Isolated yield. [c] Determined by HPLC. [d] Sequential washing method: HCOOH 2h, 1M NaOH 1 h, H_2O, MeOH, DCM, Vaccum. [e] NMR yield. Durene as the internal standard.

Scheme S4 Recovery method

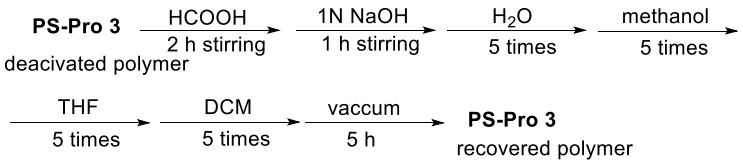

We performed catalyst recovery and reuse experiments in prolonged reaction time. (Table S5) Interestingly, the catalyst **PS-Pro 3** was still reactive after 8 runs. However, the reaction time was prolonged to 35 h for completion of the reaction, which indicated some catalyst deactivation during

recovery experiments. The catalyst in the 5% mol% amount was used to achieve reliable enantioselectivities.

Table S5 Catalyst recovery and reuse using prolonged reaction time

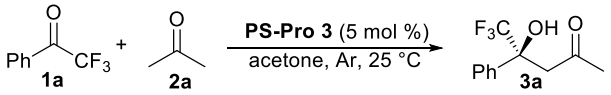

Run	Time (h)	Yield (%)[b]	Ee (%)[c]	TON	TOF (h^{-1})
1[a]	14 h	86	89	17.2	1.23
2[a]	24 h	85	90	17.0	0.71
3[a,d]	14 h	90	78	17.9	1.28
3[a,e]	16 h	90	88	17.9	1.12
4[a,e]	31 h	86	86	17.0	0.55
5[a,e]	33 h	92	87	18.5	0.56
6[a,e]	35 h	88	86	17.5	0.50
7[a,e]	35 h	93	86	18.5	0.53

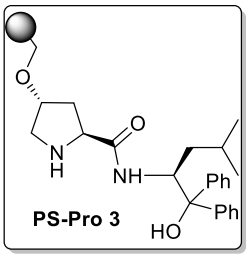

[a] Reaction conditions: **1a** (0.2 mmol), **PS-Pro 3** (0.01 mmol) in dry acetone (0.5 mL) under argon at RT. [b] Isolated yield. [c] Determined by HPLC. [d] Sequential washing method: HCOOH 2 h, 1M NaOH 5 times, H_2O, MeOH, THF, DCM, Vaccum. [e] Sequential washing method: HCOOH 2 h, 1M NaOH 1 h, H_2O, MeOH, THF, DCM, Vaccum.

Additional condition screenings in flow system (Tables S6-S8)

Table S6 Effect of 10% HFIP additive

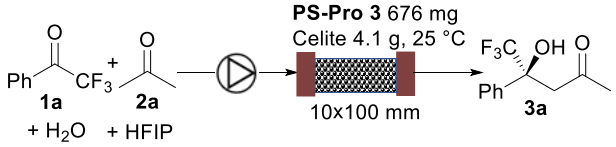

Time (h)	Volume (mL)	Flow rate (mL/min)	Yield (%)[b]	Ee (%)[c]	TOF (h^{-1})
3-4.3[a]	3.2	0.052	87	82	0.24
4.3-5.2[a]	2.7	0.055	86	82	0.27
5.2-6.3[a]	7	0.098	85	84	0.43
6.3-7.5[a]	8	0.12	84	82	0.51
7.5-8.7[a]	**10.5**	**0.14**	**64**	**84**	**0.48**
8.7-9.6[a]	**8.5**	**0.16**	**60**	**81**	**0.48**

[a] 0.05 M **1a**, 10% HFIP additive and 1 equiv. H_2O in acetone **2a** was degassed for 10 min in advance. [b] Isolated yield. [c] Determined by HPLC.

In the presence of 10% volume of HFIP and 1 equiv of water, the TOF value was improved to 0.48 h^{-1} (Table S6). However, the enantioselectivity dropped to 81% ee from 90% ee because of the existence of reversible reaction. The HFIP additive could promote the target catalytic cycle, but the reverse catalytic cycle was also accelerated at the same time.

Table S7 Effect of Acetone/H_2O (4:1) system

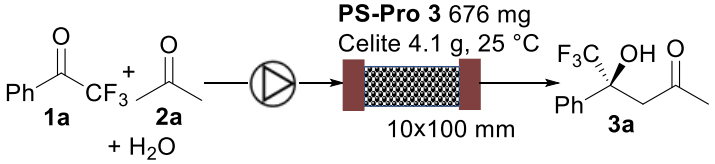

Time (h)	Volume (mL)	Flow rate (mL/min)	Yield (%)[b]	Ee (%)[c]	TOF (h^{-1})
19.6-20.5[a]	5.1	0.095	ND	ND	ND

[a] acetone/water mixture (4:1) was used to stablize the system for 10 h. 0.05 M **1a** in acetone and water (4:1) was feeded into the flow system. [b] Isolated yield. [c] Determined by HPLC.

Continuation of the above flow process, the acetone solvent was changed to a mixture of acetone and water (4:1) (Table S7). When the flow rate was increased to 0.095 mL/min, much amount of starting material remained. We could not isolate the chiral product **3a** and expected enantioselectivity wasn't detected. In the main text (Scheme 3), we found that the water could promote the hydrolysis reaction on the polymer surface and guarantee the life-time of the flow process. However, excess amount of water couldn't accelerate the catalytic reaction and improve the efficiency.

Table S8 Effect of 10% 4-nitrophenol additive

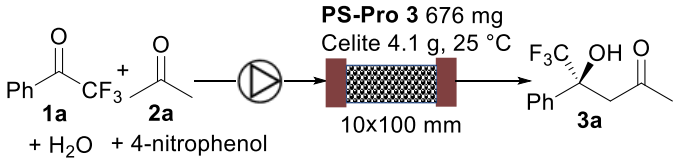

Time (h)	Volume (mL)	Flow rate (mL/min)	Yield (%)[b]	Ee (%)[c]	TOF (h^{-1})
25.5-26.5[a]	5.4	0.093	85	82	0.39
26.5-28[a]	9.0	0.1	87	81	0.44
28-29.3[a]	11	0.14	82	81	0.58
29.3-31[a]	6	0.15	84	81	0.64

[a] Acetone, H_2O and 4-nitrophenol mixture was used to stablize the flow system for 5 h. Then, 0.05 M **1a**, 10% 4-nitrophenol and 1 equiv H_2O in acetone **2a** was feeded into the flow system. [b] Isolated yield. [c] Determined by HPLC.

Continuation of the above flow process, similar phenomenon was observed with the HFIP additive. (Table S8) In our hypothesis, the 4-nitrophenol could accelerate the target aldol reaction and the reverse reaction simultaneously.

Investigation of catalyst deactivation using IR and fluorine elemental analysis (Schemes S5-6)

Scheme S5 Fluorine elemental analysis study for catalyst deactivation in flow system

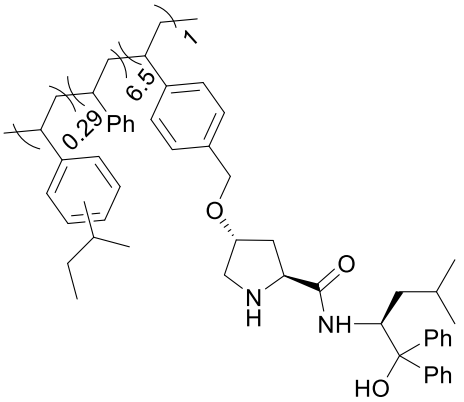

Structure of freshly prepared polymer:
Elemental analysis: F 0%, C 84.26%, H 7.76%, N 2.43%

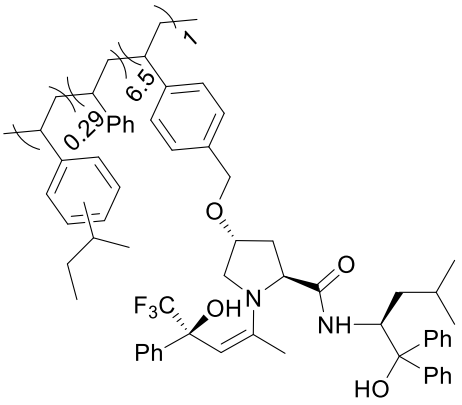

Proposed structure of deactivated polymer:
Elemental analysis: F 0.33%, C 71.01%, H 6.45%, N 1.78%

In the main text (Scheme 2), we noticed some deactivation of the flow process in the absence of water additive. The deactivated polymer was recovered from the polymer and celite mixture by extraction method (EtOAc/H_2O). And the polymer was further washed with methanol, DCM. Further evaporation under vacuum gave the final polymer. The polymer was submitted to elemental analysis. We found that 0.33% F in the deactivated polymer was observed. And IR analysis also indicated the C-F absorption peak around 1100 cm^{-1}. A possible structure of deactivated polymer **PS-Pro 3** in the flow process was proposed to explain the deactivation pathway, which could be further suppressed by the addition of water. Within the extraction process, the hydrolysis reaction of the deactivated polymer might happen and lead to the loss of F element in the polymer. (Schemes S5-6)

Scheme S6 IR study for catalyst deactivation in flow system

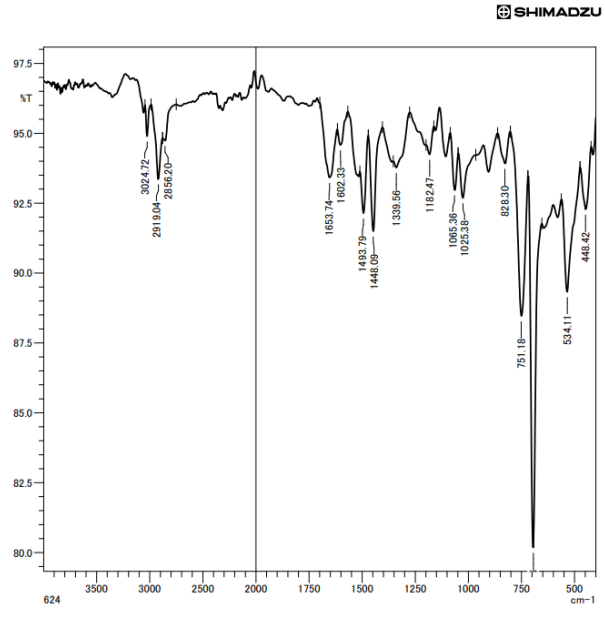

Fresh polymer: No C-F absorption.

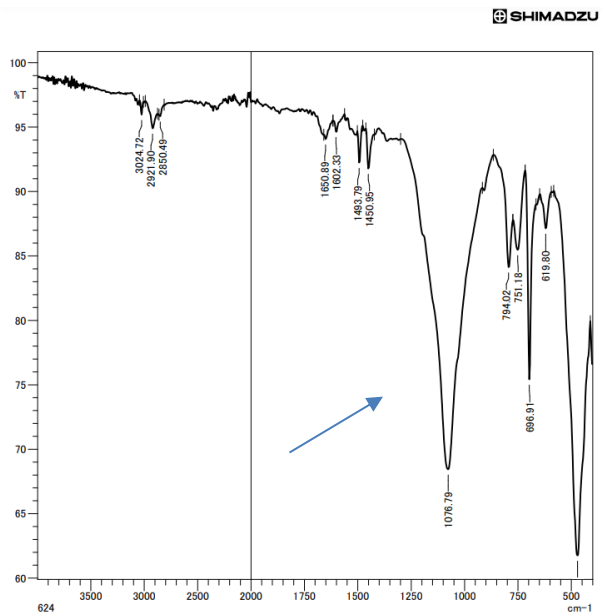

Deactivated polymer: C-F absorption at 1076.79 cm^{-1}.

Experimental Procedures

General considerations

^{1}H NMR and ^{13}C NMR spectra were recorded on JNM-ECX600 spectrometers in $CDCl_3$ unless otherwise noted. Tetramethylsilane (TMS) served as internal standard (δ = 0) for ^{1}H NMR, chemical shift values are listed in parts per million (ppm). Data are reported as follows: chemical shift (ppm on the δ scale), multiplicity (s = singlet, d = doublet, t = triplet, q = quartet, dd = doublet of doublet, m = multiplet), coupling constant *J* (Hz), and integration. ^{13}C NMR (150 MHz) chemical shifts are given in ppm relative to the $CDCl_3$ served as internal standard (δ= 77.0). Trifluorotoluene served as internal standard (δ = – 63.2) for ^{19}F NMR. High resolution mass spectra (HRMS) were recorded with an electrospray ionization time-of-flight (ESITOF) mass spectrometer. IR spectra were measured by Shimadzu IRSpirit-T with QART-S. High-performance liquid chromatography (HPLC) was carried out with a SHIMADZU LC-20AB instrument (liquid chromatograph). Optical rotation Elemental analysis experiments were conducted with an Analytic Functional Testing VarioMICRO CHNS instrument. Preparative thin-layer chromatography (PTLC) was carried out using Wakogel B-5F. CF_3TMS, Methyl ketones **1**, Benzaldehydes, Grignard reagents, dry and deuteride solvents were purchased from Wako Pure Chemical Industrials, Merk Co. and Tokyo Chemical Industries (TCI) Ltd. Trifluoroacetophenone and its derivatives **2** were prepared according to the previously reported synthetic method.[4] Styrene and divinylbenzene were purified with a short silica column before use.

Catalyst synthesis

General procedure for the monomer synthesis[2]

To a suspension of Boc-L-proline (2.15 g, 10 mmol) and Et_3N (3.0 mL, 22 mmol) in dry CH_2Cl_2 (20 mL) was slowly added ethyl chloroformate (0.95 mL, 10 mmol) at 0 °C resulting in the formation of triethylammonium hydrochloride as a white precipitate. Upon completion of the addition, the resulting slurry was stirred for an additional 30 min. The crude amino alcohol prepared from the L-Leucine (10 mmol) was then added in portions by means of a funnel (rinsing with dry CH_2Cl_2). Upon completion of the addition, the reaction mixture was stirred at 0 °C to room temperature overnight, followed by evaporation of volatiles under reduced pressure to provide the crude N-Boc proline amide as a pale-yellow solid. MeOH (16 mL) and CH_2Cl_2 (8 mL) were then added to the crude N-Boc proline amide, followed by slow addition of HCOOH (4 mL). The resulting slurry was heated to 50 °C and stirred for 7 h. During this time, the mixture became homogeneous (after ~2.5 h). After the

reaction was complete (TLC analysis), the resulting solution of the **Pro 1**·HCOOH salt was evaporated under reduced pressure and diluted with H_2O (20 mL) and EtOAc (30 mL). The mixture was cooled to 0 °C and made slightly basic (pH 8−9) with 6 N NaOH (~7 mL), with vigorous stirring, to give **Pro 1**. After separation of the organic layer, the aqueous phase was extracted with EtOAc (3 × 20 mL). The combined organic layers were washed with 1 N NaOH, H_2O, and brine and were dried over Na_2SO_4. The solution was filtered through a short pad of silica (Hexane/Ethyl estate = 3:1-1:1) and concentrated in vacuo to afford **Pro 1** as a white solid.

General procedure a for the polymer synthesis[1]

Toluene (0.5 mL) was degassed under nitrogen atmosphere during 30 min. Addition of the mixture of monomer **Pro 1** (334 mg, 1.0 mmol), styrene (1.1 mL, 9.6 mmol) and AIBN (11 mg, 0.07 mmol) in 0.5 mL of toluene was carried out. After that, the mixture was degassed for another 30 min at 20 °C. The temperature was then raised to 80 °C and the reaction mixture was stirred vigorously for 24 h. The resulting polymer beads were filtered and washed with methanol several times, then with, THF and CH_2Cl_2, followed by drying under reduced pressure for 4h, which afforded the desired cross-linked chiral polymer **PS-Pro 1**. For **PS-Pro 2** and **3**, degassed divinylbenzene (DVB) was introduced in an indicated equivalent. The catalyst loading in polymer was modified by changing the ratio of monomer/ styrene/DVB.

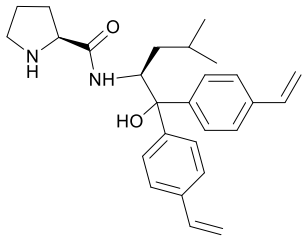

(*S*)-*N*-((*S*)-1-Hydroxy-4-methyl-1,1-bis(4-vinylphenyl)pentan-2-yl)pyrrolidine-2-carboxamide (Pro 1) Following the general procedure, monomer **Pro 1** (334 mg) (1 mmol) was obtained in 8% yield as a white solid. The low isolated yield suffered from the undesired polymerization problem of the di-styrene in the acid treatment step. ^{1}H NMR (600 MHz, $CDCl_3$) δ 7.94 (d, *J* = 8.5 Hz, 1H), 7.53 – 7.46 (m, 4H), 7.34 (d, *J* = 8.4 Hz, 2H), 7.28 (d, *J* = 8.3 Hz, 2H), 6.69 – 6.60 (m, 2H), 5.72 – 5.64 (m, 2H), 5.36 (br, 1H), 5.22 – 5.10 (m, 2H), 4.61 (t, *J* = 9.6 Hz, 1H), 3.48 (dd, *J* = 9.3, 4.7 Hz, 1H), 2.81 (dt, *J* = 10.1, 6.6 Hz, 1H), 2.63 – 2.51 (m, 1H), 1.96 – 1.75 (m, 3H), 1.62 – 1.39 (m, 3H), 1.34 – 1.16 (m, 2H), 0.92 (d, *J* = 6.6 Hz, 3H), 0.86 (t, *J* = 6.5 Hz, 3H) ppm; ^{13}C NMR (151 MHz, $CDCl_3$) δ 176.1, 146.1, 144.6, 136.4, 136.3, 135.9, 135.8, 126.1, 125.9, 125.8, 125.7, 113.7, 113.5, 80.8, 60.2, 56.4, 47.0, 37.5, 30.5, 25.7, 25.3, 23.8, 21.5 ppm; IR 3480.28, 3257.50, 2959.03, 2870.48, 1636.60, 1508.08, 1446.67, 1132.48, 1081.07, 903.99 cm^{-1}; $[\alpha]_D^{26}$ – 34.6 (c 0.50, $CHCl_3$); HRMS (DART): m/z calcd. for $C_{27}H_{34}N_2O_2$ [M + H$^+$] 419.2698; found 419.2690.

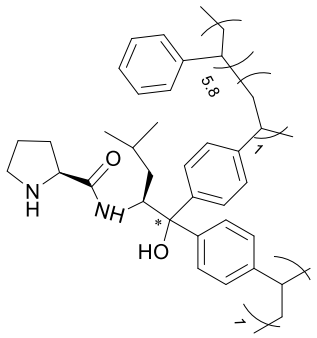

Following the general procedure, **PS-Pro 1** (652 mg) was obtained as a colorless solid. Polymerization yield was 89% according to the polymerization degree of monomer.
Elemental analysis: %C, 83.76; %H, 7.95; %N, 2.50

Actual loading was 0.89 mmol/g; Target loading was 0.70 mmol/g
IR analysis: 2969.02, 2921.90, 2866.20, 1650.89, 1492.37, 1453.81, 1055.37, 1032.52, 1015.38, 754.04 cm^{-1}

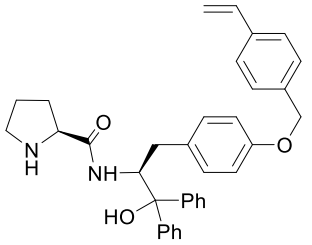

(*S*)-*N*-((*S*)-1-Hydroxy-1,1-diphenyl-3-(4-((4-vinylbenzyl)oxy)phenyl) propan-2-yl)pyrrolidine-2-carboxamide (Pro 2) Following the general procedure, monomer **Pro 2** (4.2 g) was obtained in 80% yield as a white solid. 532 mg of **Pro 2** (1 mmol) was used in the polymerization step. ^{1}H NMR (600 MHz, $CDCl_3$) δ 7.97 (d, *J* = 7.8 Hz, 1H), 7.67 (d, *J* = 7.7 Hz, 2H), 7.55 (d, *J* = 7.6 Hz, 2H), 7.40 (d, *J* = 8.1 Hz, 2H), 7.36 – 7.27 (m, 4H), 7.26 – 7.18 (m, 3H), 7.11 (t, *J* = 7.4 Hz, 1H), 6.97 (d, *J* = 8.4 Hz, 2H), 6.84 (d, *J* = 8.3 Hz, 2H), 6.70 (dd, *J* = 17.6, 10.9 Hz, 1H), 6.40 (br, 1H), 5.74 (d, *J* = 17.5 Hz, 1H), 5.24 (d, *J* = 10.9 Hz, 1H), 5.00 (s, 2H), 4.53 (t, *J* = 8.5 Hz, 1H), 3.46 – 3.42 (m, 1H), 3.14 (dd, *J* = 13.9, 11.6 Hz, 1H), 2.76 (dd, *J* = 14.2, 2.1 Hz, 1H), 2.69 (dt, *J* = 9.8, 7.0 Hz, 1H), 2.45 – 2.33 (m, 1H), 1.95 – 1.68 (m, 2H), 1.33 (tt, *J* = 12.5, 6.3 Hz, 1H), 1.22 (td, *J* = 12.5, 5.4 Hz, 1H), 1.00 (dt, *J* = 12.8, 7.2 Hz, 1H) ppm; ^{13}C NMR (151 MHz, $CDCl_3$) δ 176.5, 157.2, 146.7, 145.1, 137.2, 136.6, 136.4, 132.1, 130.0, 128.3, 127.8, 127.6, 126.7, 126.4, 126.3, 125.6, 125.6, 114.7, 114.0, 80.3, 69.7, 62.1, 60.0, 46.8, 33.1, 30.3, 25.4 ppm; IR 3648.80, 3346.04, 3277.49, 2929.04, 2867.63, 1639.46, 1510.93, 1446.67, 1406.68, 825.44, 749.75 cm^{-1}; $[\alpha]_D^{26}$ – 68.8 (c 0.50, $CHCl_3$); HRMS (DART): m/z calcd. for $C_{35}H_{36}N_2O_3$ $[M + H^+]$ 533.2804; found 533.2778.

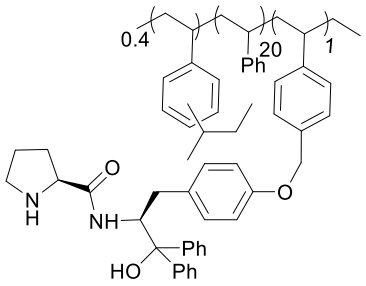

Following the general procedure, **PS-Pro 2** (2.3 g) was obtained as a colorless solid. Polymerization yield was 92% according to the polymerization degree of monomer.
Elemental analysis: %C, 84.62; %H, 7.21; %N, 1.11
Actual loading was 0.40 mmol/g; Target loading was 0.38 mmol/g
IR analysis: 3648.80, 2970.45, 2923.32, 2866.20, 1650.89, 1558.06, 1509.50, 1490.94, 1452.38, 1103.95, 754.04 cm^{-1}

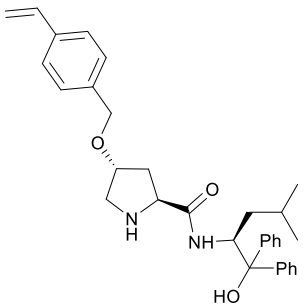

(2*S*,4*R*)-*N*-((*S*)-1-Hydroxy-4-methyl-1,1-diphenylpentan-2-yl)-4-((4-vinylbenzyl)oxy)pyrrolidi-e-2-carboxamide (Pro 3) Following the general procedure, monomer **Pro 3** (2.7 g) was obtained in 54% yield as a white solid. 500 mg of **Pro 3** (1 mmol) was used in the polymerization step. ^{1}H NMR (600 MHz, $CDCl_3$) δ 8.01 (d, *J* = 8.3 Hz, 1H), 7.55 – 7.53 (m, 4H), 7.37 (d, *J* = 8.0 Hz, 2H), 7.30 (t,

J = 7.5 Hz, 2H), 7.22 (t, *J* = 7.1 Hz, 4H), 7.18 (td, *J* = 7.5, 1.0 Hz, 1H), 7.10 (td, *J* = 7.5, 1.0 Hz, 1H), 6.70 (dd, *J* = 17.6, 10.9 Hz, 1H), 5.73 (d, *J* = 17.6 Hz, 1H), 5.47 (br, 1H), 5.23 (d, *J* = 10.9 Hz, 1H), 4.56 (t, *J* = 9.6 Hz, 1H), 4.40 – 4.31 (m, 2H), 3.79 (br, 1H), 3.68 (t, *J* = 8.2 Hz, 1H), 2.94 (d, *J* = 12.4 Hz, 1H), 2.26 – 2.05 (m, 3H), 1.96 – 1.86 (m, 1H), 1.63 – 1.49 (m, 1H), 1.43 – 1.33 (m, 1H), 1.28 – 1.15 (m, 1H), 0.91 (d, *J* = 6.5 Hz, 3H), 0.85 (d, *J* = 6.6 Hz, 3H) ppm; ^{13}C NMR (151 MHz, $CDCl_3$) δ 175.4, 146.7, 145.0, 137.6, 137.1, 136.4, 128.2, 127.9, 127.8, 126.7, 126.4, 126.3, 126.3, 125.7, 125.5, 113.9, 80.9, 80.0, 70.3, 59.5, 52.2, 37.2, 36.0, 25.4, 23.8, 21.5 ppm; IR 3314.62, 2953.31, 2867.63, 1633.75, 1525.21, 1493.79, 1448.09, 1062.51, 826.87, 744.04 cm^{-1}; $[\alpha]_D^{26}$ – 42.6 (c 0.10, $CHCl_3$); HRMS (DART): m/z calcd. for $C_{32}H_{38}N_2O_3$ [M + H^+] 499.2961; found 499.2944.

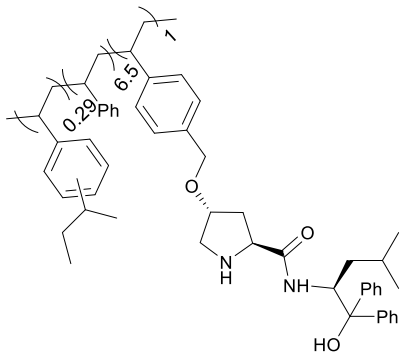

Following the general procedure, **PS-Pro 3** (1.16 g) was obtained as a colorless solid. Polymerization yield was 97% according to the polymerization degree of monomer.
Elemental analysis: %C, 86.08; %H, 7.56; %N, 0.95.
Actual loading was 0.34 mmol/g; Target loading was 0.37 mmol/g.
Elemental analysis: %C, 81.97; %H, 7.36; %N, 2.22.
Actual loading was 0.79 mmol/g; Target loading was 0.81 mmol/g.
Elemental analysis: %C, 82.62; %H, 7.50; %N, 2.40.
Actual loading was 0.86 mmol/g; Target loading was 0.81 mmol/g.
Elemental analysis: %C, 84.26; %H, 7.76; %N, 2.43.
Actual loading was 0.87 mmol/g; Target loading was 0.81 mmol/g.
IR analysis: 3026.15, 2923.32, 2866.20, 1649.46, 1600.90, 1512.36, 1492.37, 1449.52, 1053.94, 751.18 cm^{-1}

Continuous-flow synthesis for the chiral trifluoromethyl carbinols (Scheme S7-8)

To examine the substrate scope, 676 mg **PS-Pro 3** (0.86 mmol/g) and 4.1 g celite were packed into the flow reactor (10×100 mm). For all samples, degassed toluene under argon atmosphere was fed into the flow column in 1 mL/min for 1 h. After this rinsing process, the bubble in the flow reactor could be completely removed. To examine the substrate scope, all the flow samples were pre-prepared by mixing the ketones (2 mmol, 1.0 equivalent), H_2O (2 mmol, 36 mg, 1 equivalent) and acetone (40 mL), and further degassed in the ultrasonic instrument for 10 min. In low flow rate case, this degassing procedure could effectively solve the blocking problem caused by the bubble gathering in the flow pipe. Flow rate was set as 0.05 mL/min. All data collected could match the previously reported results. The sequential synthesis of chiral trifluoromethyl carbinols was conducted at room temperature under argon atmosphere. One batch of **PS-Pro 3** was employed for the samples from **3a** to **3a'**. After pumping each solution for 10 h, the system was rinsed by pumping acetone/H_2O for 30 min. The collected sample was evaporated, and further purified with the PTLC (Hexane/Ethyl estate = 5:1). Flow efficiency slightly dropped by contrast of isolated yields and ee values between the beginning **3a** and the end **3a'**. The deactivated **PS-Pro 3** was recovered with above introduced washing method, and reused for the unsymmetric ketones. (Scheme S7)
The recovered **PS-Pro 3** and celite were repacked intro the flow reactor for the unsymmetric ketones. After pumping each solution for 5 h, THF/H_2O mixture was introduced to wash the flow system in 1 mL/min for 30 min, and Toluene/H_2O mixture for another 30 min. The collected sample was

evaporated, and further purified with the PTLC (Hexane/Ethyl estate = 5:1). (Scheme S8)

Scheme S7 Substrate scope with the freshly prepared **PS-Pro 3**

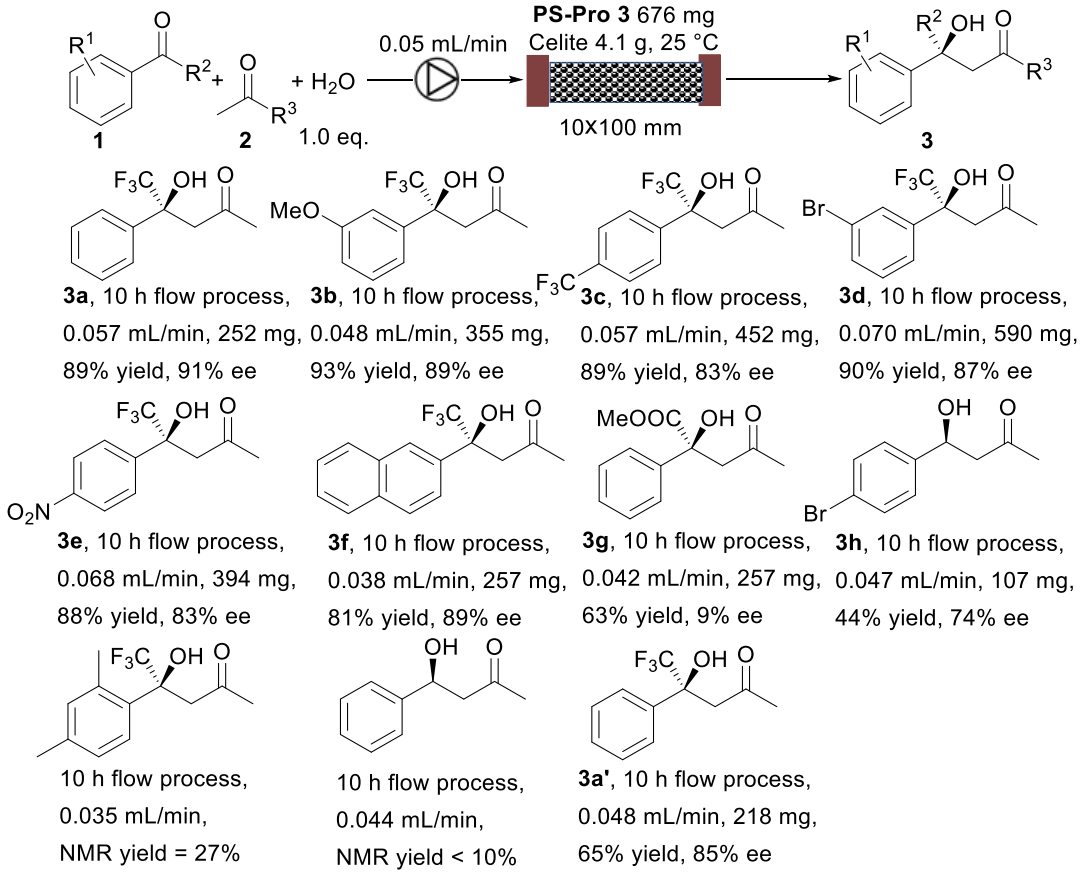

Scheme S8 Substrate scope with the recovered **PS-Pro 3**

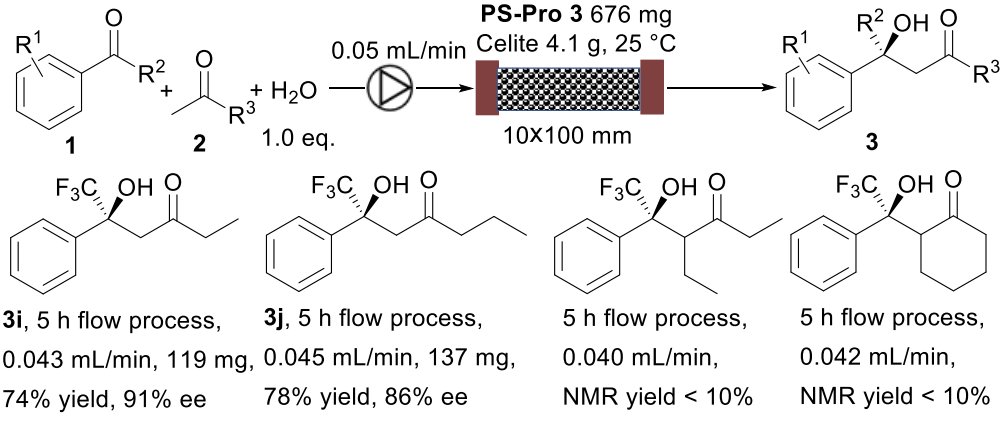

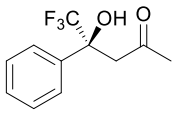

(*S*)-5,5,5-Trifluoro-4-hydroxy-4-phenylpentan-2-one (3a) 3a (252 mg) was obtained in 89% yield and 91% ee using the freshly prepared **PS-Pro 3** packed flow reactor. Purification was carried out by the preparative TLC using hexane/EtOAc (5:1) as the eluent. All spectroscopic data matched results previously reported in the literature.[5] ^{1}H NMR (600 MHz, $CDCl_3$) δ 7.57 (d, J = 7.5 Hz, 2H), 7.45 – 7.32 (m, 3H), 5.45 (s, 1H), 3.29 (dd, J = 94.3, 17.2 Hz, 2H), 2.20 (s, 3H) ppm; ^{13}C NMR (151 MHz, $CDCl_3$) δ 208.9, 137.4, 128.8, 128.4, 126.1, 123.5, 76.0 (d, J = 29.1), 45.07, 32.06 ppm; ^{19}F NMR (564 MHz, $CDCl_3$, $PhCF_3$) – 80.8 ppm; HPLC Chiralcel OD-3 column, hexane/i-PrOH (95:5), flow rate 1.0 mL/min, 215 nm, t_R minor = 8.3 min, t_S major = 10.6 min.

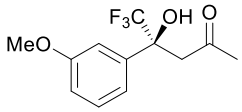

(*S*)-5,5,5-Trifluoro-4-hydroxy-4-(3-methoxyphenyl)pentan-2-one (3b) 3b (355 mg) was obtained in 93% yield and 89% ee using the freshly prepared **PS-Pro 3** packed flow reactor. Purification was carried out by the preparative TLC using hexane/EtOAc (5:1) as the eluent. All spectroscopic data matched results previously reported in the literature.[6] ^{1}H NMR (600 MHz, $CDCl_3$) δ 7.30 (t, *J* = 8.0 Hz, 1H), 7.17 (s, 1H), 7.08 (d, *J* = 7.7 Hz, 1H), 6.89 (dd, *J* = 8.2, 2.4 Hz, 1H), 5.44 (s, 1H), 3.82 (s, 3H), 3.37 – 3.13 (m, 2H), 2.20 (s, 3H) ppm; ^{13}C NMR (151 MHz, $CDCl_3$) δ 209.0, 159.7, 139.0, 129.4, 125.8, 124.4 (q, *J* = 285.3 Hz), 118.2, 114.0, 112.5, 76.0 (q, *J* = 29.0 Hz), 55.3, 45.1, 32.1 ppm; ^{19}F NMR (564 MHz, $CDCl_3$, $PhCF_3$) – 80.8 ppm; HPLC Chiralcel OD-3 column, hexane/i-PrOH (95:5), flow rate 1.0 mL/min, 215 nm. t_R minor = 16.6 min, t_S major = 20.5 min.

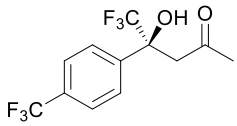

(*S*)-5,5,5-Trifluoro-4-hydroxy-4-(4-(trifluoromethyl)phenyl)pentan-2-one (3c) 3c (452 mg) was obtained in 89% yield and 83% ee using the freshly prepared **PS-Pro 3** packed flow reactor. Purification was carried out by the preparative TLC using hexane/EtOAc (3:1) as the eluent. All spectroscopic data matched results previously reported in the literature.[6] ^{1}H NMR (600 MHz, $CDCl_3$) δ 7.30 (t, *J* = 8.0 Hz, 1H), 7.17 (s, 1H), 7.08 (d, *J* = 7.7 Hz, 1H), 6.89 (dd, *J* = 8.2, 2.4 Hz, 1H), 3.82 (s, 3H), 3.39 – 3.15 (m, 2H), 2.20 (s, 3H) ppm; ^{13}C NMR (151 MHz, $CDCl_3$) δ 208.9, 137.4, 128.8, 128.4, 126.1, 123.5, 76.0 (d, *J* = 29.1), 45.1, 32.1 ppm; ^{19}F NMR (564 MHz, $CDCl_3$, $PhCF_3$) – 80.5 ppm; HPLC Chiralcel OJ-3 column, hexane/i-PrOH (90:10), flow rate 1.0 mL/min, 215 nm. t_R minor = 5.6 min, t_S major = 6.2 min.

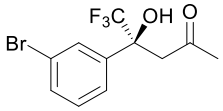

(*S*)-4-(3-Bromophenyl)-5,5,5-trifluoro-4-hydroxypentan-2-one (3d) 3d (590 mg) was obtained in 90% yield and 87% ee using the freshly prepared **PS-Pro 3** packed flow reactor. Purification was carried out by the preparative TLC using hexane/EtOAc (5:1) as the eluent. All spectroscopic data matched results previously reported in the literature.[6] ^{1}H NMR (600 MHz, $CDCl_3$) δ 7.74 (s, 1H), 7.50 – 7.14 (m, 2H), 7.29 – 7.25 (m, 1H), 5.55 (s, 1H), 3.41 – 3.17 (m, 2H), 2.23 (s, 3H) ppm; ^{13}C NMR (151 MHz, $CDCL_3$) δ 208.7, 139.8, 132.0, 123.0, 129.5, 124.8, 123.3, 122.8, 75.6 (d, *J* = 30.2), 44.9, 32.0 ppm; ^{19}F NMR (564 MHz, $CDCl_3$, $PhCF_3$) – 80.7 ppm; HPLC Chiralcel OJ-3 column, hexane/i-PrOH (90:10), flow rate 1.0 mL/min, 215 nm. t_R minor = 8.0 min, t_S major = 9.0 min.

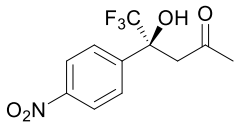

(*S*)-5,5,5-Trifluoro-4-hydroxy-4-(4-nitrophenyl)pentan-2-one (3e) 3e (394 mg) was obtained in 88% yield and 83% ee using the freshly prepared **PS-Pro 3** packed flow reactor. Purification was carried out by the preparative TLC using hexane/EtOAc (3:1) as the eluent. All spectroscopic data matched results previously reported in the literature.[6] ^{1}H NMR (600 MHz, $CDCl_3$) δ 8.25 (d, *J* = 8.9 Hz, 2H), 7.77 (d, *J* = 8.8 Hz, 2H), 5.66 (s, 1H), 3.32 (s, 2H), 2.25 (s, 3H) ppm; ^{13}C NMR (151 MHz, $CDCl_3$) δ 208.4, 148.2, 144.5, 127.4, 124.0 (q, *J* = 286.2 Hz), 123.6, 77.2, 75.5 (d, *J* = 151.2 Hz), 44.91, 31.91 ppm; ^{19}F NMR (564 MHz, $CDCl_3$, $PhCF_3$) – 80.1 ppm; HPLC Chiralcel OJ-3 column, hexane/i-PrOH (90:10), flow rate 1.0 mL/min, 215 nm. t_R minor = 21.4 min, t_S major = 23.8 min.

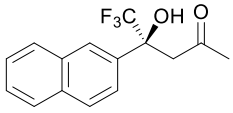

(*S*)-5,5,5-Trifluoro-4-hydroxy-4-(naphthalen-2-yl)pentan-2-one (3f) 3f (257 mg) was obtained in 81% yield and 89% ee using the freshly prepared **PS-Pro 3** packed flow reactor. Purification was carried out by the preparative TLC using hexane/EtOAc (5:1) as the eluent. All spectroscopic data matched results previously reported in the literature.[6] ^{1}H NMR (600 MHz, $CDCl_3$) δ 8.10 (s, 1H), 7.92 – 7.82 (m, 3H), 7.65 (d, *J* = 8.2 Hz, 1H), 7.56 – 7.49 (m, 2H), 5.62 (s, 1H), 3.50 – 3.15 (m, 2H), 2.21 (s, 3H) ppm; ^{13}C NMR (151 MHz, $CDCl_3$) δ 209.0, 134.8, 133.2, 132.8, 128.5, 128.3, 127.5, 126.8, 126.5, 126.1, 123.6, 123.3, 76.2 (q, *J* = 29.1 Hz), 45.2, 32.1 ppm; ^{19}F NMR (564 MHz, $CDCl_3$, $PhCF_3$) – 80.5 ppm; HPLC Chiralcel OD-3 column, hexane/i-PrOH (95:5), flow rate 1.0 mL/min, 254 nm. t_R minor = 9.3 min, t_S major = 13.7 min.

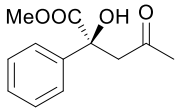

Methyl (*S*)-2-hydroxy-4-oxo-2-phenylpentanoate (3g) 3g (175 mg) was obtained in 63% yield and 9% ee using the freshly prepared **PS-Pro 3** packed flow reactor. Purification was carried out by the preparative TLC using hexane/EtOAc (5:1) as the eluent. All spectroscopic data matched results previously reported in the literature.[6] ^{1}H NMR (600 MHz, $CDCl_3$) δ 7.58 – 7.53 (m, 2H), 7.35 (t, *J* = 7.6 Hz, 2H), 7.31 – 7.21 (m, 1H), 4.43 (br, 1H), 3.75 (s, 3H), 3.55 (d, *J* = 17.7 Hz, 1H), 3.01 (d, *J* = 17.7 Hz, 1H), 2.20 (s, 3H) ppm; ^{13}C NMR (151 MHz, $CDCl_3$) δ 207.8, 174.3, 140.2, 128.4, 128.1, 128.0, 124.8, 76.3, 53.1, 53.0, 30.6 ppm; HPLC Chiralcel OJ-3 column, hexane/i-PrOH (90:10), flow rate 1.0 mL/min, 215 nm. t_S major = 18.8 min, t_R minor = 20.8 min.

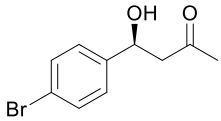

(*S*)-4-(4-Bromophenyl)-4-hydroxybutan-2-one (3h) 3h (107 mg) was obtained in 44% yield and 74% ee using the freshly prepared **PS-Pro 3** packed flow reactor. Purification was carried out by the preparative TLC using hexane/EtOAc (5:1) as the eluent. All spectroscopic data matched results previously reported in the literature.[6] ^{1}H NMR (600 MHz, $CDCl_3$) δ 7.47 (d, *J* = 8.3 Hz, 2H), 7.23 (d, *J* = 8.4 Hz, 2H), 5.13 – 5.00 (m, 1H), 3.37 (br, 1H), 2.87 – 2.76 (m, 2H), 2.19 (s, 3H) ppm; ^{13}C NMR (151 MHz, $CDCl_3$) δ 208.9, 141.7, 131.6, 127.4, 121.4, 69.2, 51.7, 30.8 ppm; HPLC Chiralcel OJ-3 column, hexane/i-PrOH (90:10), flow rate 1.0 mL/min, 215 nm. t_S major = 12.0 min, t_R minor = 12.7 min.

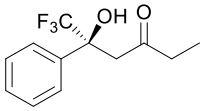

(*S*)-6,6,6-Trifluoro-5-hydroxy-5-phenylhexan-3-one (3i) 3i (119 mg) was obtained in 74% yield and 91% ee using the recovered **PS-Pro 3** packed flow reactor. Purification was carried out by the preparative TLC using hexane/EtOAc (5:1) as the eluent. All spectroscopic data matched results previously reported in the literature.[6] ^{1}H NMR (600 MHz, $CDCl_3$) δ 7.56 (d, *J* = 7.5 Hz, 2H), 7.43 – 7.30 (m, 3H), 5.60 (s, 1H), 3.32 – 3.15 (m, 2H), 2.59 – 2.30 (m, 2H), 0.99 (t, *J* = 7.8 Hz, 3H) ppm; ^{13}C NMR (151 MHz, $CDCl_3$) δ 211.8, 137.5, 128.8, 128.4, 126.1, 124.5 (q, *J* = 285.9 Hz), 76.0 (q, *J* = 29.6 Hz), 44.0, 38.2, 7.1 ppm; ^{19}F NMR (564 MHz, $CDCl_3$, $PhCF_3$) – 80.7 ppm; HPLC Chiralcel OJ-3 column, hexane/i-PrOH (95:5), flow rate 1.0 mL/min, 215 nm. t_R minor = 9.0 min, t_S major = 12.2 min.

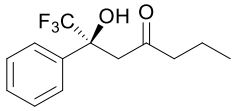

(*S*)-1,1,1-Trifluoro-2-hydroxy-2-phenylheptan-4-one (3j) 3j (137 mg) was obtained in 78% yield and 86% ee using the recovered **PS-Pro 3** packed flow reactor. Purification was carried out by the preparative TLC using hexane/EtOAc (5:1) as the eluent. All spectroscopic data matched results previously reported in the literature.[6] ^{1}H NMR (600 MHz, $CDCl_3$) δ 7.57 (d, *J* = 7.6 Hz, 2H), 7.43 – 7.32 (m, 3H), 5.62 (s, 1H), 3.36 – 3.12 (m, 2H), 2.51 – 2.33 (m, 2H), 1.58 – 1.47 (m, 2H), 0.84 (t, *J* = 7.4 Hz, 3H) ppm; ^{13}C NMR (151 MHz, $CDCl_3$) δ 211.4, 137.5, 128.7, 128.4, 126.1, 124.5 (q, *J* = 283.4 Hz), 75.9, 46.8, 44.3, 16.5, 13.3 ppm; ^{19}F NMR (564 MHz, $CDCl_3$, $PhCF_3$) – 80.7 ppm; HPLC Chiralcel OJ-3 column, hexane/i-PrOH (95:5), flow rate 1.0 mL/min, 215 nm. t_R minor = 7.3 min, t_S minor = 10.2 min.

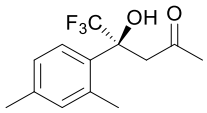

(*S*)-4-(2,4-Dimethylphenyl)-5,5,5-trifluoro-4-hydroxypentan-2-one 27% NMR yield was obtained using the freshly prepared **PS-Pro 3** packed flow reactor. Durene (0.25 equivalent) was used as the internal standard. Crude ^{1}H NMR (600 MHz, $CDCl_3$) 7.17 (d, *J* = 8.4 Hz, 2H), 7.04 – 6.95 (m, 2H), 5.36 (s, 1H), 3.60 – 3.55 (m, 1H), 3.19 – 3.14 (m, 1H), 2.59 (s, 3H), 2.30 (s, 3H), 2.26 (s, 3H), 2.21 (s, 11H) ppm.

Formal continuous-flow synthesis of chiral Fenpentadiol analogue 4 (Schemes S9-10)

676 mg **PS-Pro 3** (0.86 mmol/g) and 4.1 g celite were packed into the flow reactor (10×100 mm). Degassed toluene under argon atmosphere was fed into the flow column in 1 mL/min for 1 h. After this rinsing process, the bubble in the flow reactor could be completely removed. Flow sample were pre-prepared by mixing the **1i** (3 mmol, 1.0 equivalent, 0.05 N), H_2O (3 mmol, 54 mg, 1 equiv) and acetone (60 mL), and further degassed in the ultrasonic instrument for 10 min. In low flow rate case, this degassing procedure could effectively solve the blocking problem caused by the bubble gathering in the flow pipe. Flow rate was set as 0.05 mL/min. All data collected could match the previously reported results. This flow process was conducted for 20 h, and the collected sample was evaporated and purified with PTLC (Hexane/EtOAc = 5:1). (Scheme S9)

Scheme S9 Continuous synthesis of chiral **3k** under the optimal flow condition

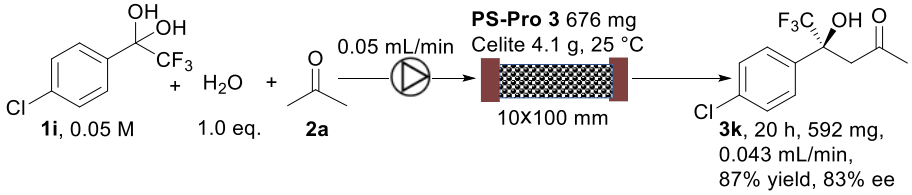

Next Grignard reaction of **3k** (592 mg, 2.2 mmol) and methyl magnesium bromide (4 equivalent) at 50 °C smoothly delivered the desired Fenpentadiol analogue **4** (600 mg). Crude ^{1}H NMR analysis of analogue **4** showed 7% of **3k** remained. Further crystallization (200 mg **4)** in hexane/DCM could produce 108 mg of **4** with improved enantioselectivity. (Scheme S10)

Scheme S10 Fenpentadiol analogue **4**

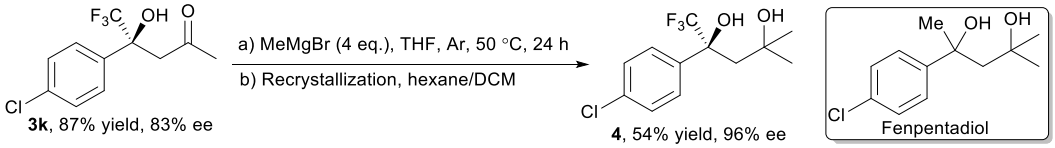

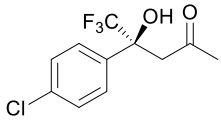

(*S*)-4-(4-Chlorophenyl)-5,5,5-trifluoro-4-hydroxypentan-2-one (3k) 3k (592 mg) was obtained in 87% yield and 83% ee using the freshly prepared **PS-Pro 3** packed flow reactor. Purification was carried out by the preparative TLC using hexane/EtOAc (5:1) as the eluent. All spectroscopic data matched results previously reported in the literature.[7] ^{1}H NMR (600 MHz, $CDCl_3$) δ 7.42 (d, J = 8.5 Hz, 2H), 7.31 – 7.25 (m, 2H), 5.43 (s, 1H), 3.25 – 3.09 (m, 2H), 2.13 (s, 3H) ppm; ^{13}C NMR (151 MHz, $CDCl_3$) δ 208.8, 136.0, 135.0, 128.7, 127.6, 124.2 (q, J = 286.0 Hz) , 75.7 (q, J = 30.1 Hz), 44.9, 32.0 ppm; ^{19}F NMR (564 MHz, $CDCl_3$, $PhCF_3$) – 80.9 ppm; HPLC Chiralcel OJ-3 column, hexane/i-PrOH (90:10), flow rate 1.0 mL/min, 215 nm. t_R minor = 8.2 min, t_S minor = 13.2 min.

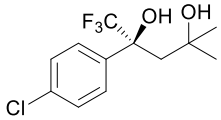

(*S*)-2-(4-Chlorophenyl)-1,1,1-trifluoro-4-methylpentane-2,4-diol (4) 4 (108 mg) was obtained in 54% yield and 96% ee with one step Grignard reaction. Crystallization in hexane/DCM was conducted to improve the enantioselectivity. All spectroscopic data matched results previously reported in the literature.[7] ^{1}H NMR (600 MHz, $CDCl_3$) δ 7.60 (d, J = 8.4 Hz, 2H), 7.36 (d, J = 8.5 Hz, 2H), 6.21 (br, 1H), 2.46 (d, J = 15.0 Hz, 1H), 2.31 (d, J = 15.0 Hz, 1H), 1.82 (br, 1H), 1.34 (s, 3H), 0.83 (s, 3H) ppm; ^{13}C NMR (151 MHz, $CDCl_3$) δ 137.6, 134.4, 128.4, 126.0, 124.1, 73.6, 42.4, 33.9, 28.5 ppm; ^{19}F NMR (564 MHz, $CDCl_3$, $PhCF_3$) – 82.5 ppm; HPLC Chiralpak AD-H column, hexane/i-PrOH (95:5), flow rate 1.0 mL/min, 215 nm. t_R minor = 6.6 min, t_S minor = 7.8 min.

Proposed transition state for the target aldol reaction (Scheme S11)

Scheme S11 Proposed anti-re face attack transition state for the target aldol reaction

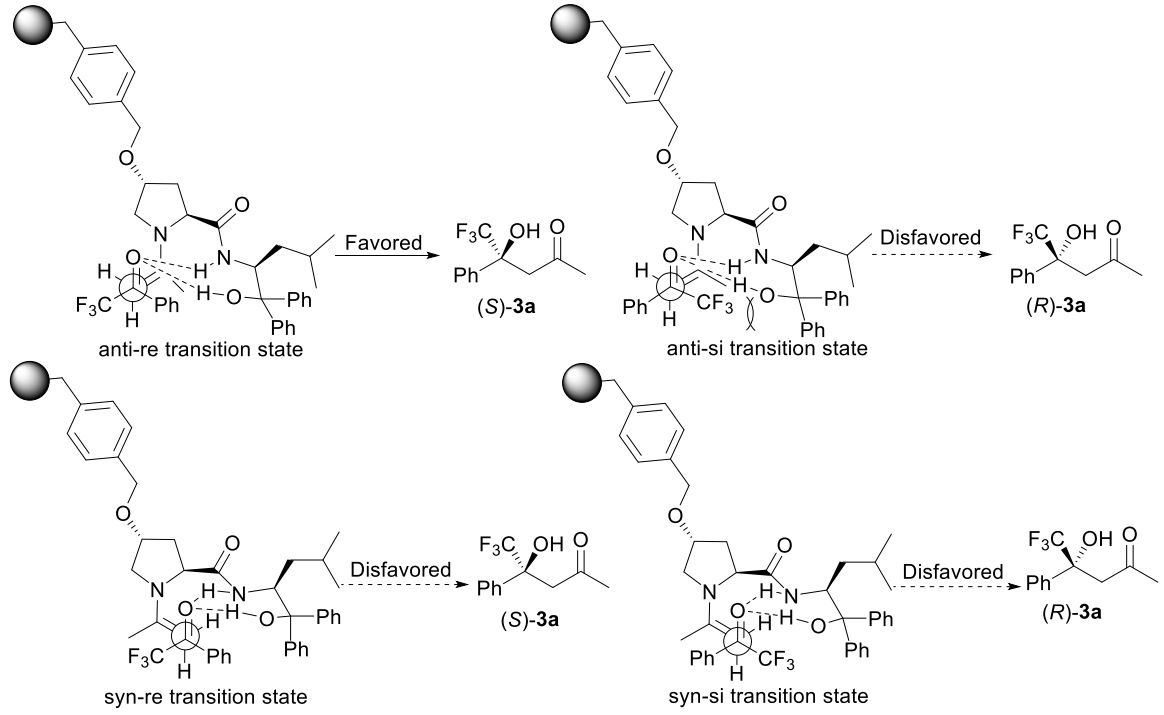

To explain the stereochemical outcome of the aldol reaction, four different possible transition states were proposed in Newman projection. (Scheme S11) Syn transition states are very likely higher in energy than anti transition states, and successfully excluded according to the previous DFT investigation[8]. The aldol reaction of acetone to trifluoroacetophenone proceeds more preferably through anti-re transition state giving (*S*)-**3a**, because anti-si transition state is destabilized by steric

repulsion between the bulky trifluoromethyl group and methyl or phenyl groups in enamine intermediate. [9]

NMR and IR spectra of catalysts

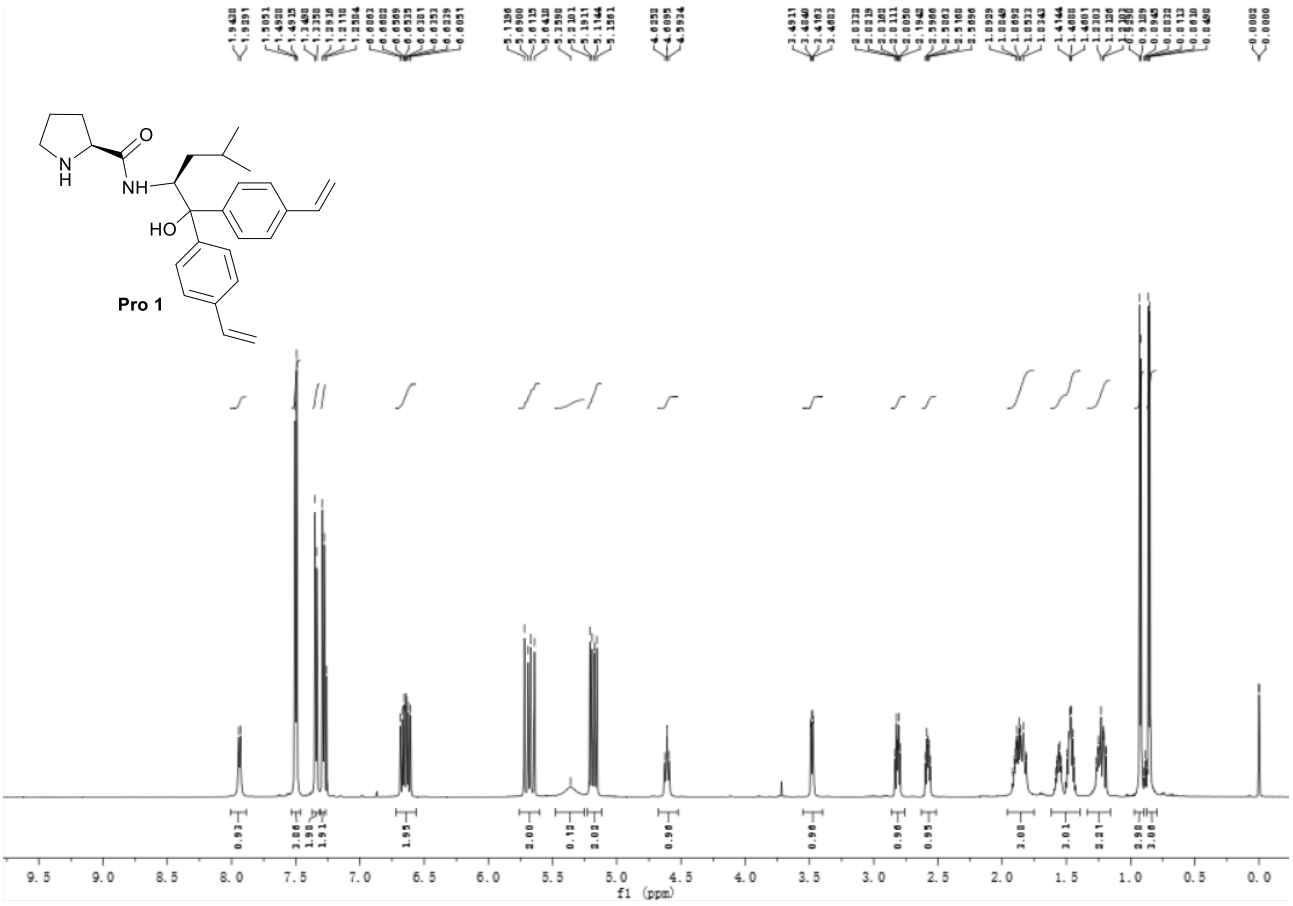

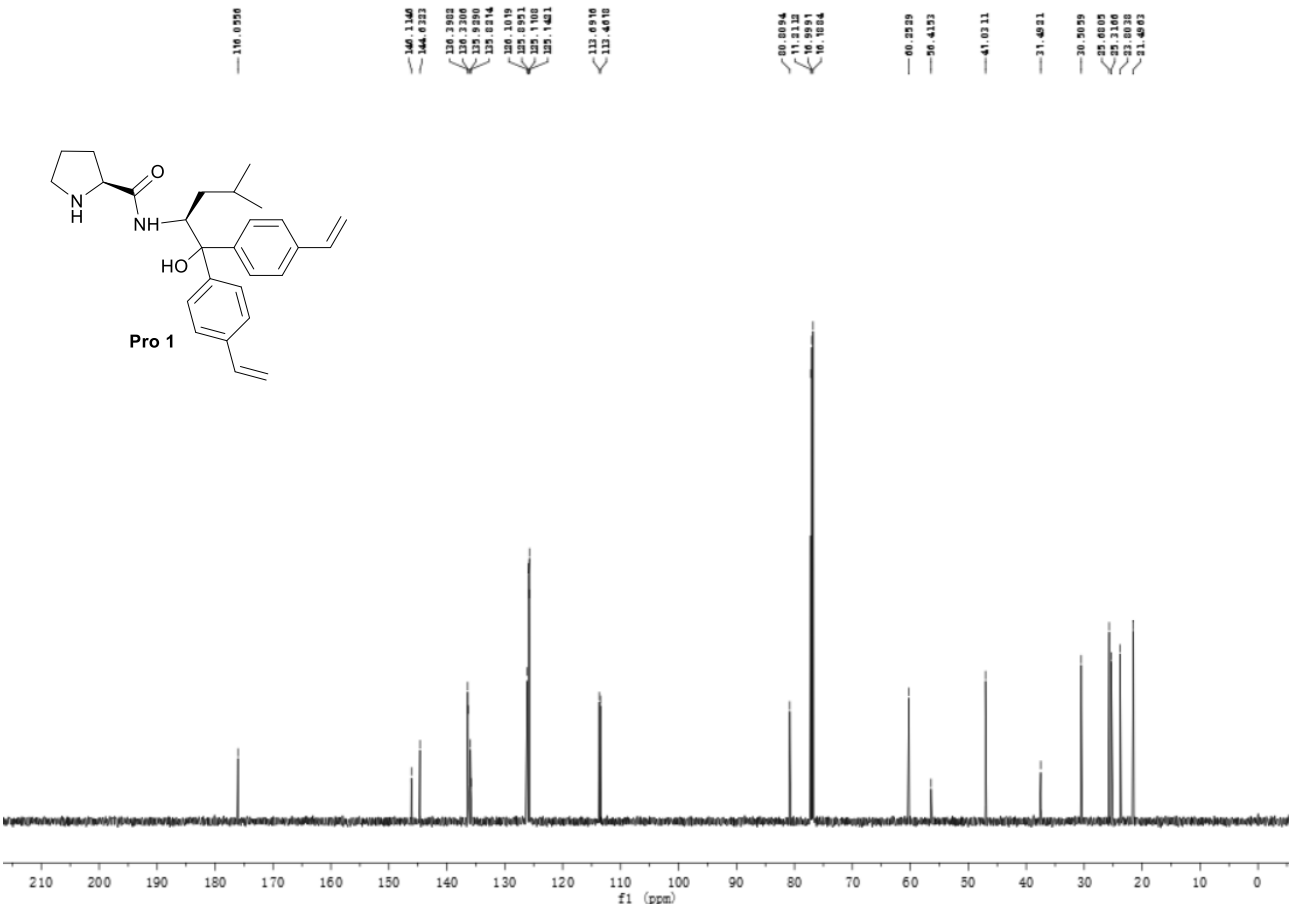

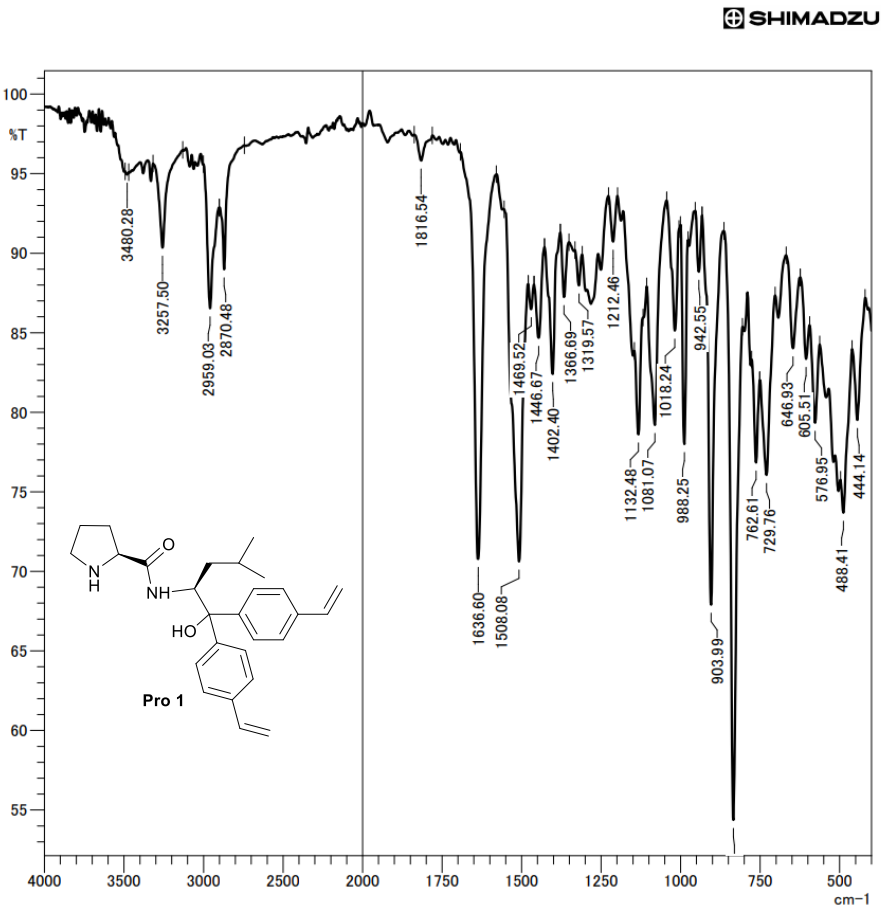
SHIMADZU
%T
3480.28
3257.50
2959.03
2870.48
1816.54
1636.60
1508.08
1469.52
1446.67
1402.40
1366.69
1319.57
1212.46
1132.48
1081.07
1018.24
988.25
942.55
903.99
762.61
729.76
646.93
605.51
576.95
488.41
444.14
Pro 1
cm-1

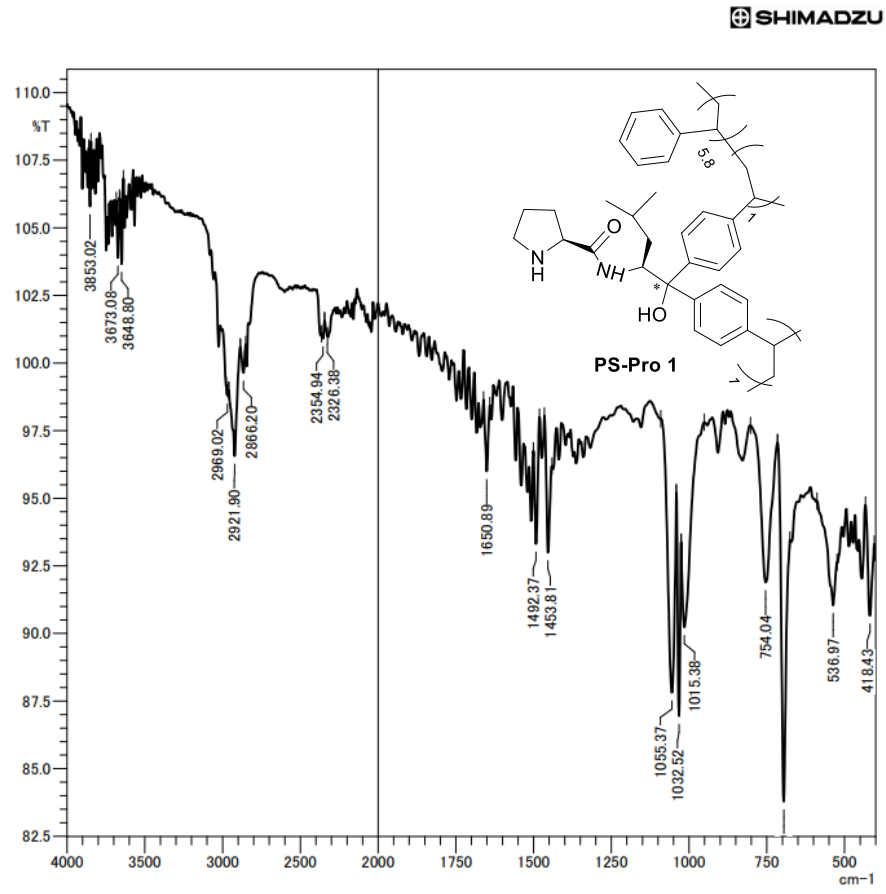
SHIMADZU
%T
3853.02
3673.08
3648.80
2969.02
2921.90
2866.20
2354.94
2326.38
1650.89
1492.37
1453.81
1055.37
1032.52
1015.38
754.04
536.97
418.43
PS-Pro 1
cm-1

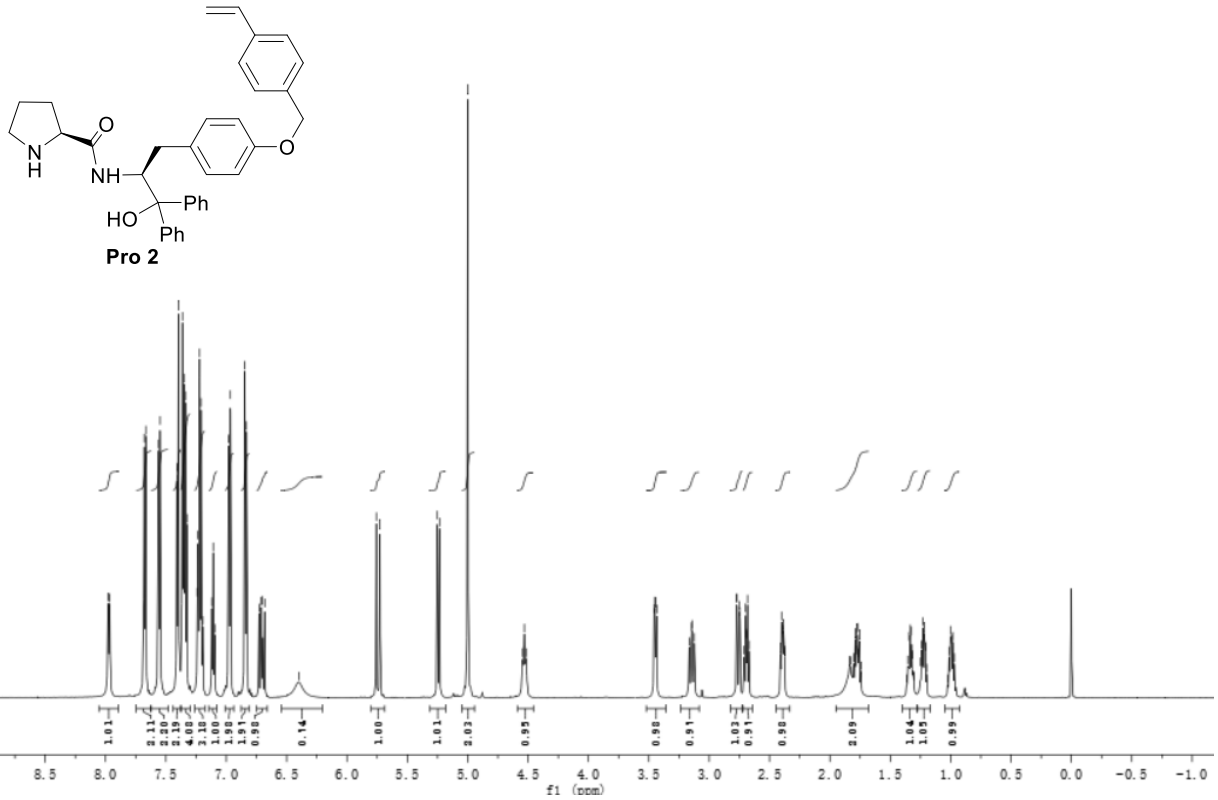

Pro 2

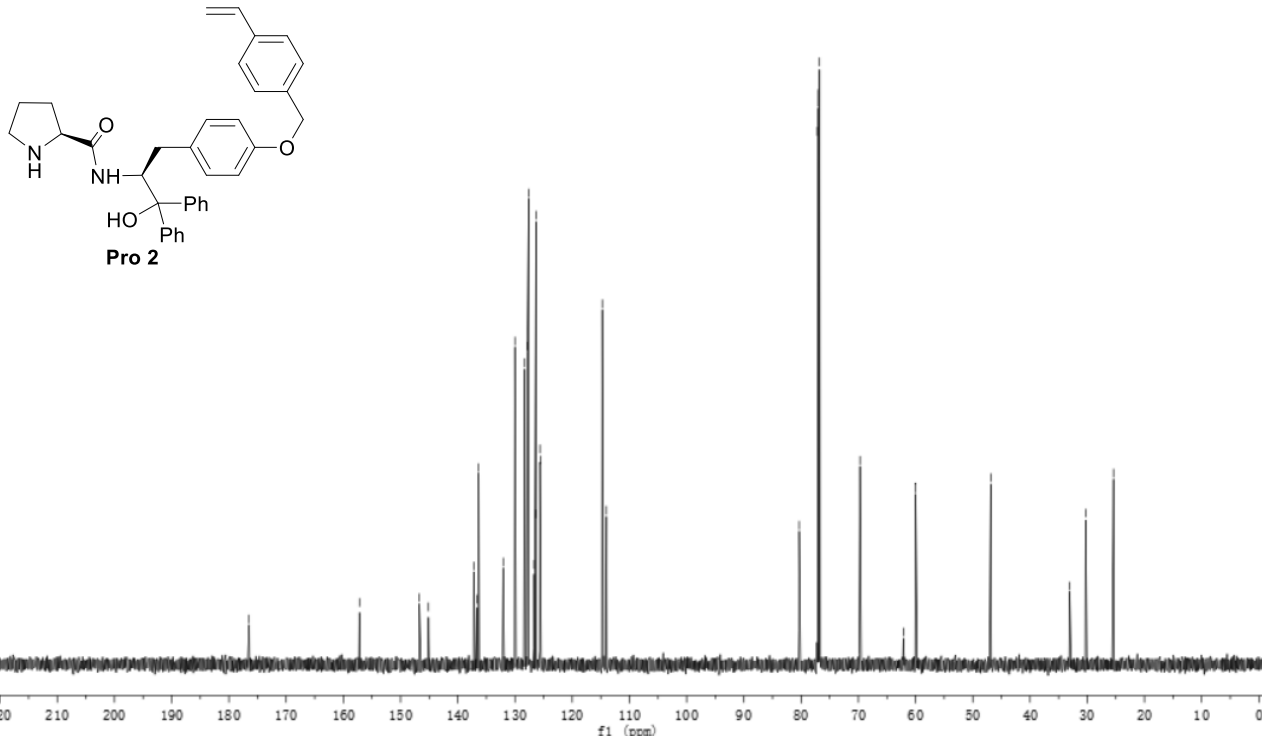

Pro 2

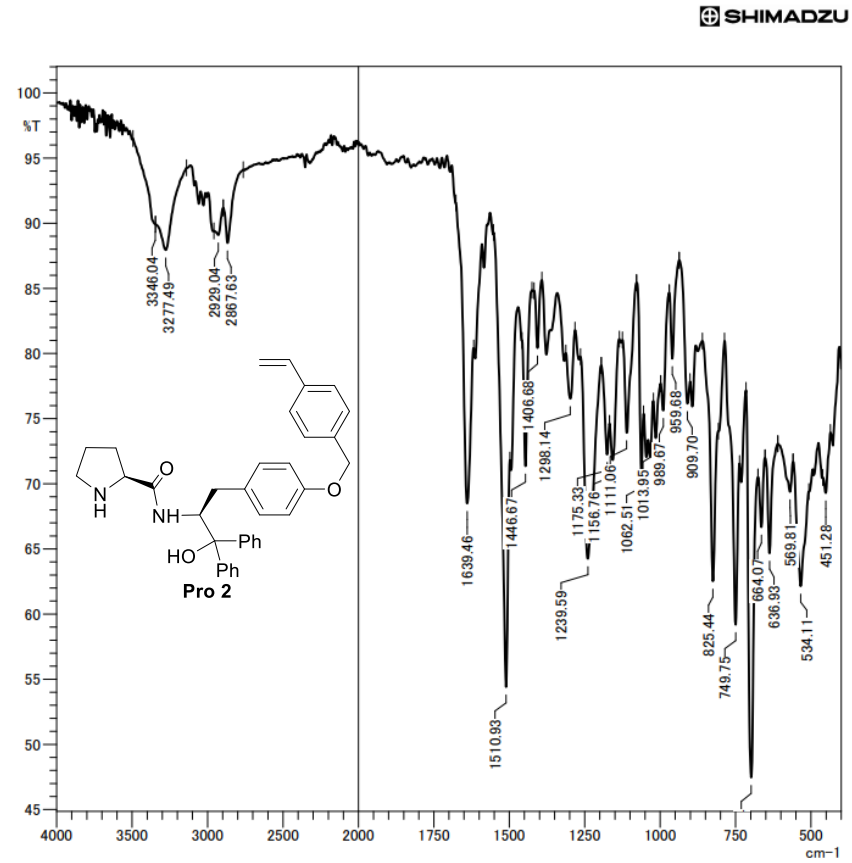
SHIMADZU
%T
cm-1
3346.04
3277.49
2929.04
2867.63
1639.46
1510.93
1446.67
1406.68
1298.14
1239.59
1175.33
1156.76
1111.06
1062.51
1013.95
989.67
959.68
909.70
825.44
749.75
664.07
636.93
569.81
534.11
451.28
Pro 2

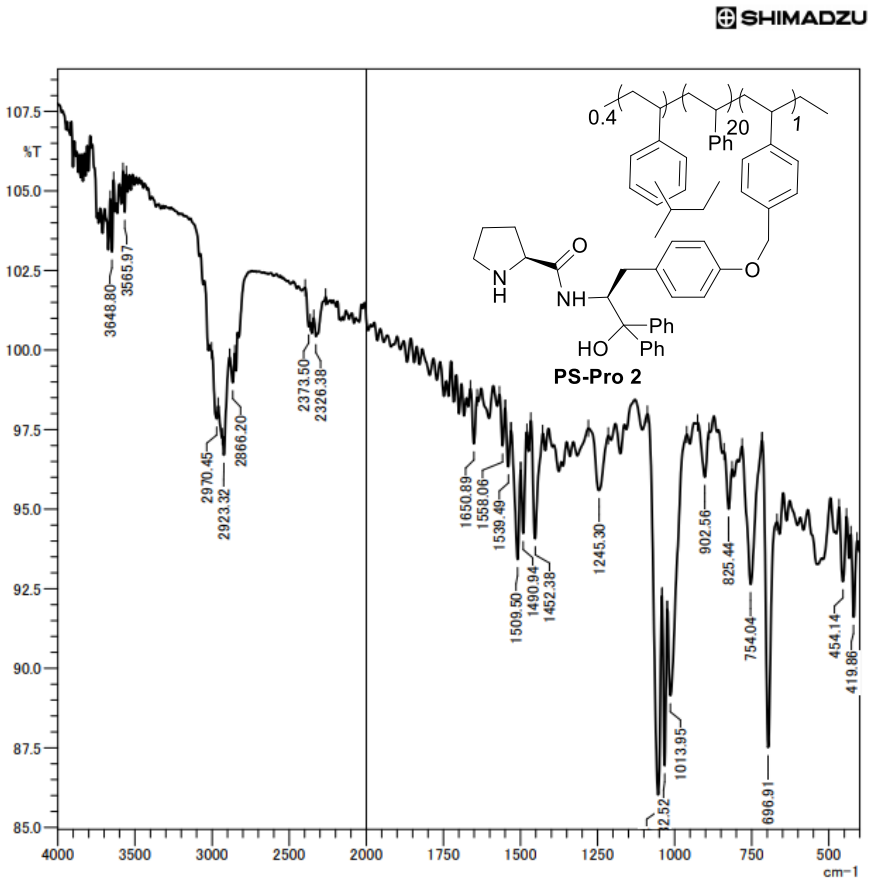
SHIMADZU
%T
cm-1
3648.80
3565.97
2970.45
2923.32
2866.20
2373.50
2326.38
1650.89
1558.06
1539.49
1509.50
1490.94
1452.38
1245.30
1013.95
902.56
825.44
754.04
696.91
454.14
419.86
0.4
20
1
Ph
PS-Pro 2

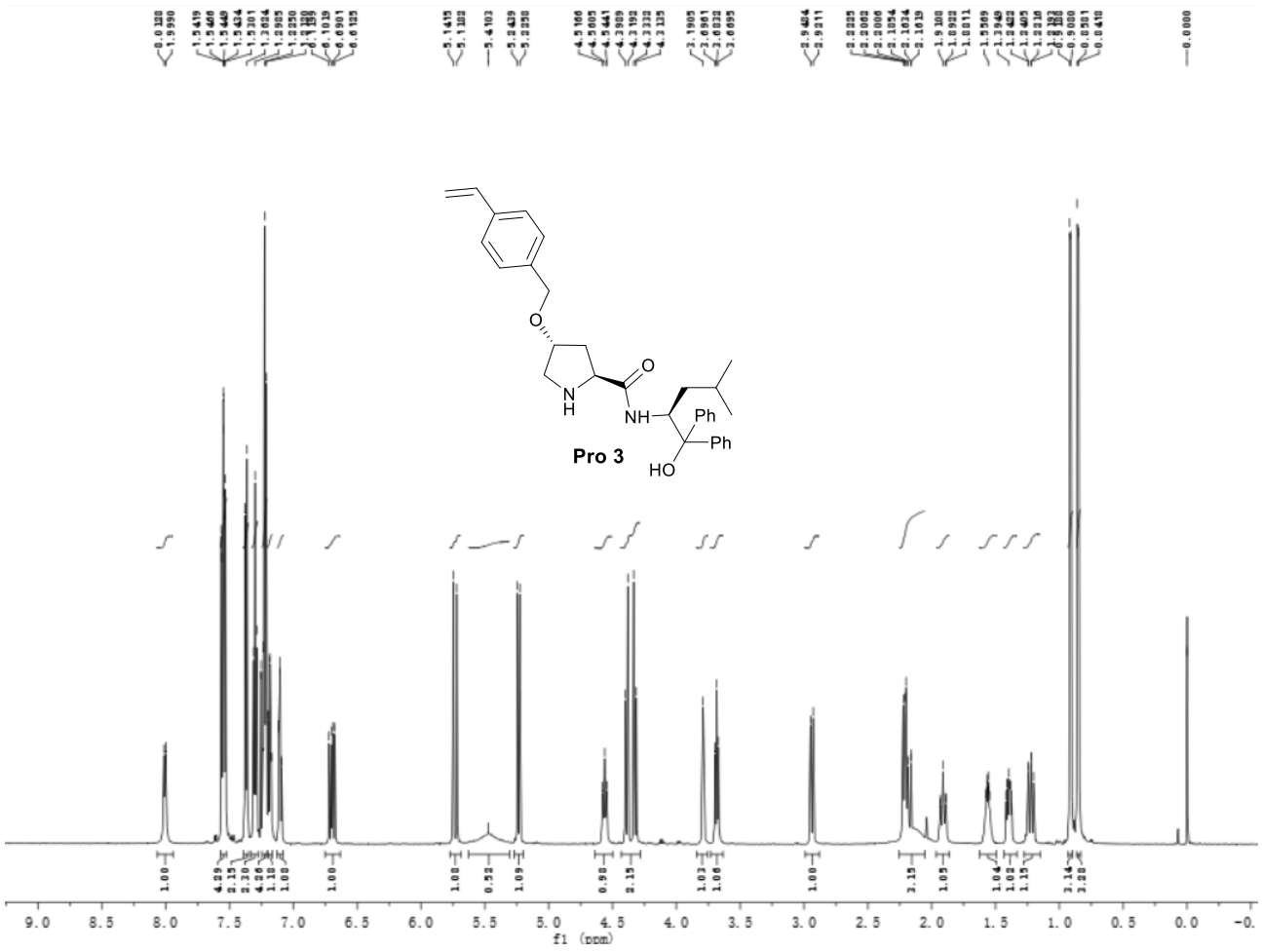
Pro 3
f1 (ppm)

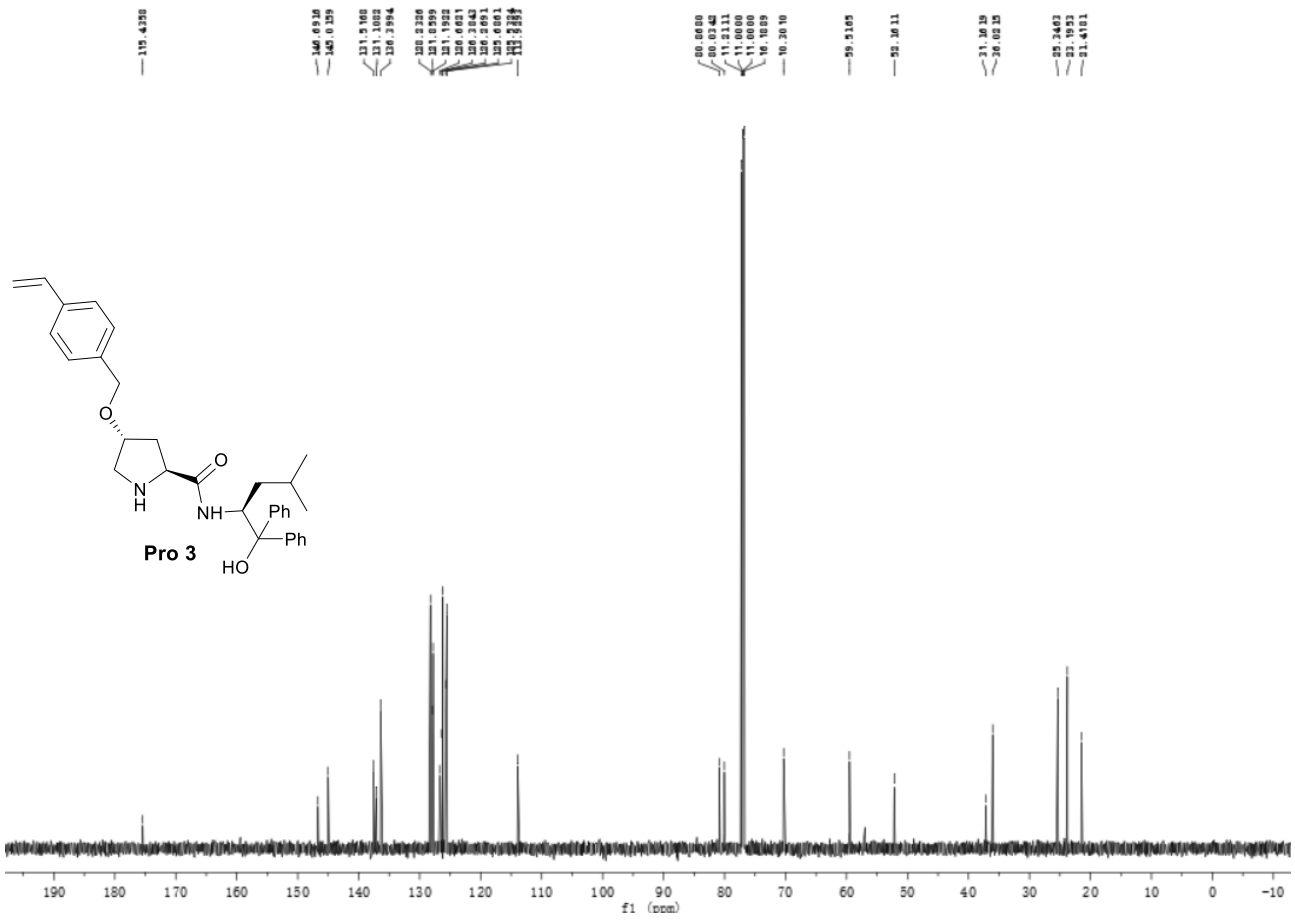
Pro 3
f1 (ppm)

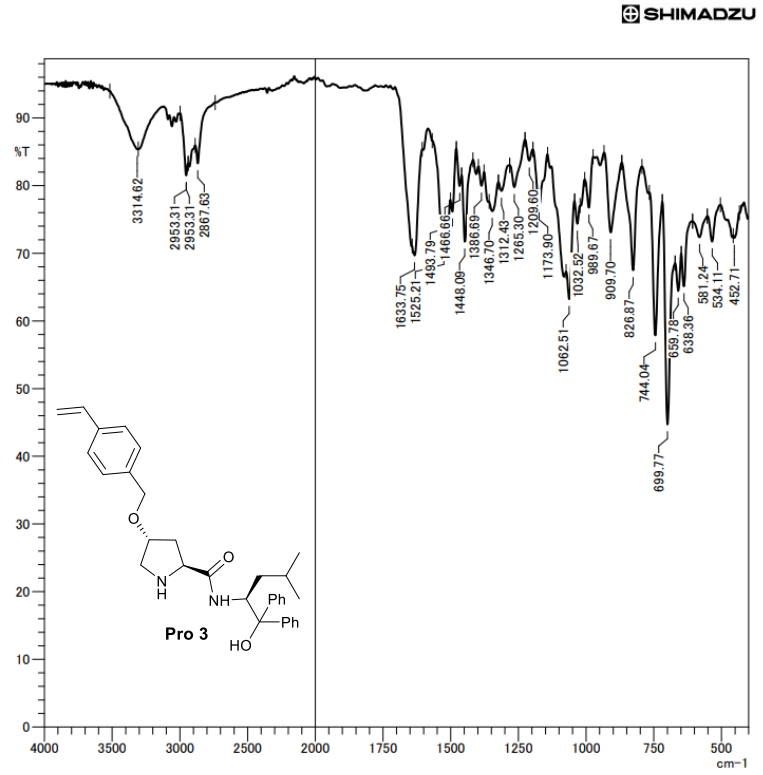
SHIMADZU
%T
3314.62
2953.31
2953.31
2867.63
1633.75
1525.21
1493.79
1466.66
1448.09
1386.69
1346.70
1312.43
1265.30
1209.60
1173.90
1062.51
1032.52
989.67
909.70
826.87
744.04
699.77
659.78
638.36
581.24
534.11
452.71
Pro 3
cm-1

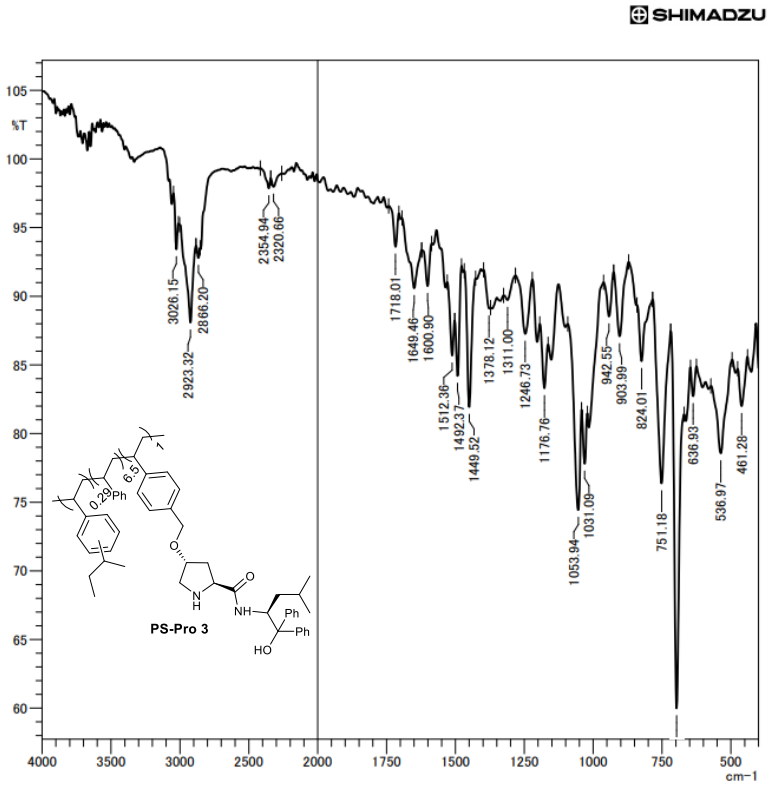
SHIMADZU
%T
3026.15
2923.32
2866.20
2354.94
2320.66
1718.01
1649.46
1600.90
1512.36
1492.37
1449.52
1378.12
1311.00
1246.73
1176.76
1053.94
1031.09
942.55
903.99
824.01
751.18
636.93
536.97
461.28
PS-Pro 3
cm-1

^{1}H NMR, ^{13}C NMR, ^{19}F NMR and HPLC spectra of products

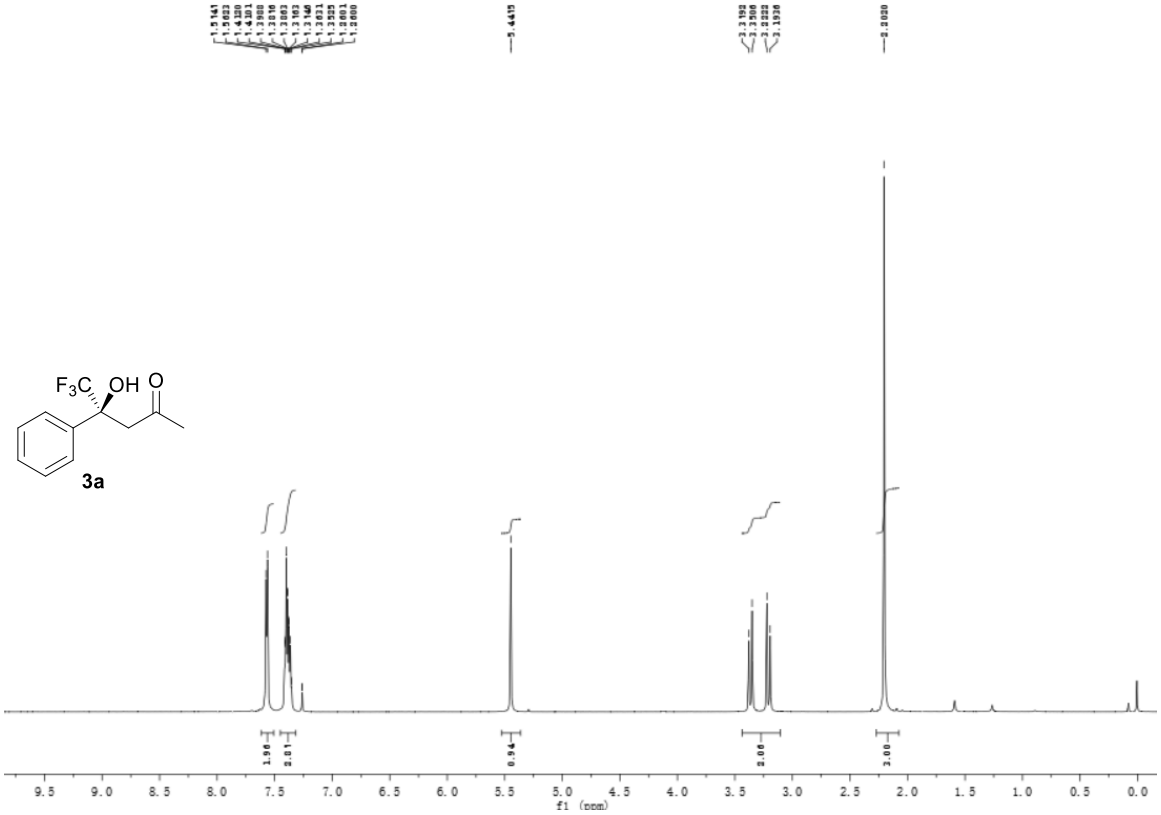

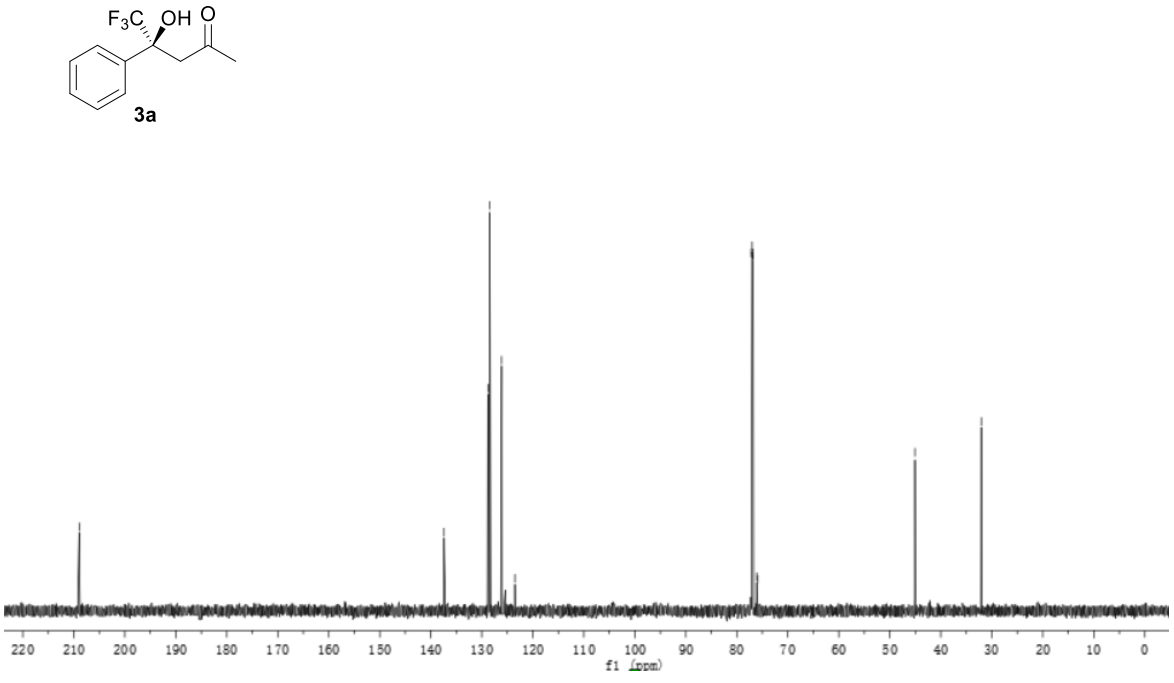

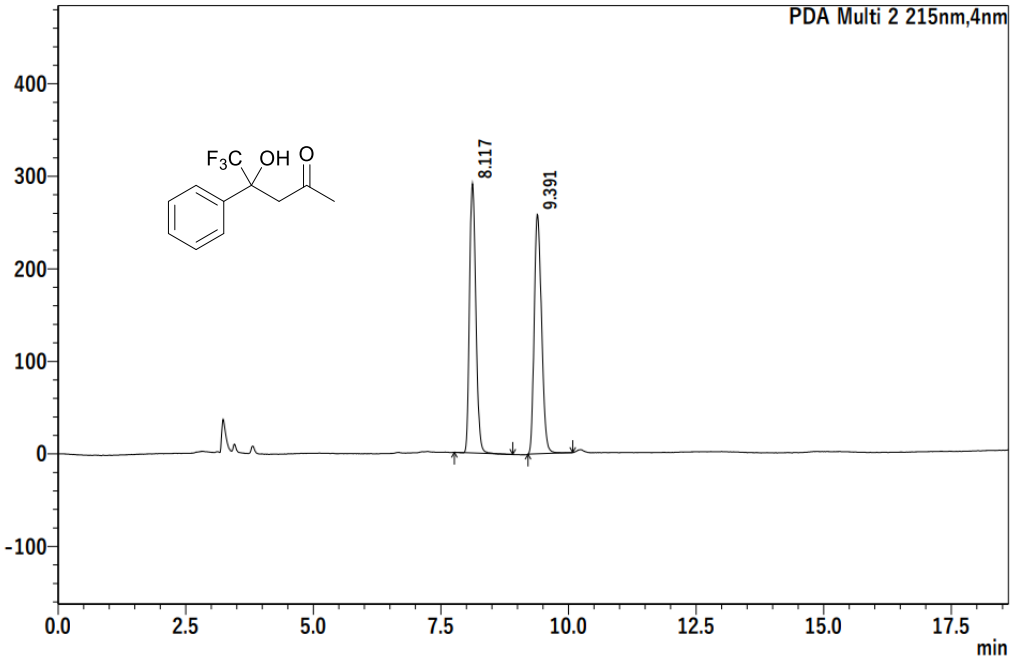

Peak Table

PDA Ch2 215nm

Peak#	Ret. Time	Area	Height	Area%
1	8.117	2516228	291110	49.155
2	9.391	2602772	258613	50.845
‡Œv		5119000	549723	100.000

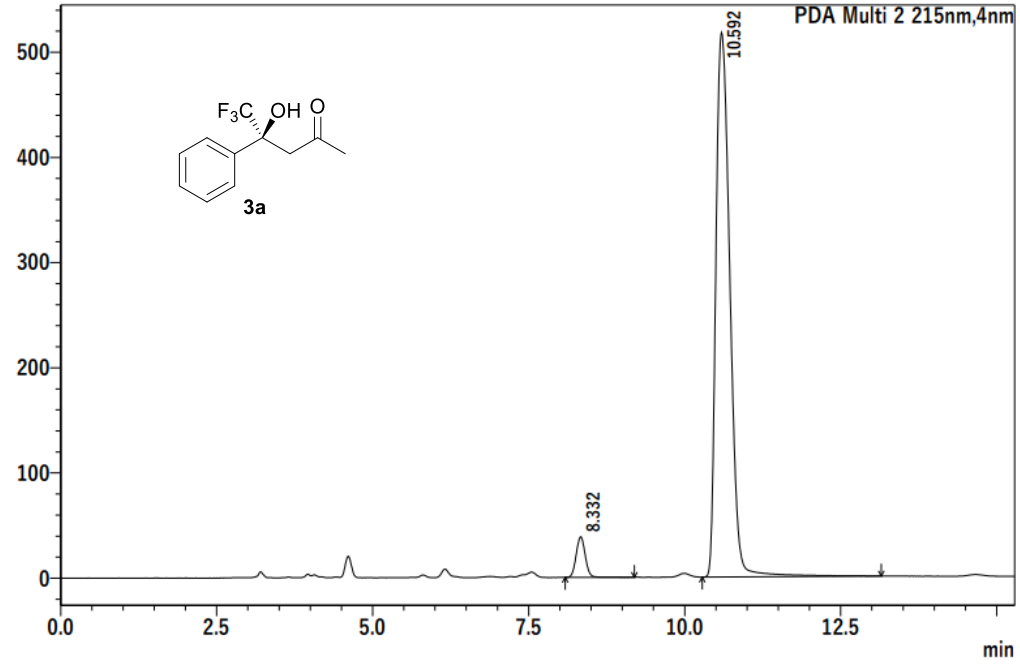

Peak Table

PDA Ch2 215nm

Peak#	Ret. Time	Area	Height	Area%
1	8.332	392306	38749	4.620
2	10.592	8099984	517734	95.380
‡Œv		8492290	556483	100.000

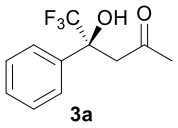

3a

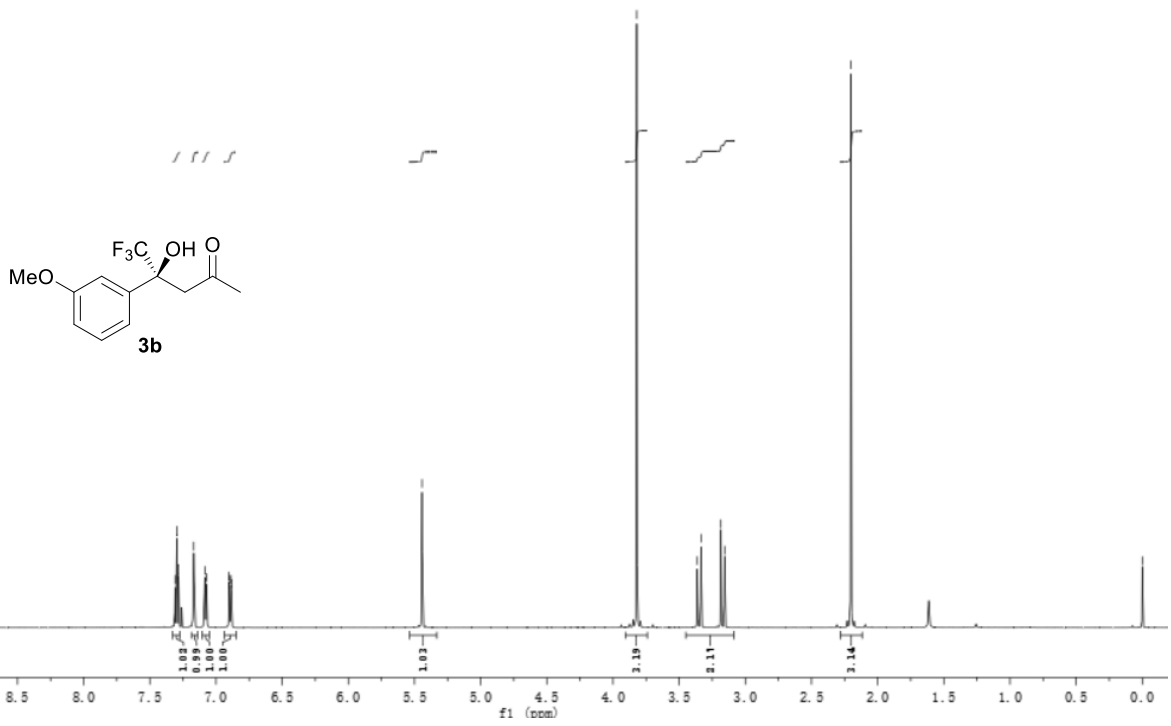

3b

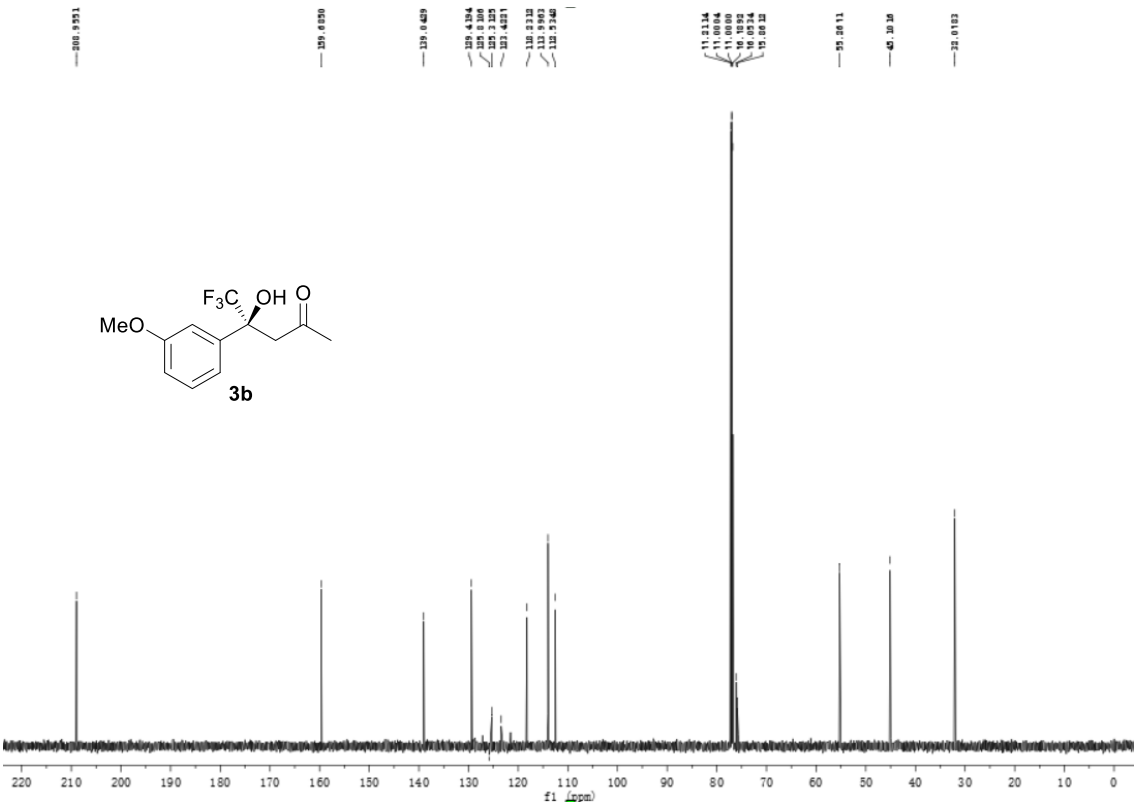

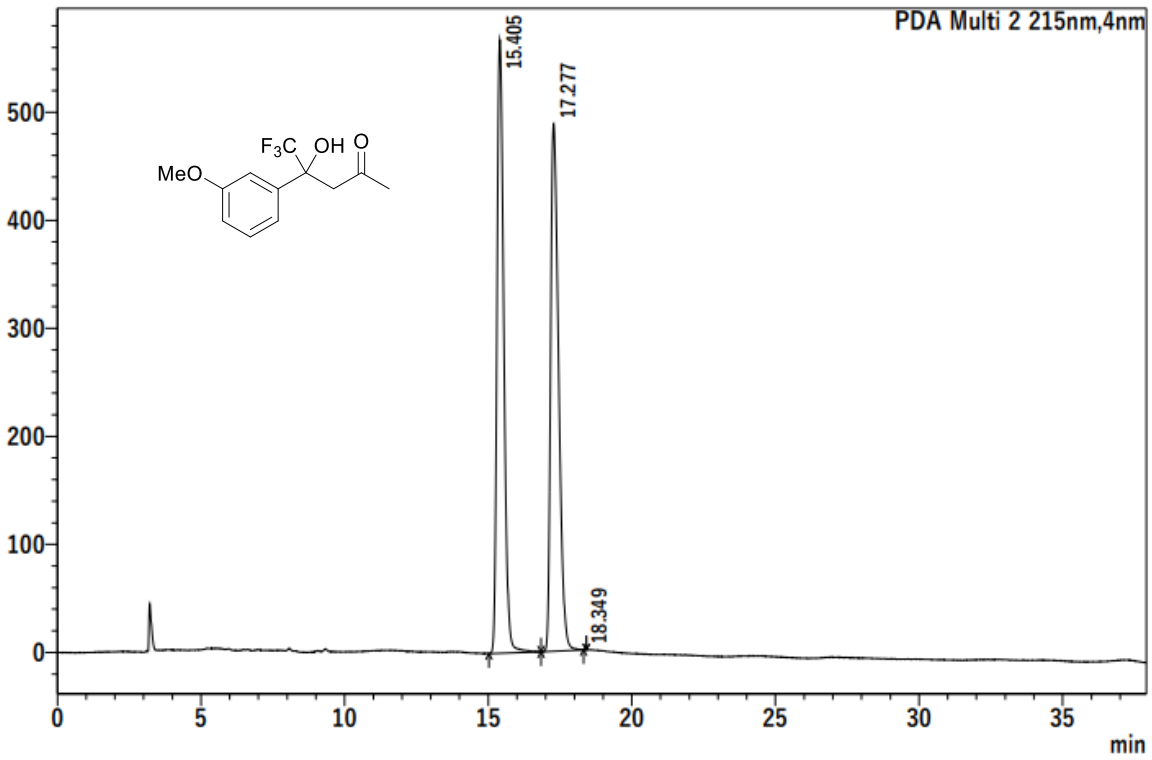

Peak Table

PDA Ch2 215nm

Peak#	Ret. Time	Area	Height	Area%
1	15.405	9505743	568068	49.902
2	17.277	9542055	488144	50.093
3	18.349	978	299	0.005
‡Œv		19048776	1056511	100.000

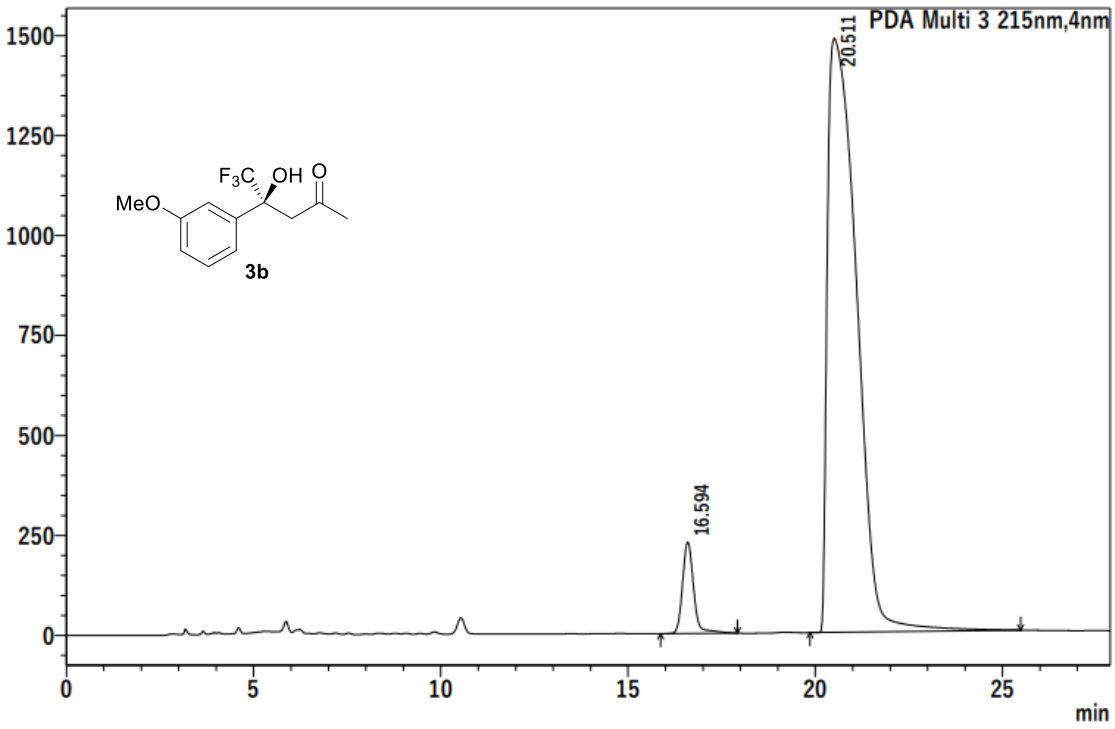

Peak Table

PDA Ch3 215nm

Peak#	Ret. Time	Area	Height	Area%
1	16.594	4718138	228498	5.574
2	20.511	79929190	1485833	94.426
‡Œv		84647328	1714331	100.000

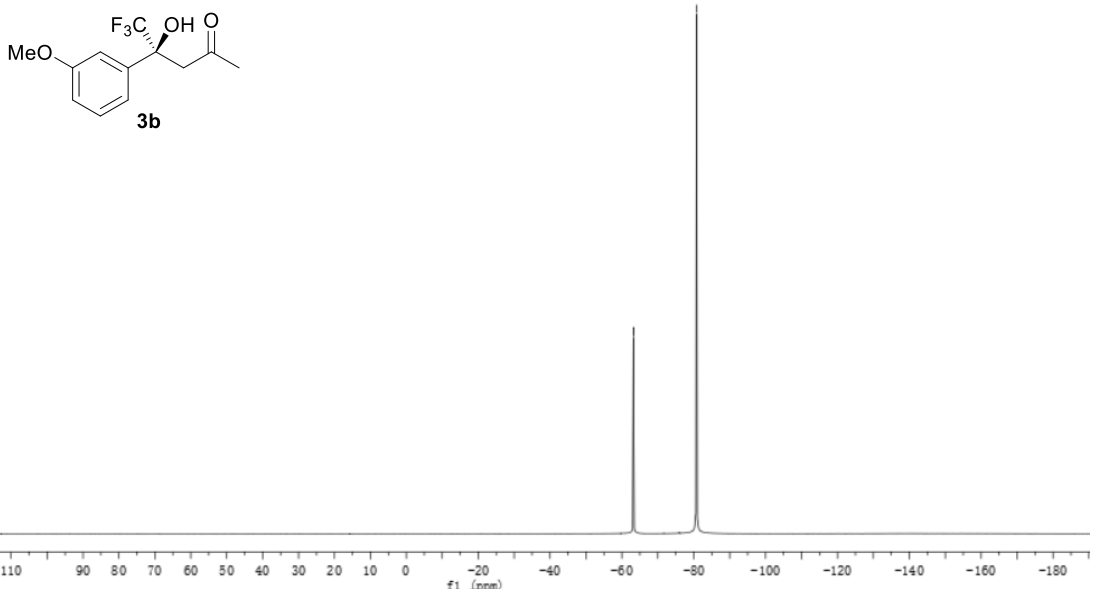

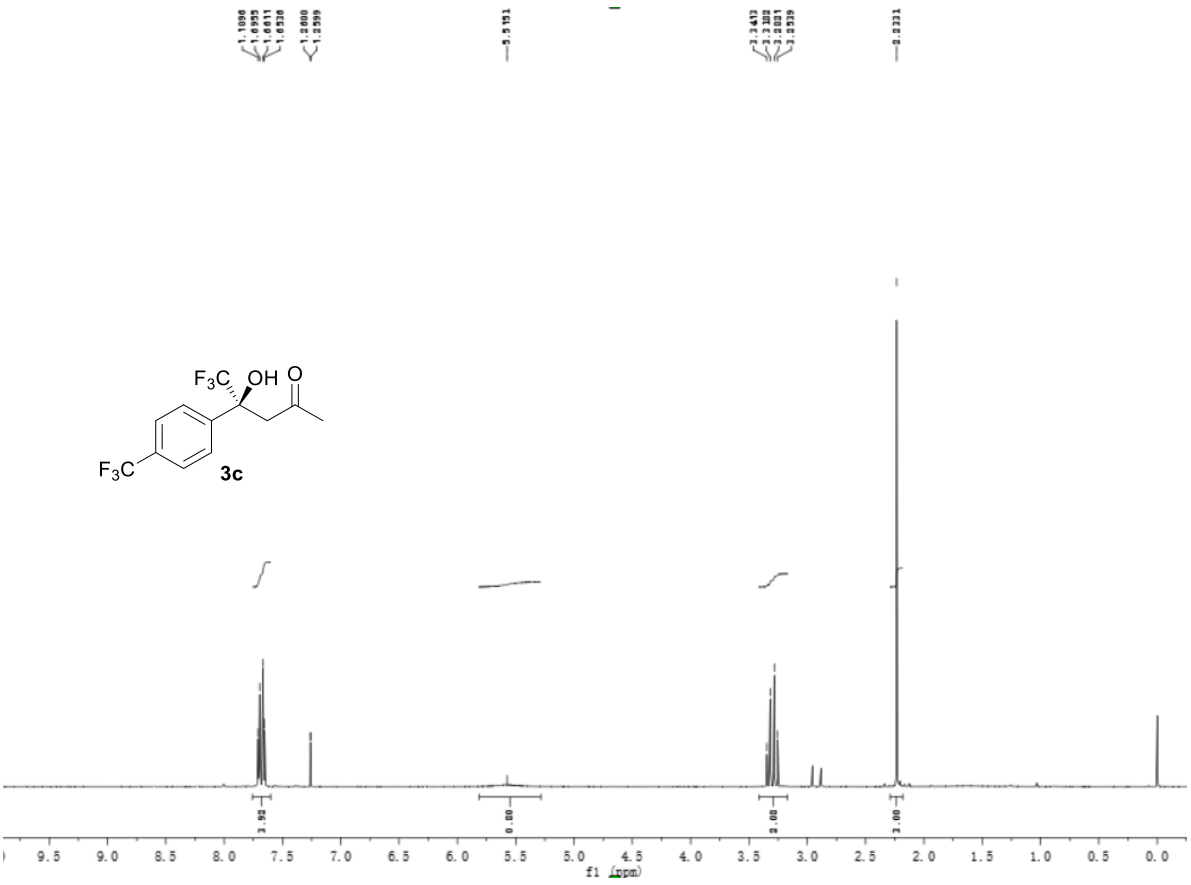
F3C
OH
O
F3C
3c
9.5
9.0
8.5
8.0
7.5
7.0
6.5
6.0
5.5
5.0
4.5
4.0
3.5
3.0
2.5
2.0
1.5
1.0
0.5
0.0
f1 (ppm)

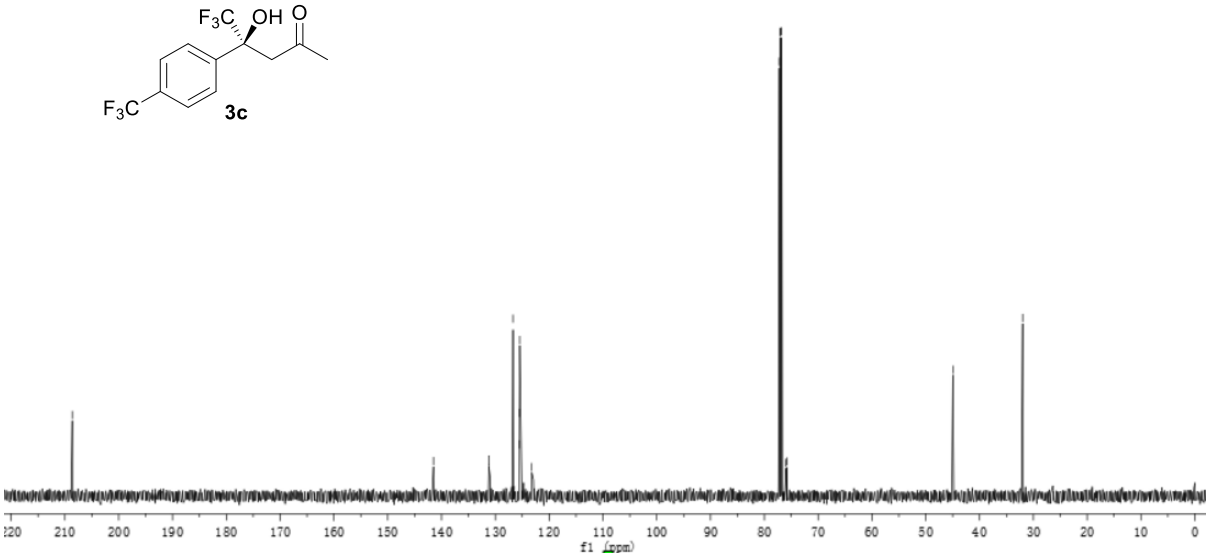
F3C
OH
O
F3C
3c
220
210
200
190
180
170
160
150
140
130
120
110
100
90
80
70
60
50
40
30
20
10
0
f1 (ppm)

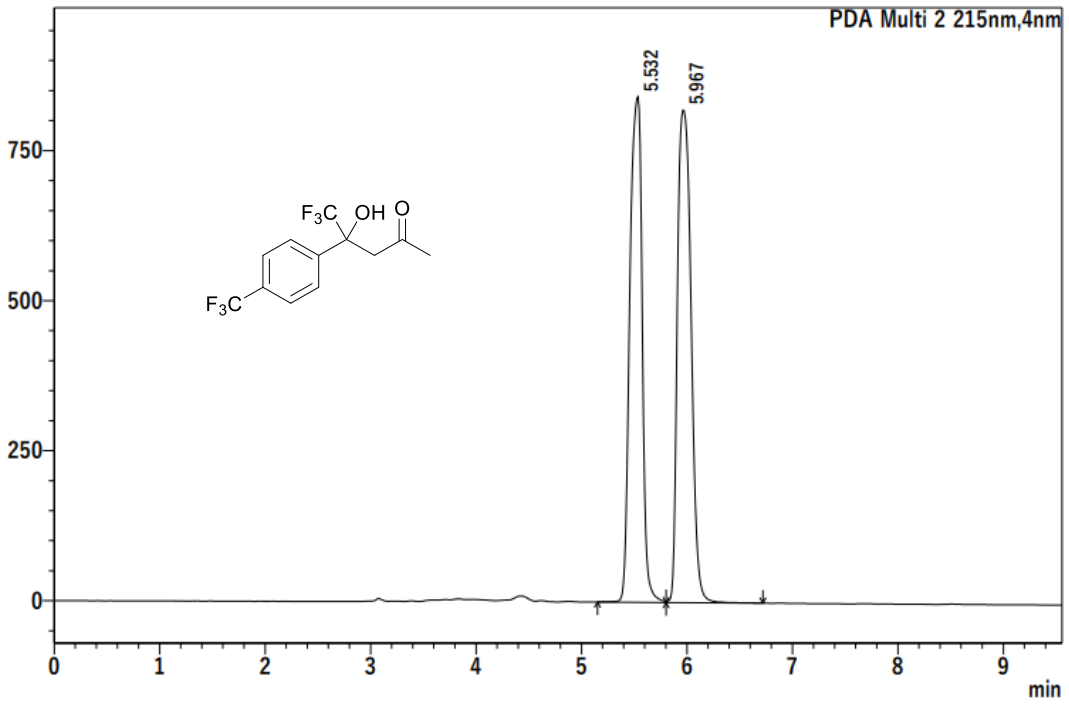

Peak Table

PDA Ch2 215nm

Peak#	Ret. Time	Area	Height	Area%
1	5.532	6898623	842634	48.510
2	5.967	7322502	820813	51.490
‡Œv		14221125	1663448	100.000

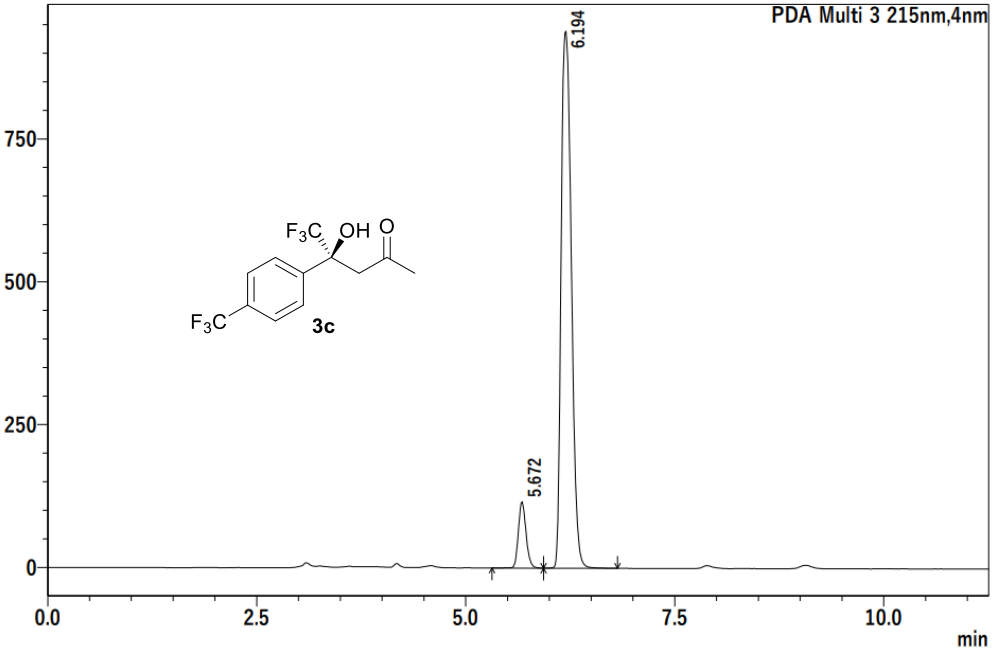

Peak Table

PDA Ch3 215nm

Peak#	Ret. Time	Area	Height	Area%
1	5.672	745390	115924	8.519
2	6.194	8004183	939525	91.481
‡Œv		8749572	1055449	100.000

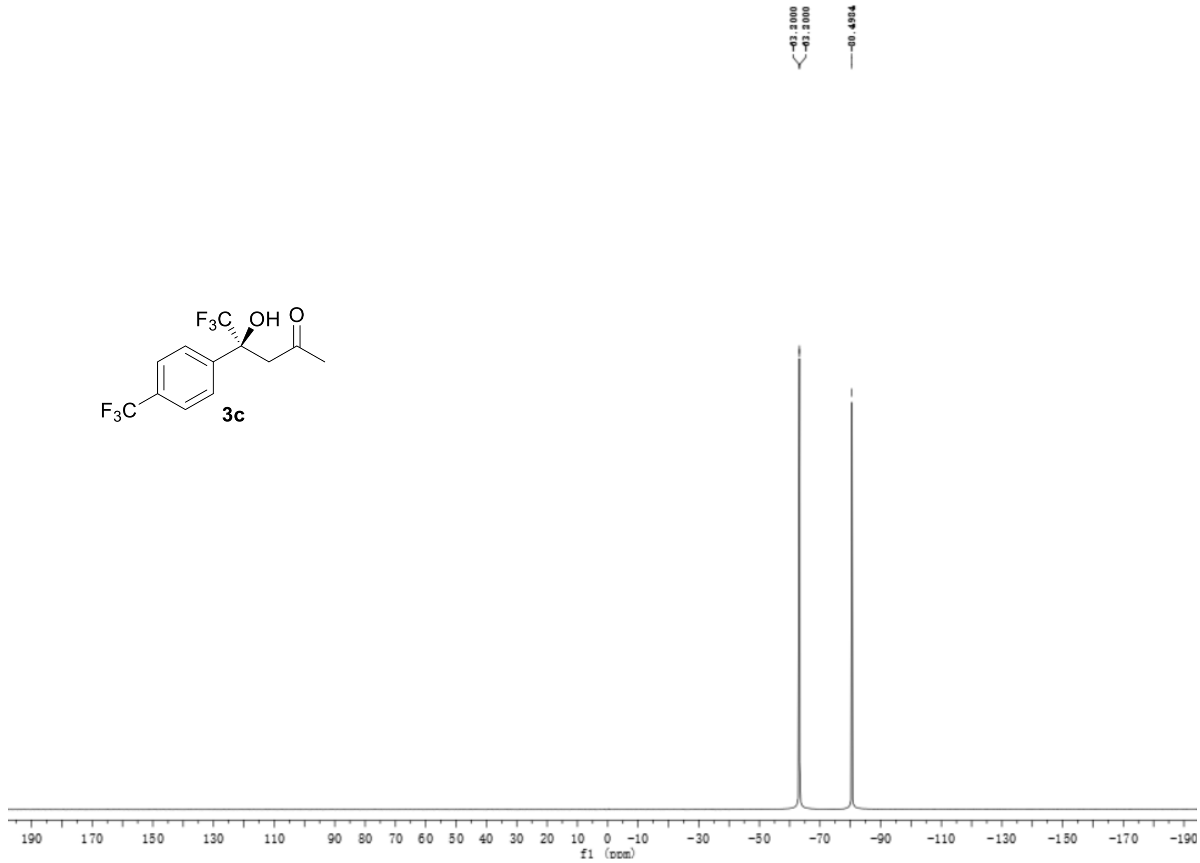

F_3C OH O
F_3C
3c
190 170 150 130 110 90 80 70 60 50 40 30 20 10 0 −10 −30 −50 −70 −90 −110 −130 −150 −170 −190
f1 (ppm)

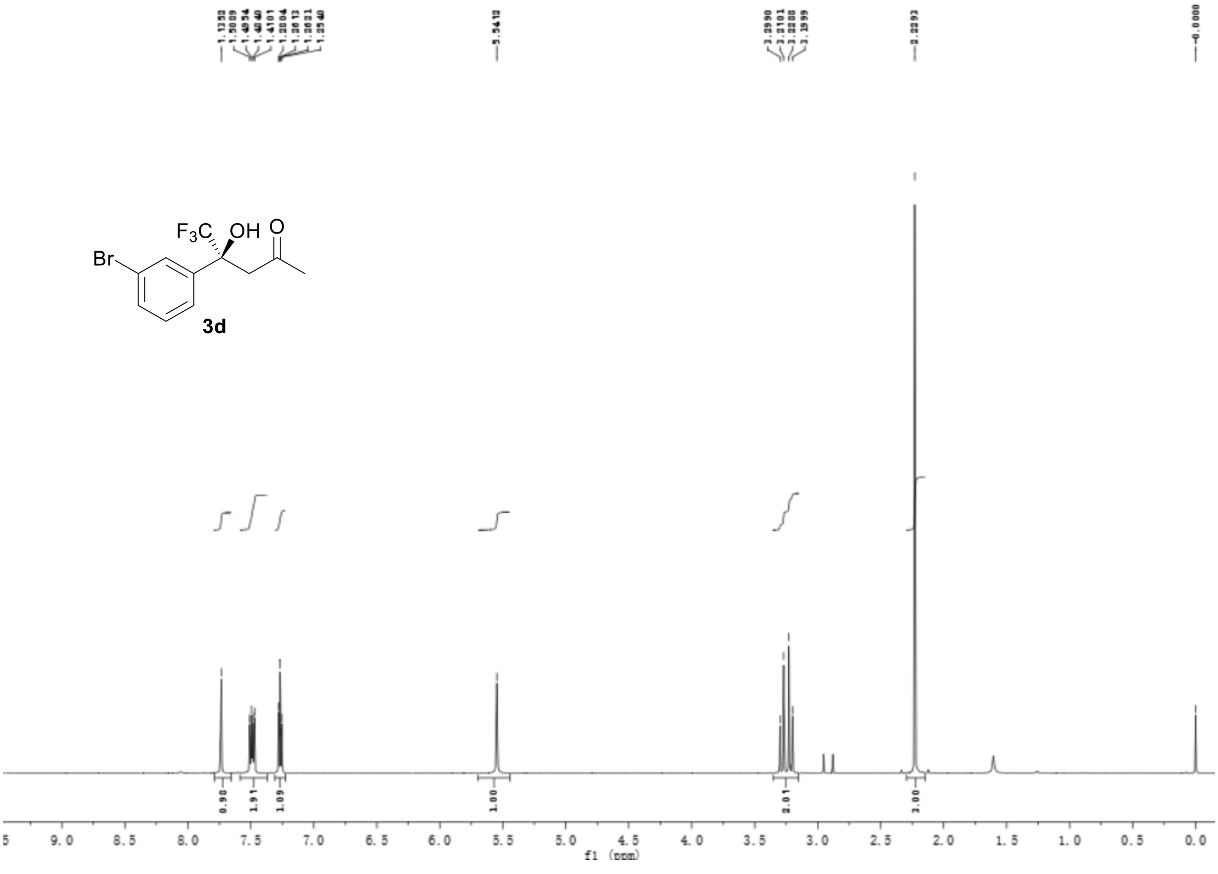

F_3C OH O
Br
3d
0.98 1.91 1.09 1.00 2.01 3.00
9.0 8.5 8.0 7.5 7.0 6.5 6.0 5.5 5.0 4.5 4.0 3.5 3.0 2.5 2.0 1.5 1.0 0.5 0.0
f1 (ppm)

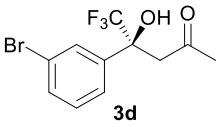

3d

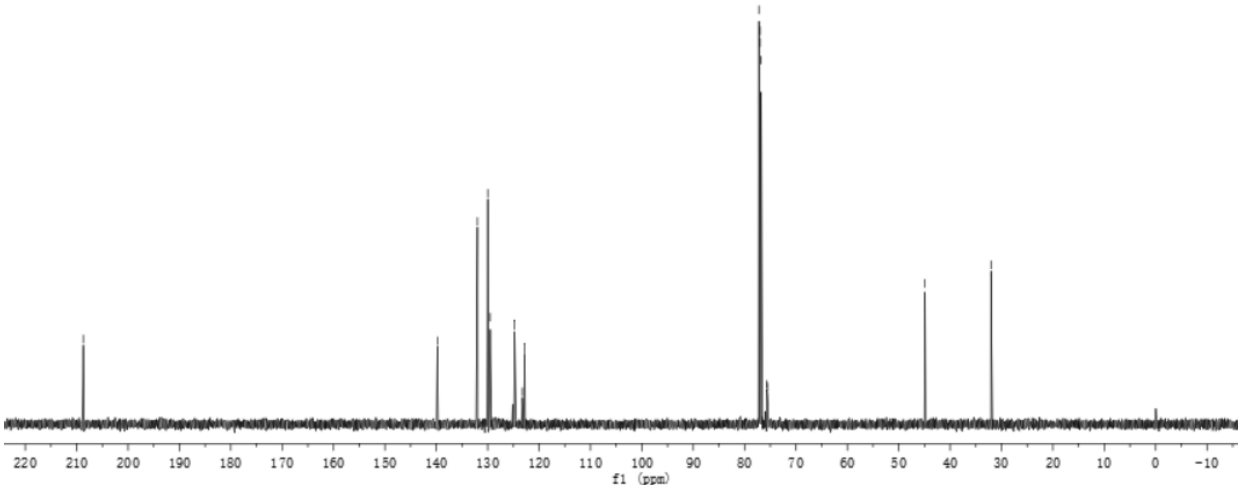

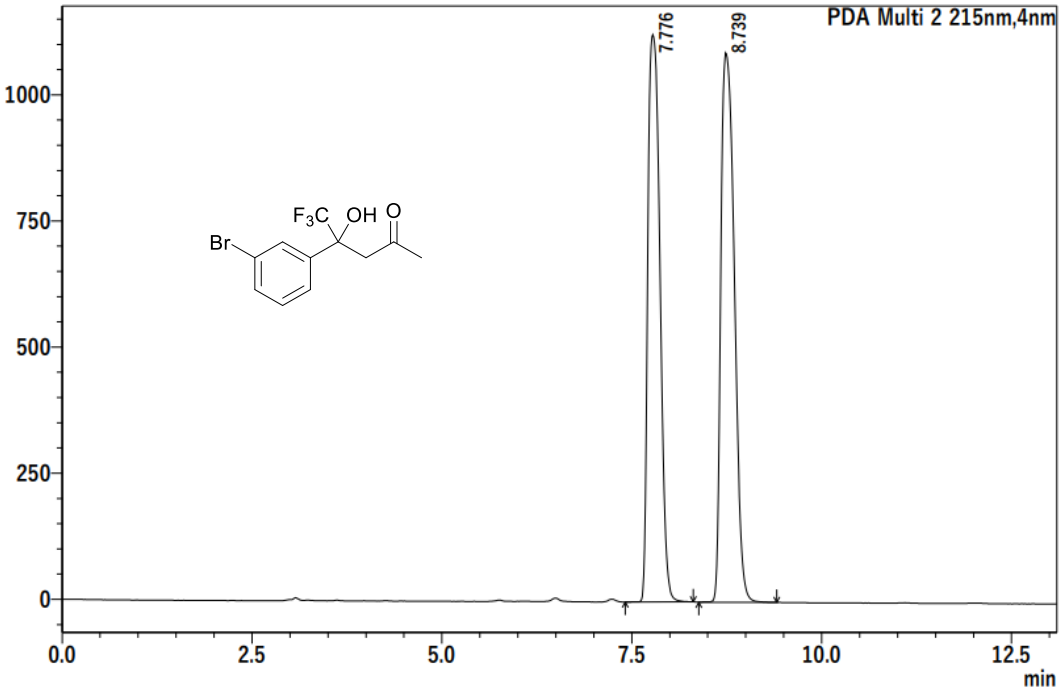

Peak Table

PDA Ch2 215nm

Peak#	Ret. Time	Area	Height	Area%
1	7.776	12460776	1124807	47.941
2	8.739	13530933	1089492	52.059
‡Œv		25991709	2214299	100.000

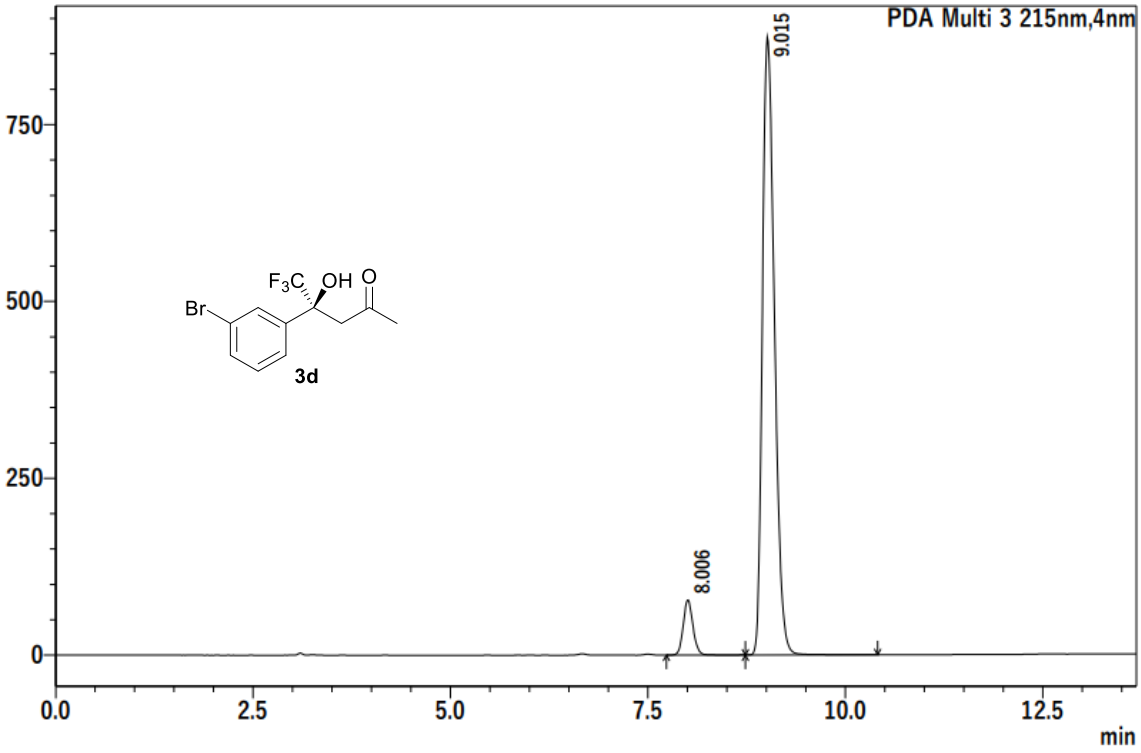

Peak Table

PDA Ch3 215nm

Peak#	Ret. Time	Area	Height	Area%
1	8.006	671565	77839	6.743
2	9.015	9287317	873686	93.257
‡Œv		9958883	951525	100.000

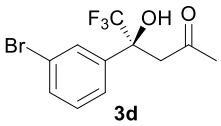

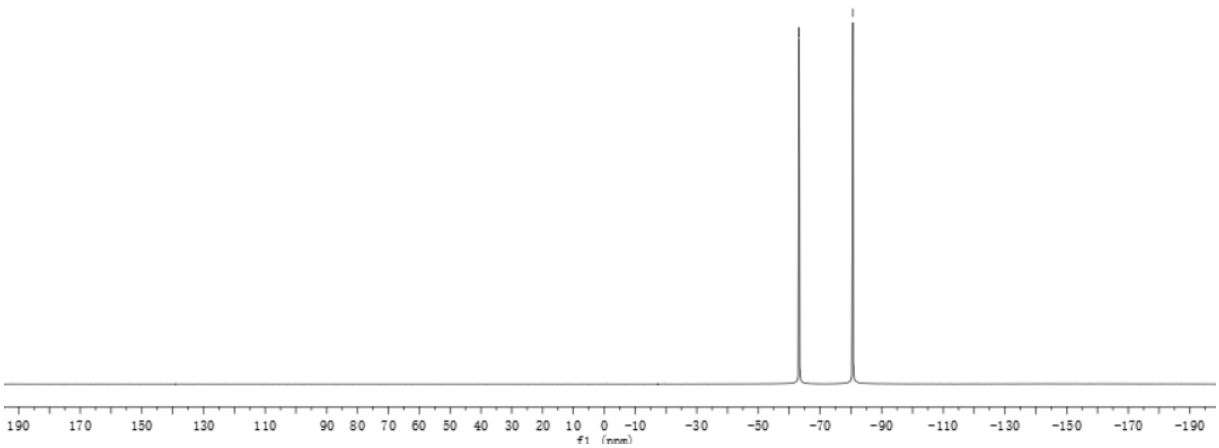

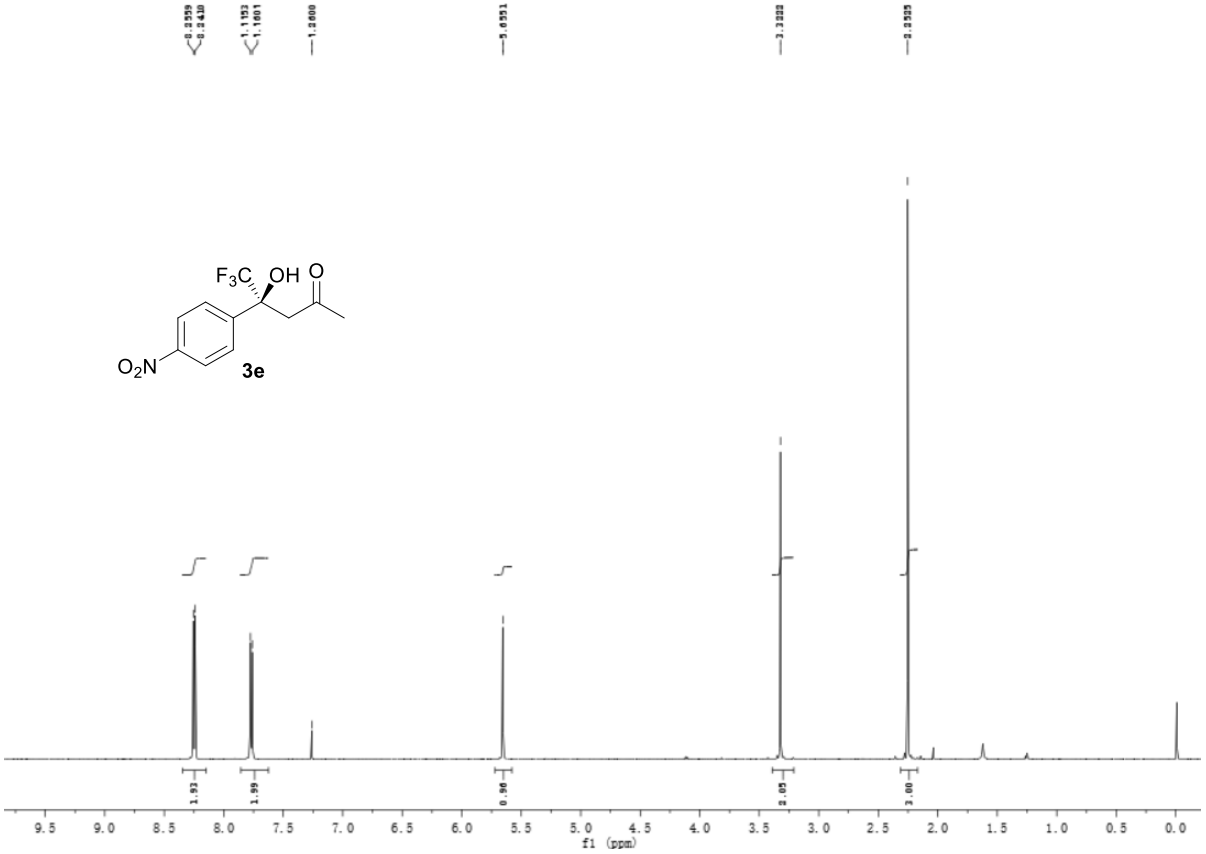
F3C
OH
O
O2N
3e
f1 (ppm)

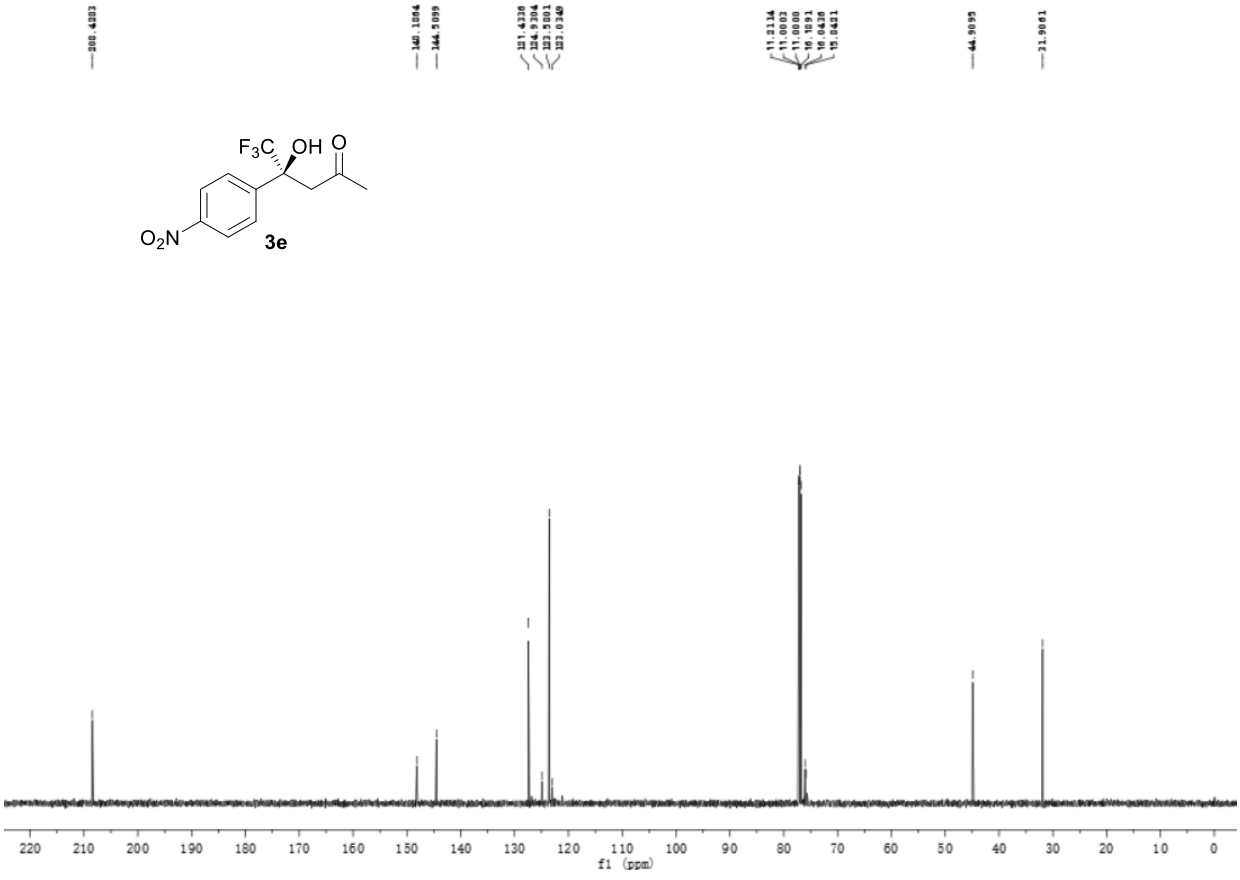
F3C
OH
O
O2N
3e
f1 (ppm)

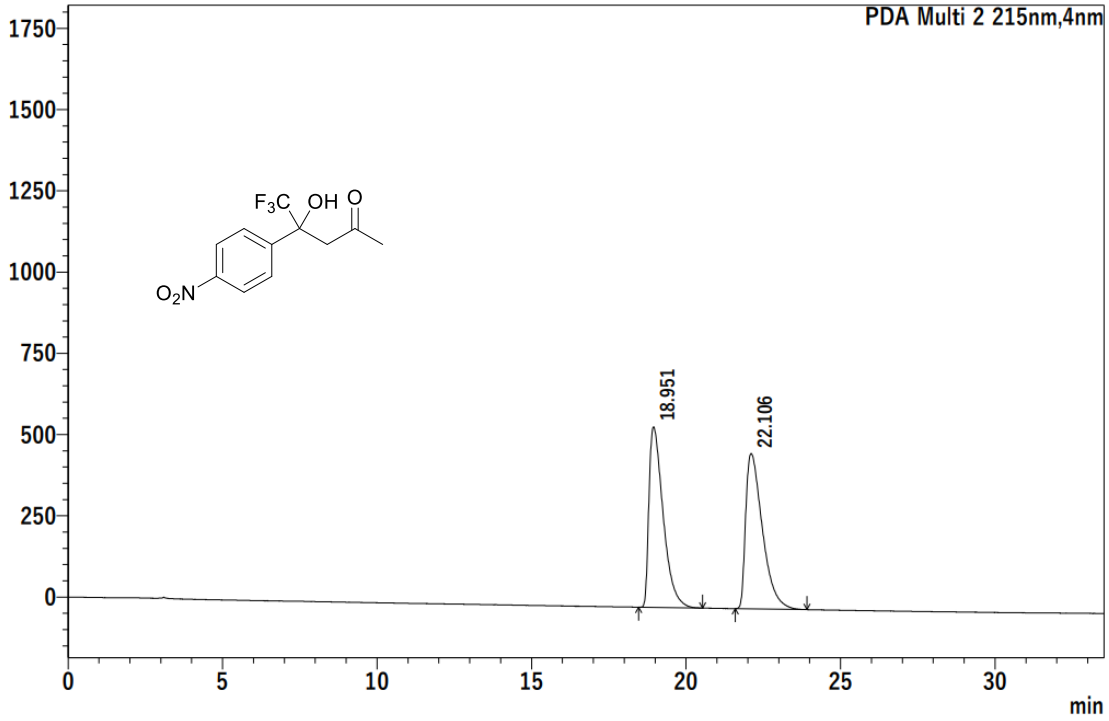

Peak Table

PDA Ch2 215nm

Peak#	Ret. Time	Area	Height	Area%
1	18.951	17754734	555917	49.649
2	22.106	18005595	478284	50.351
‡Œv		35760329	1034200	100.000

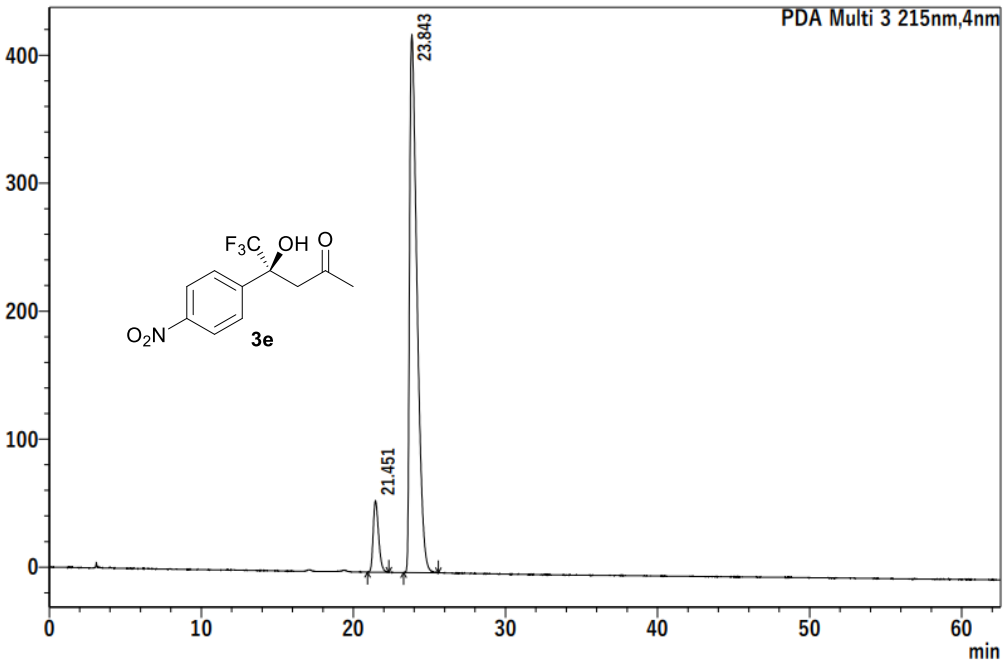

Peak Table

PDA Ch3 215nm

Peak#	Ret. Time	Area	Height	Area%
1	21.451	1369870	55716	8.746
2	23.843	14292545	420216	91.254
‡Œv		15662415	475932	100.000

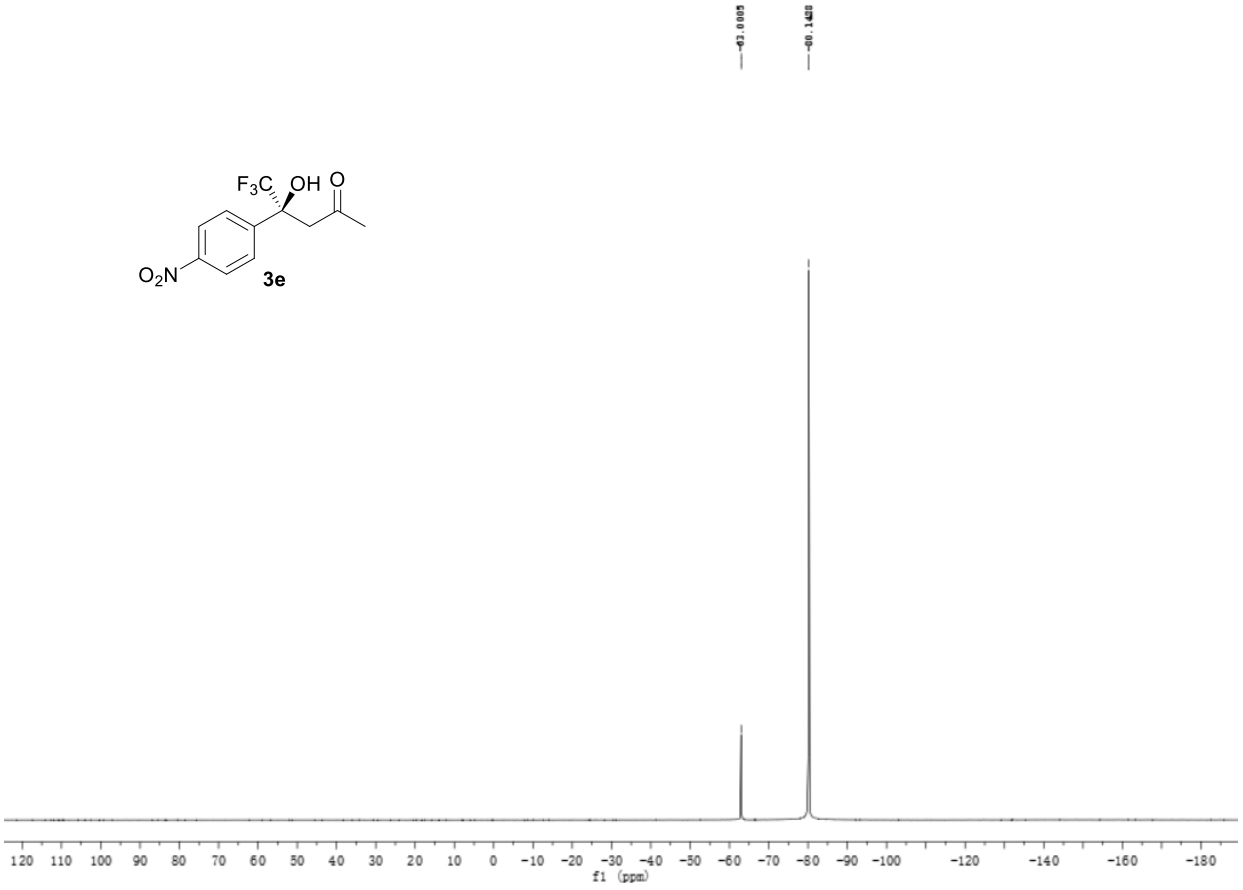
F3C
OH
O
O2N
3e
f1 (ppm)

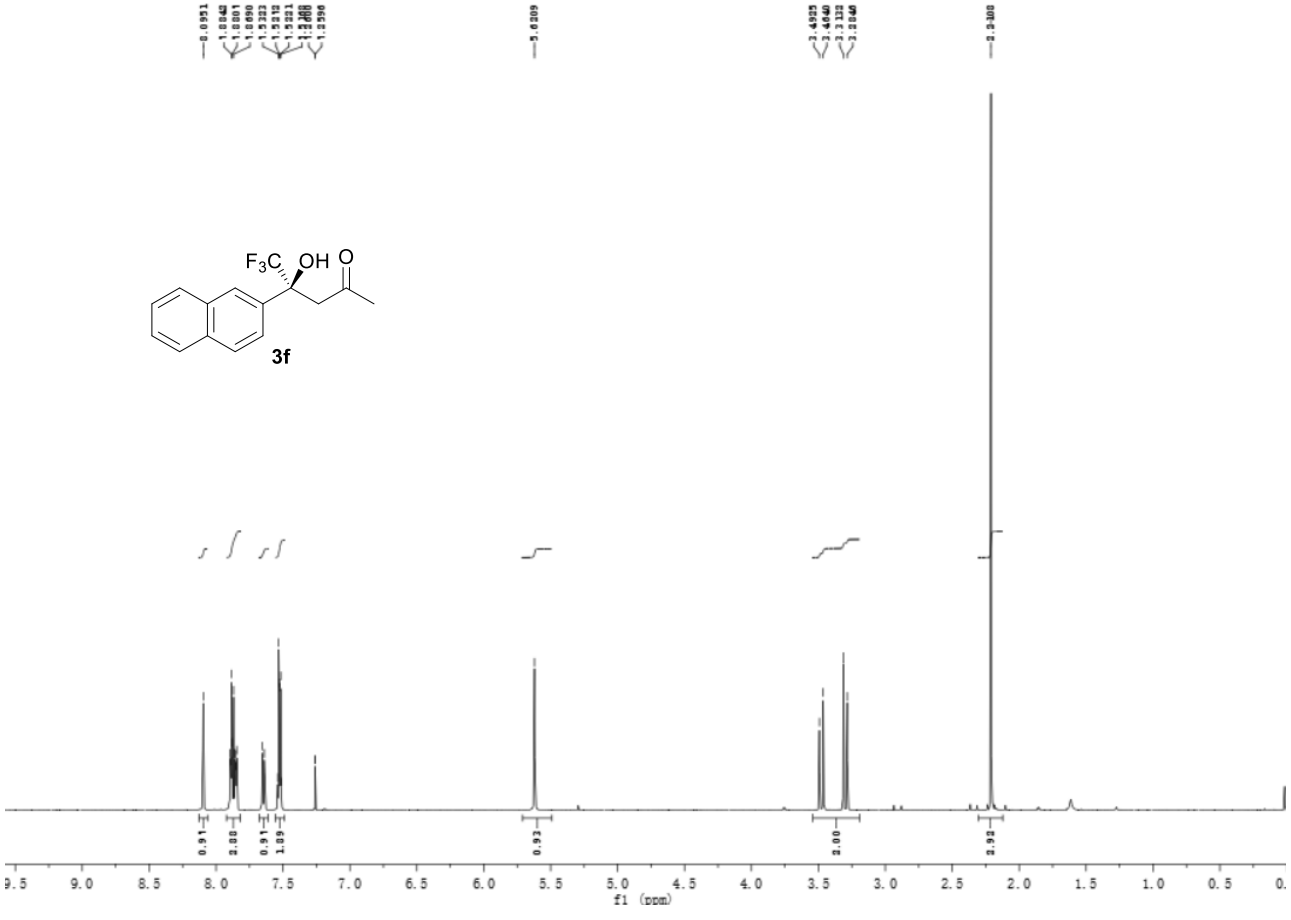
F3C
OH
O
3f
f1 (ppm)

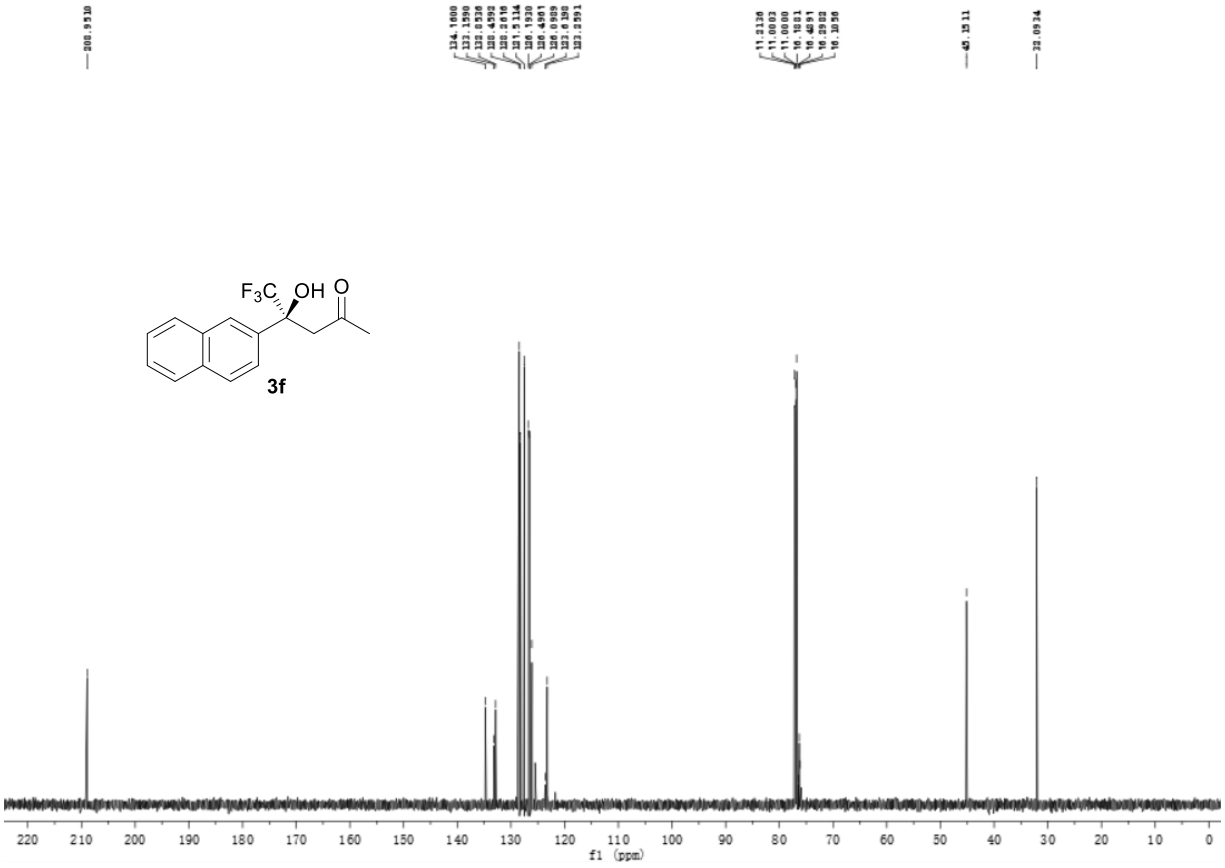

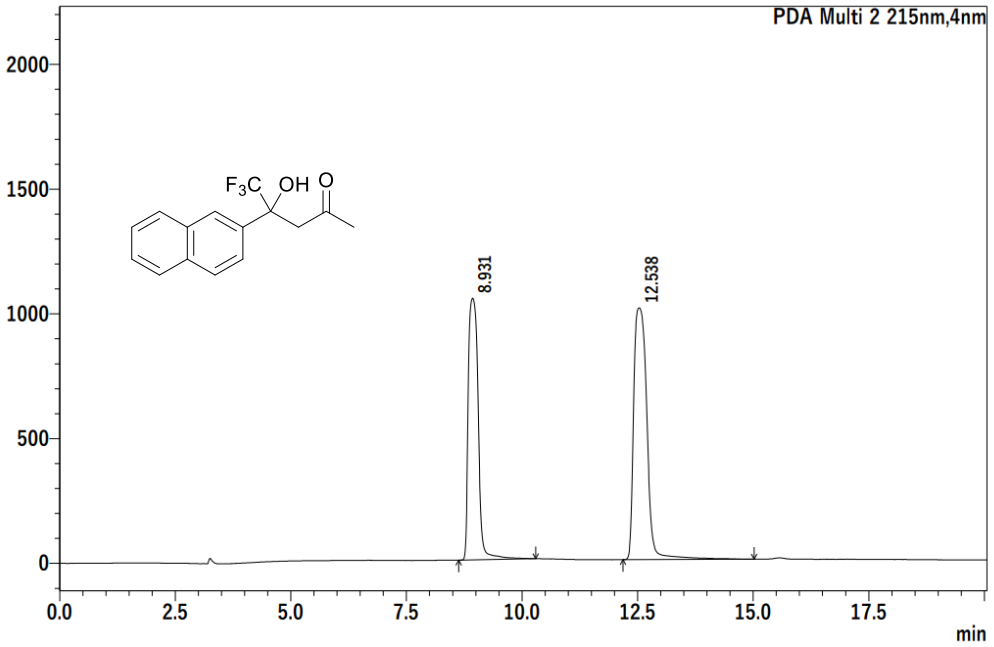

Peak Table

PDA Ch2 215nm

Peak#	Ret. Time	Area	Height	Area%
1	8.931	15612239	1049144	43.713
2	12.538	20102797	1009010	56.287
‡Œv		35715036	2058153	100.000

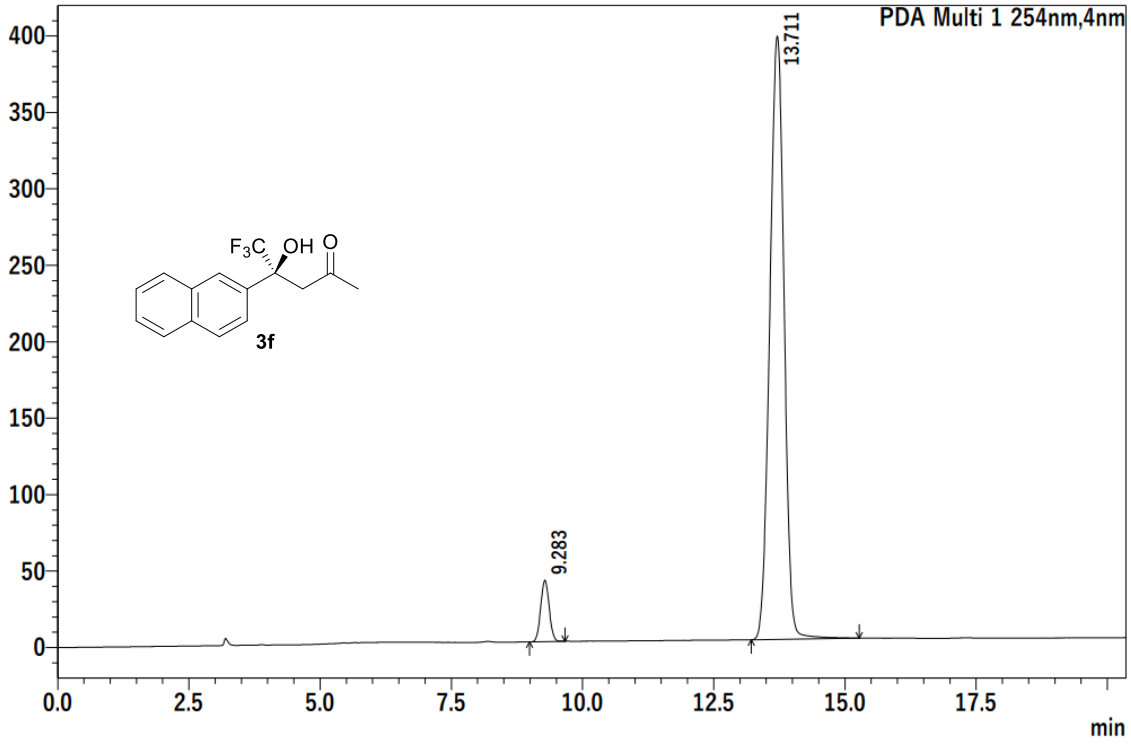

Peak Table

PDA Ch1 254nm

Peak#	Ret. Time	Area	Height	Area%
1	9.283	451885	40195	5.709
2	13.711	7463609	394524	94.291
‡Œv		7915494	434719	100.000

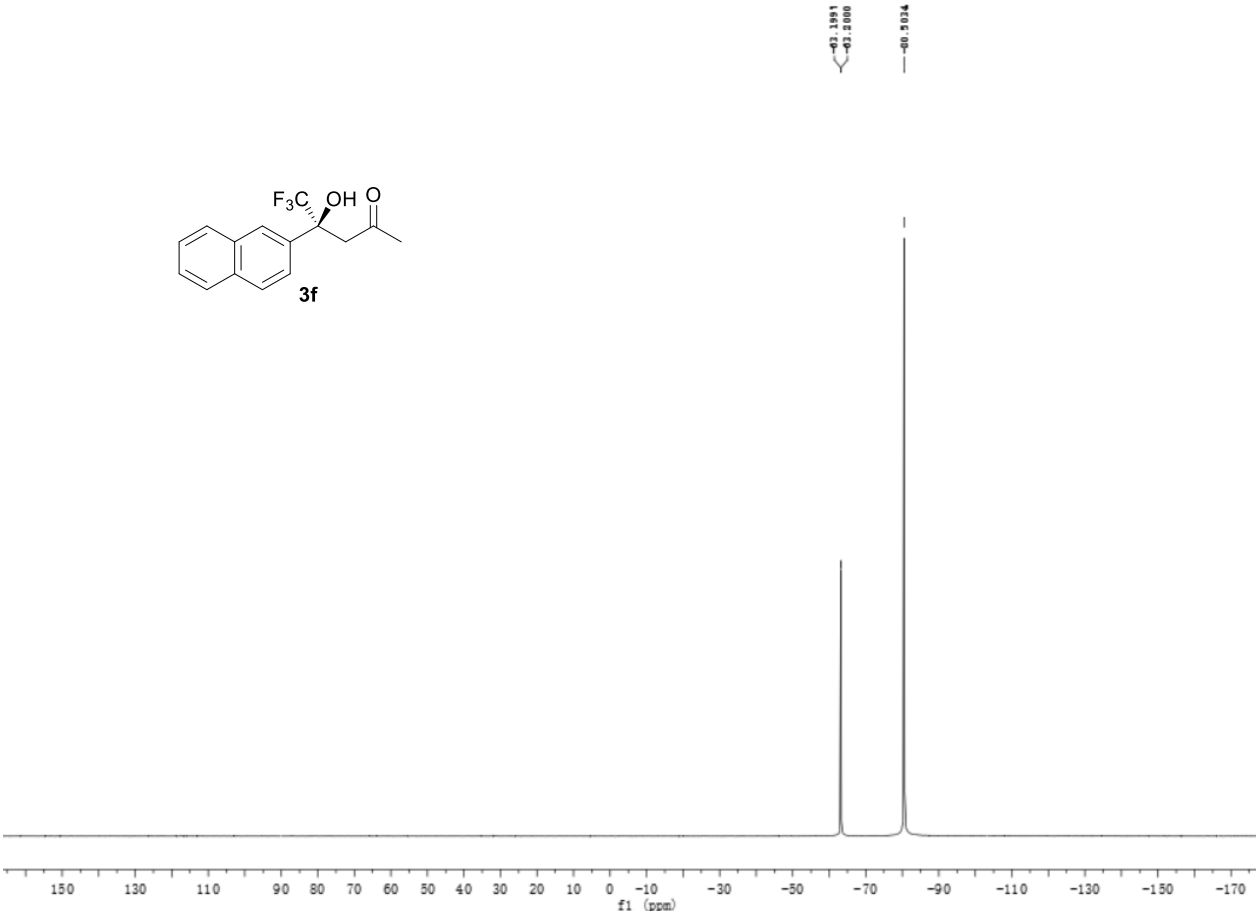

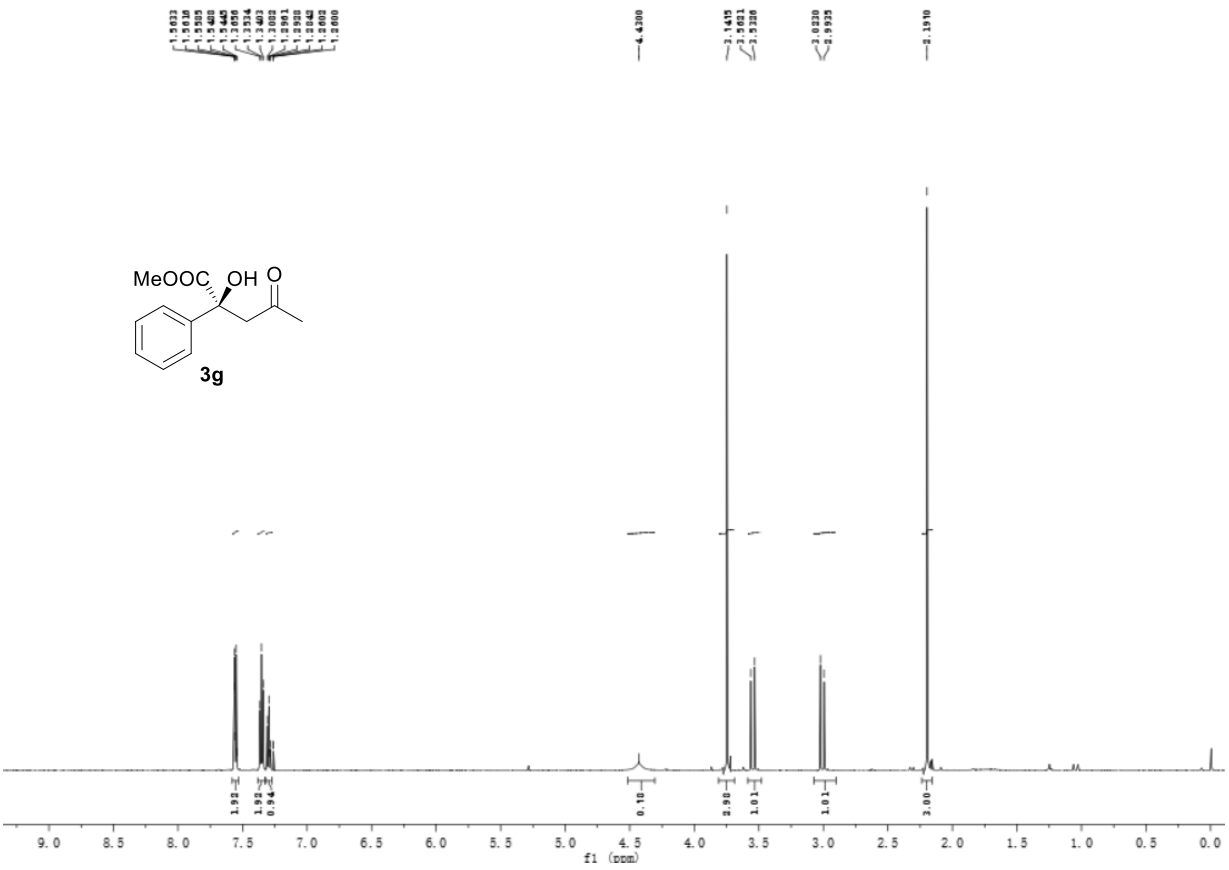
MeOOC
OH
O
3g
f1 (ppm)

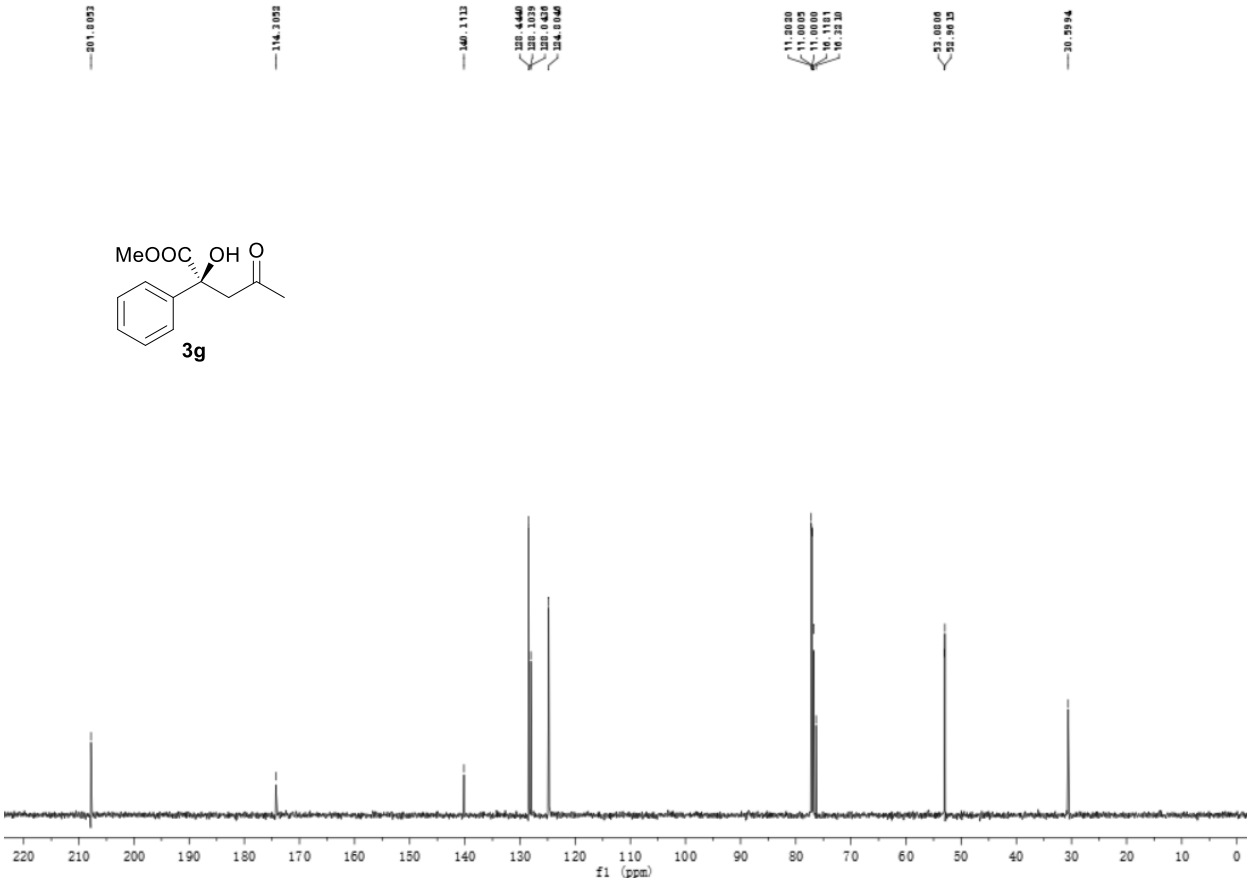
MeOOC
OH
O
3g
f1 (ppm)

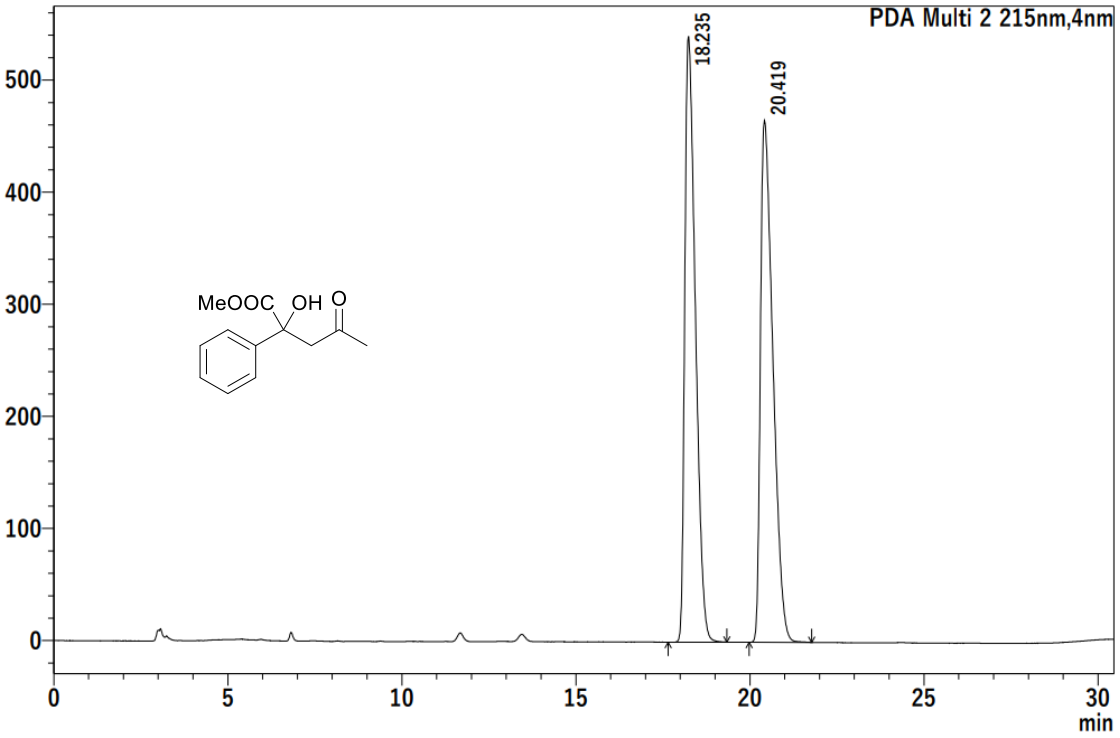

Peak Table

PDA Ch2 215nm

Peak#	Ret. Time	Area	Height	Area%
1	18.235	11502539	540219	49.797
2	20.419	11596410	465451	50.203
‡Œv		23098950	1005671	100.000

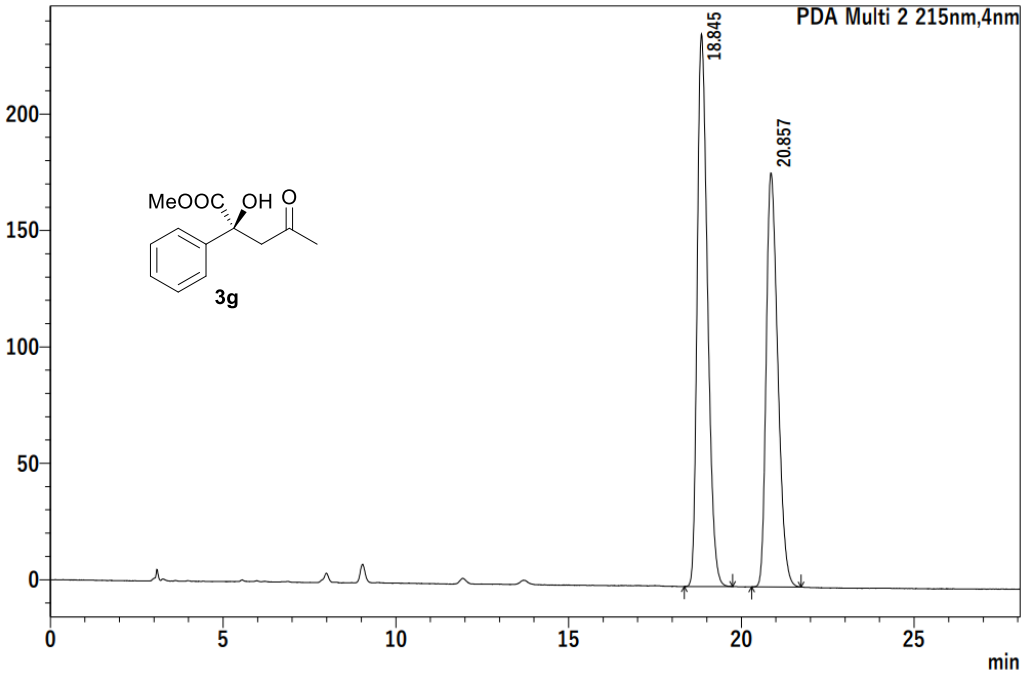

Peak Table

PDA Ch2 215nm

Peak#	Ret. Time	Area	Height	Area%
1	18.845	4952009	237421	54.441
2	20.857	4144159	177855	45.559
‡Œv		9096167	415276	100.000

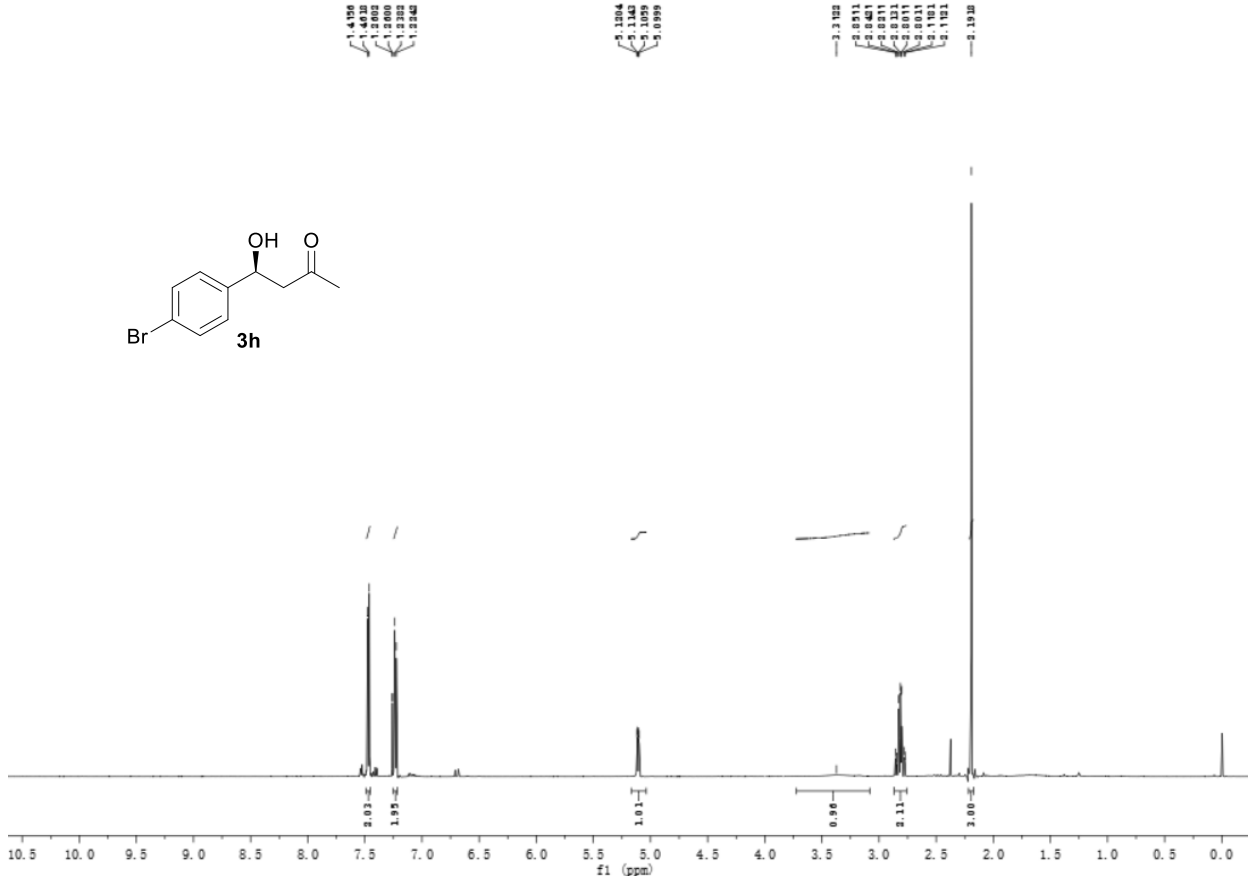
OH
O
Br
3h
10.5 10.0 9.5 9.0 8.5 8.0 7.5 7.0 6.5 6.0 5.5 5.0 4.5 4.0 3.5 3.0 2.5 2.0 1.5 1.0 0.5 0.0
f1 (ppm)

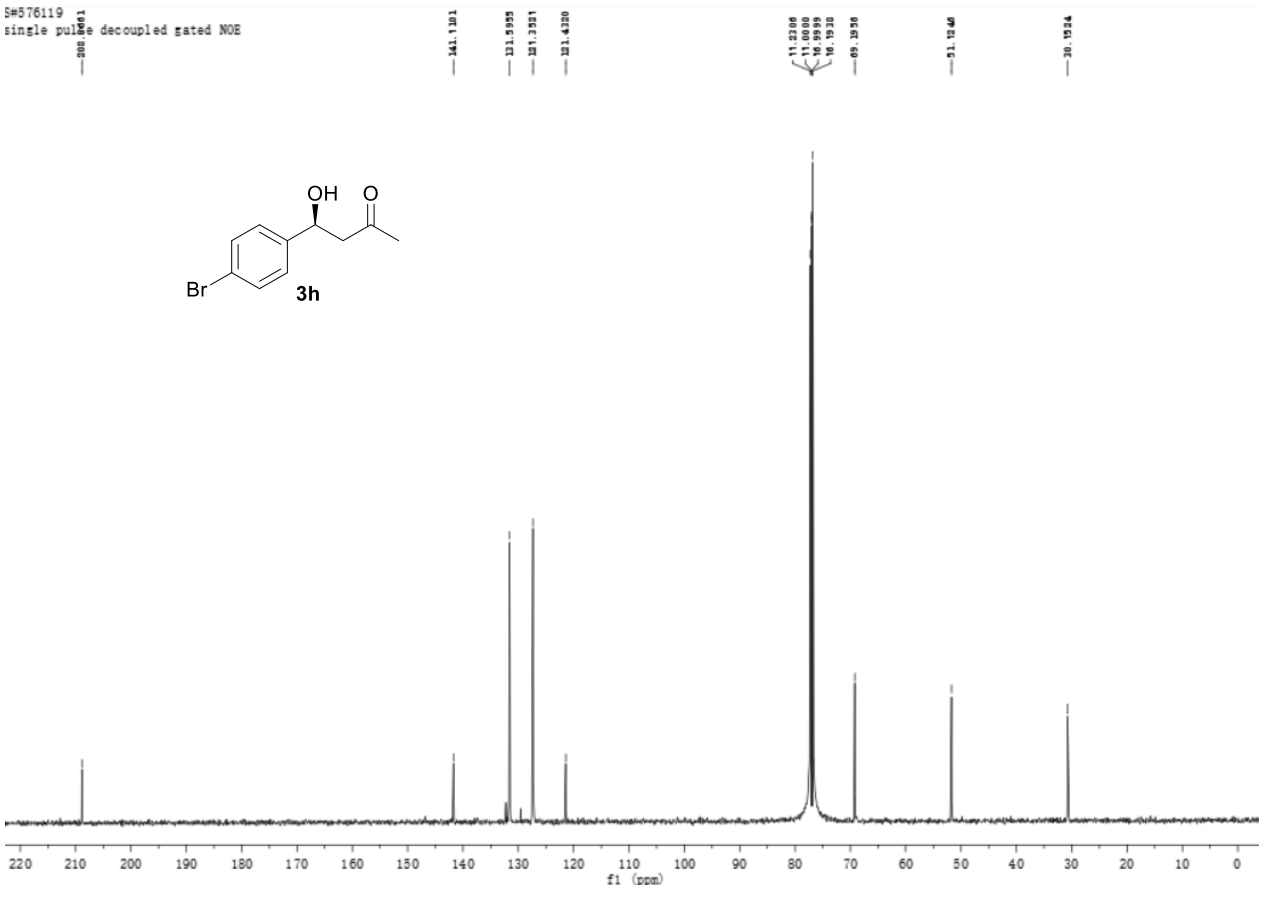
S#576119
single pulse decoupled gated NOE
OH
O
Br
3h
220 210 200 190 180 170 160 150 140 130 120 110 100 90 80 70 60 50 40 30 20 10 0
f1 (ppm)

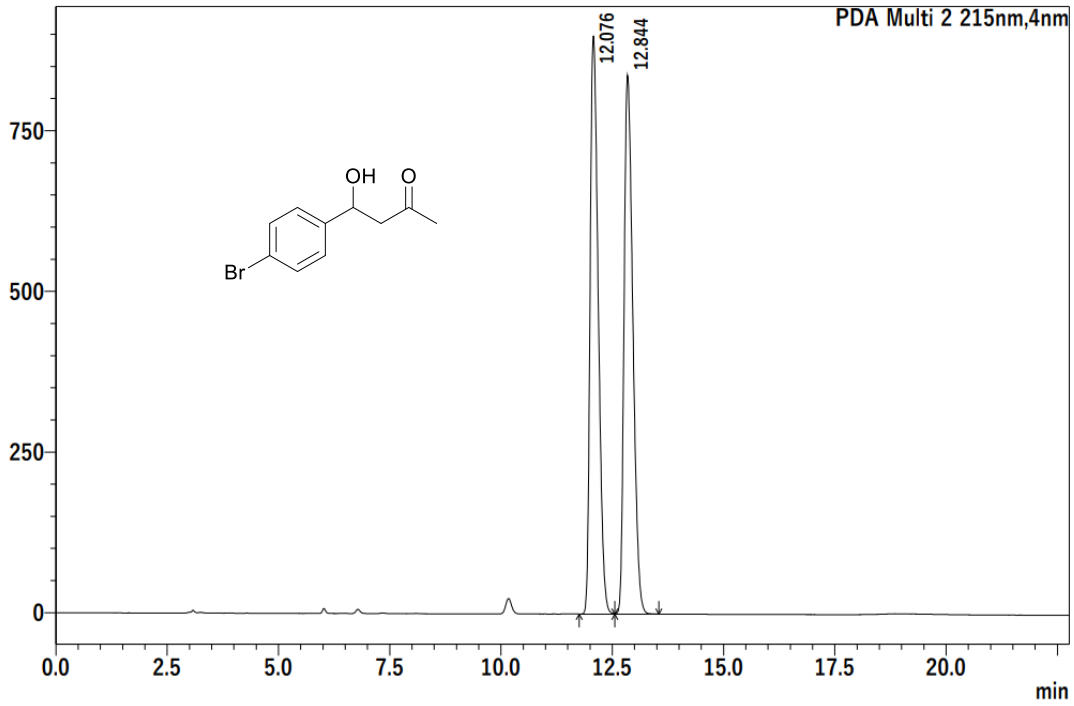

Peak Table

PDA Ch2 215nm

Peak#	Ret. Time	Area	Height	Area%
1	12.076	11449214	900044	49.796
2	12.844	11542950	838388	50.204
‡Œv		22992163	1738432	100.000

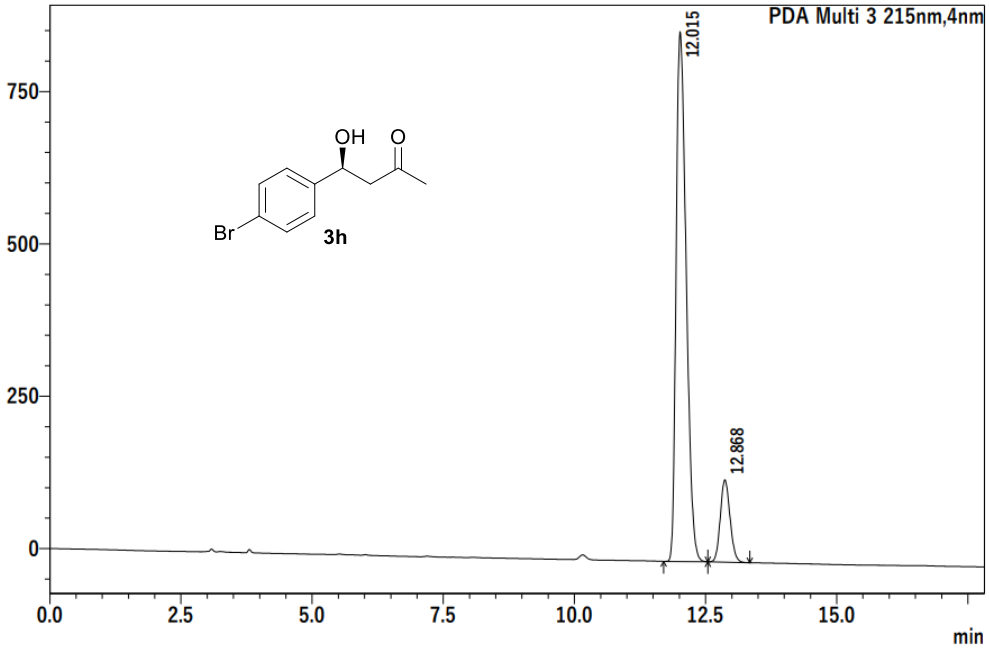

Peak Table

PDA Ch3 215nm

Peak#	Ret. Time	Area	Height	Area%
1	12.015	11561970	868695	86.932
2	12.868	1738055	135093	13.068
‡Œv		13300025	1003788	100.000

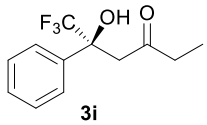

3i

3i

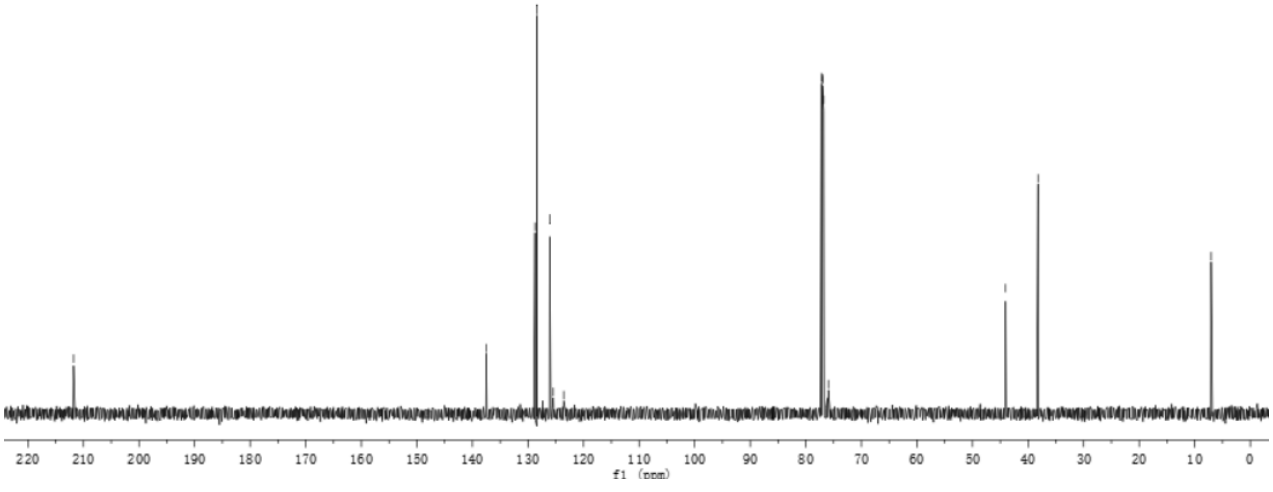

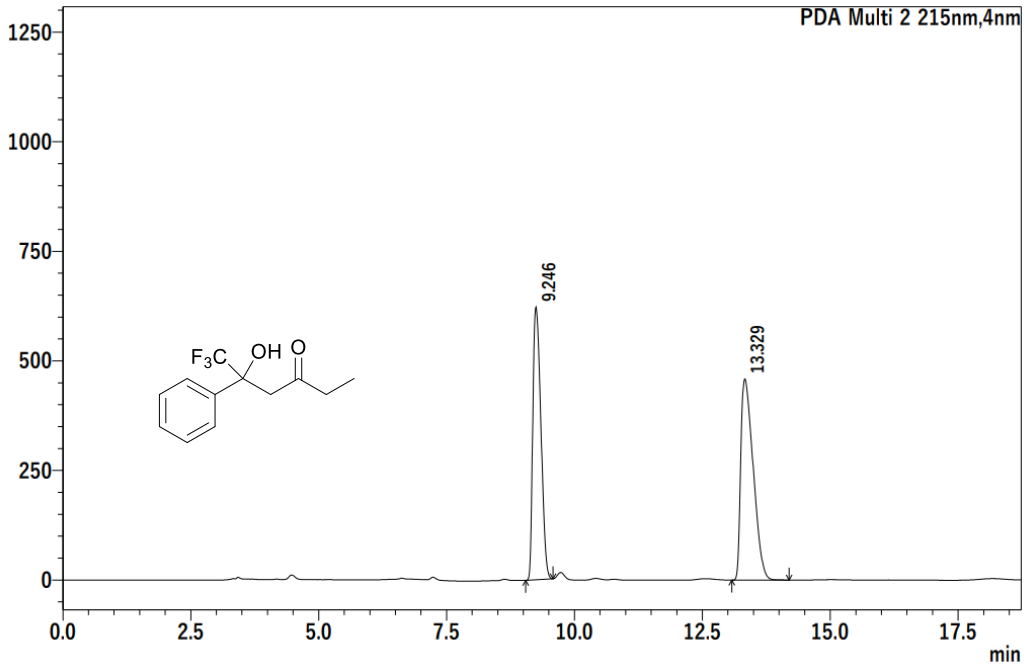

Peak Table

PDA Ch2 215nm

Peak#	Ret. Time	Area	Height	Area%
1	9.246	6841405	621905	46.844
2	13.329	7763115	459029	53.156
‡Œv		14604521	1080935	100.000

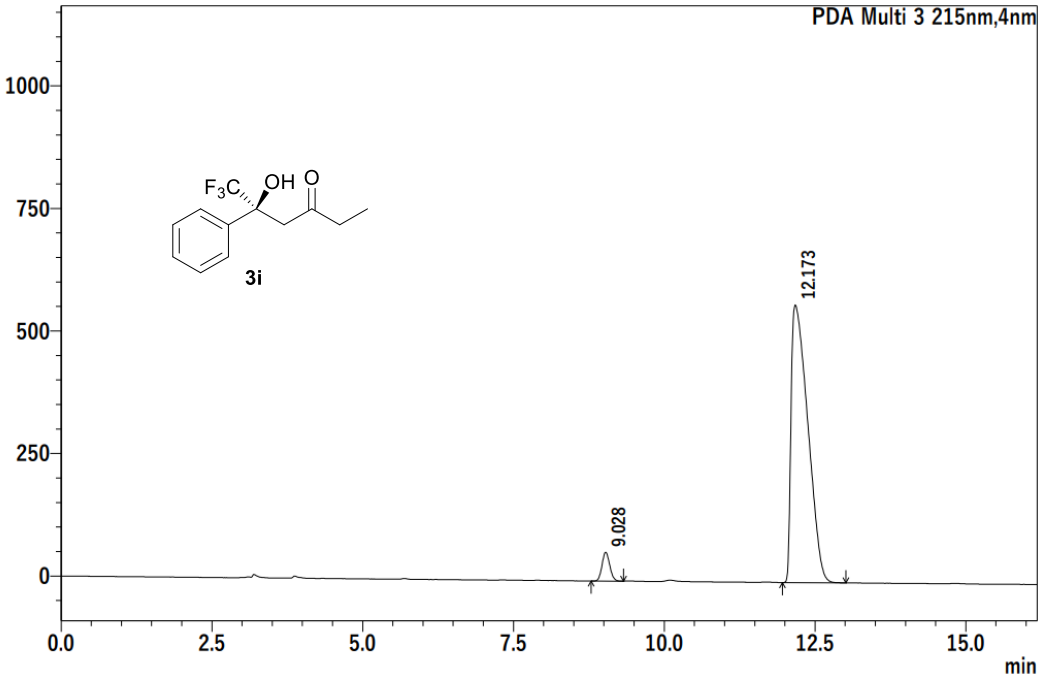

Peak Table

PDA Ch3 215nm

Peak#	Ret. Time	Area	Height	Area%
1	9.028	521713	58622	4.559
2	12.173	10921906	566476	95.441
‡Œv		11443619	625099	100.000

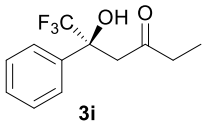

3i

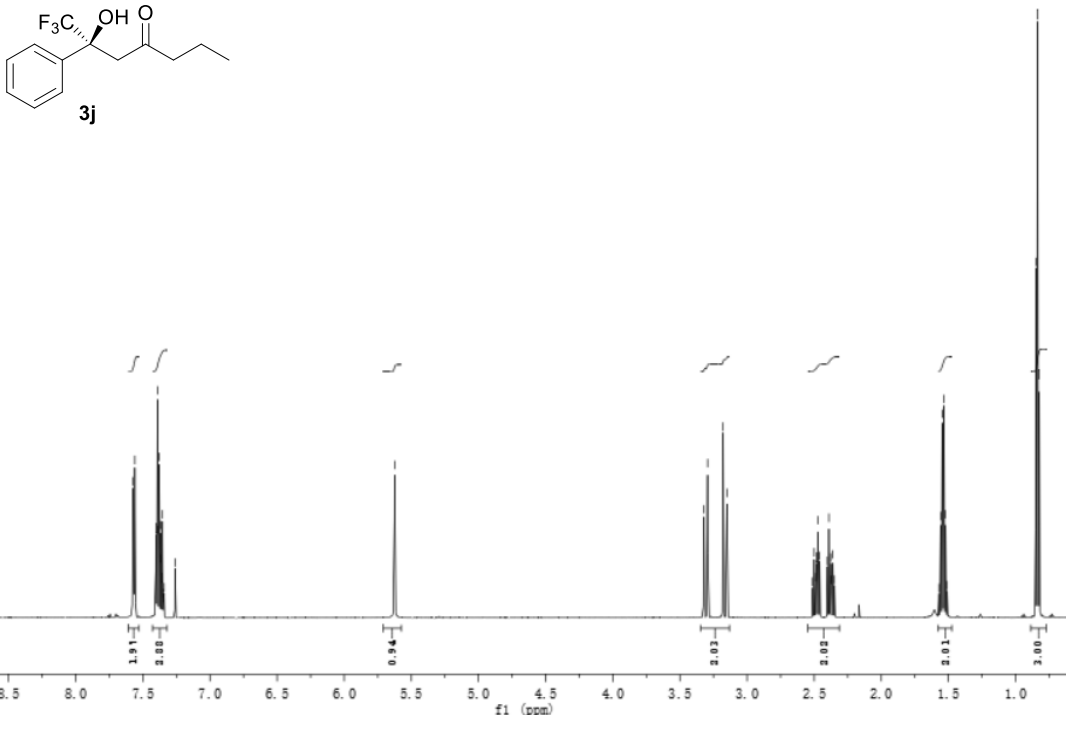

3j

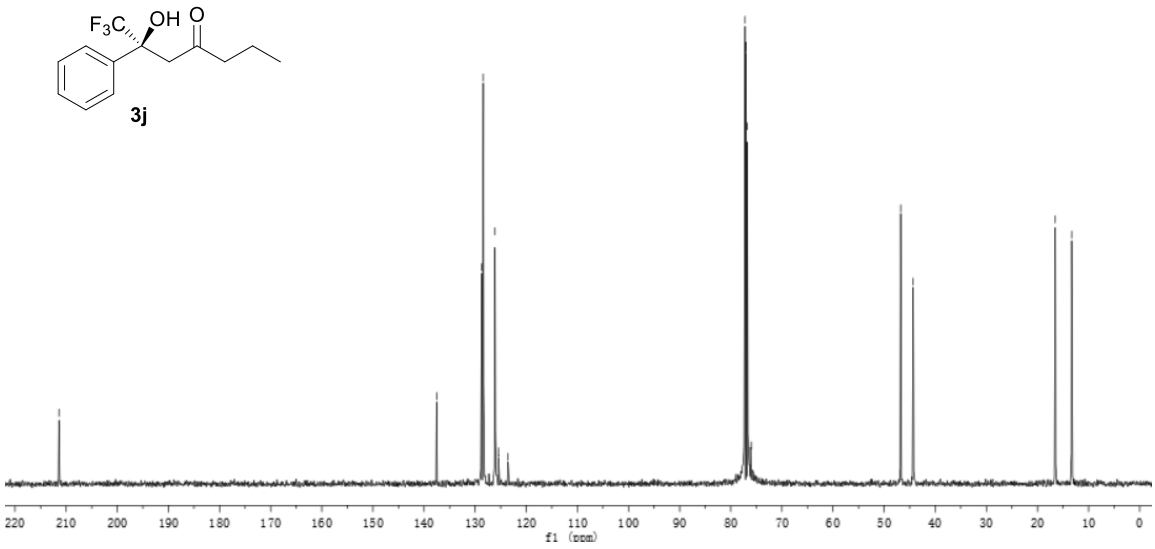

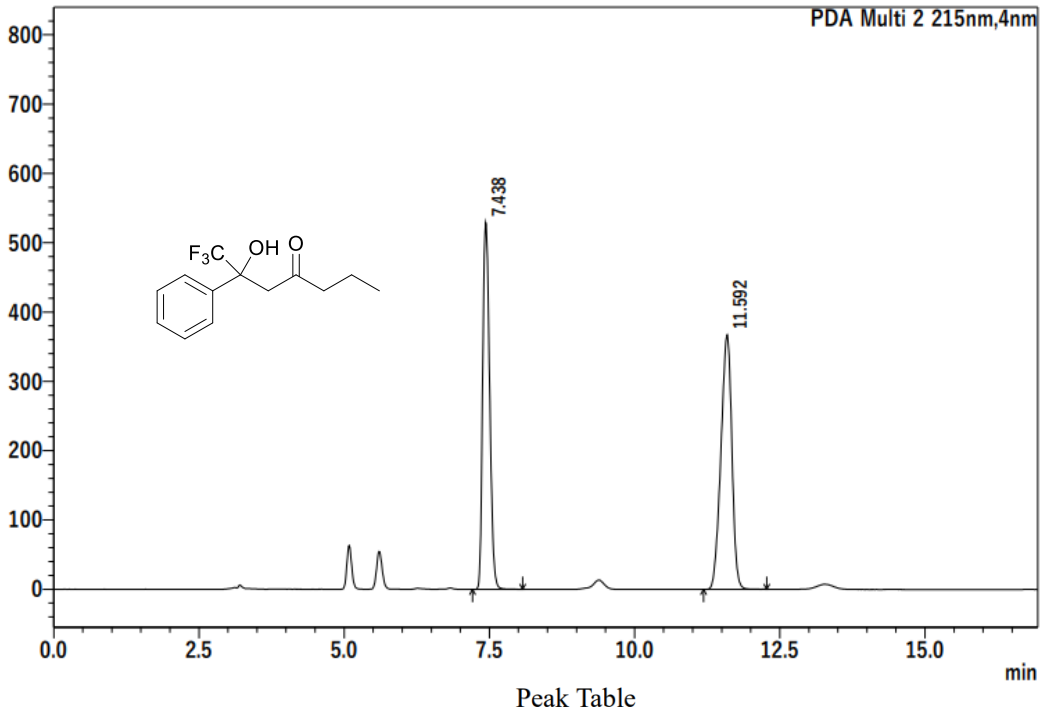

Peak Table

PDA Ch2 215nm

Peak#	Ret. Time	Area	Height	Area%
1	7.438	4417378	529438	47.798
2	11.592	4824392	366822	52.202
‡Œv		9241771	896260	100.000

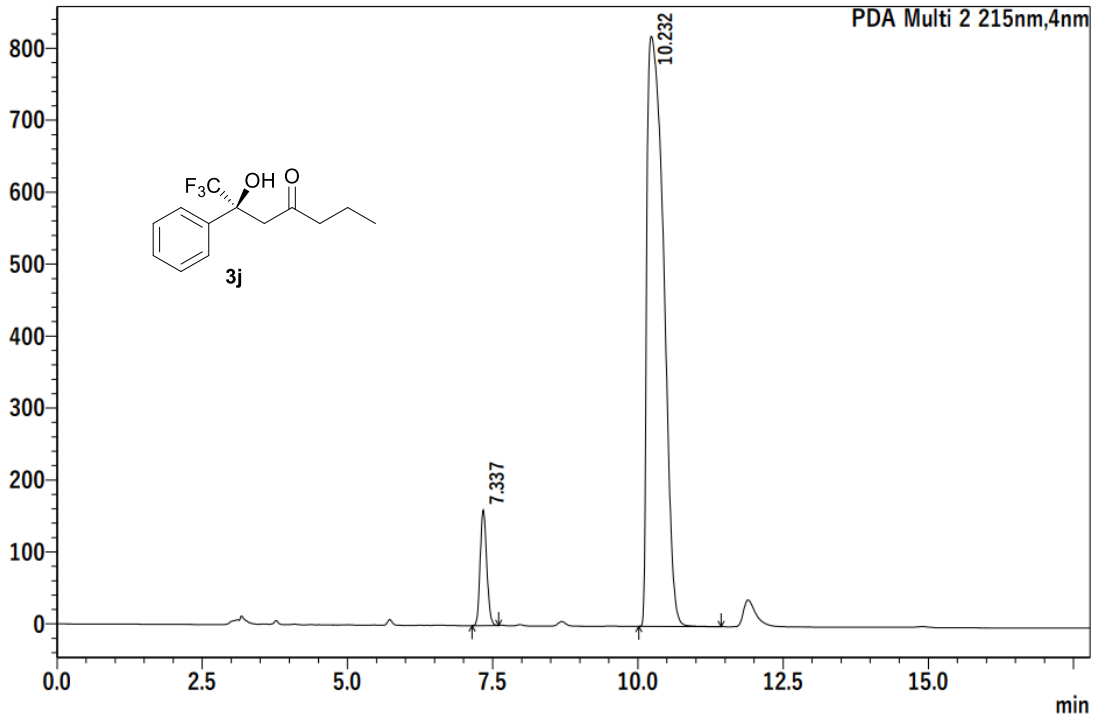

Peak Table

PDA Ch2 215nm

Peak#	Ret. Time	Area	Height	Area%
1	7.337	1261058	160506	7.180
2	10.232	16303114	820279	92.820
‡Œv		17564172	980785	100.000

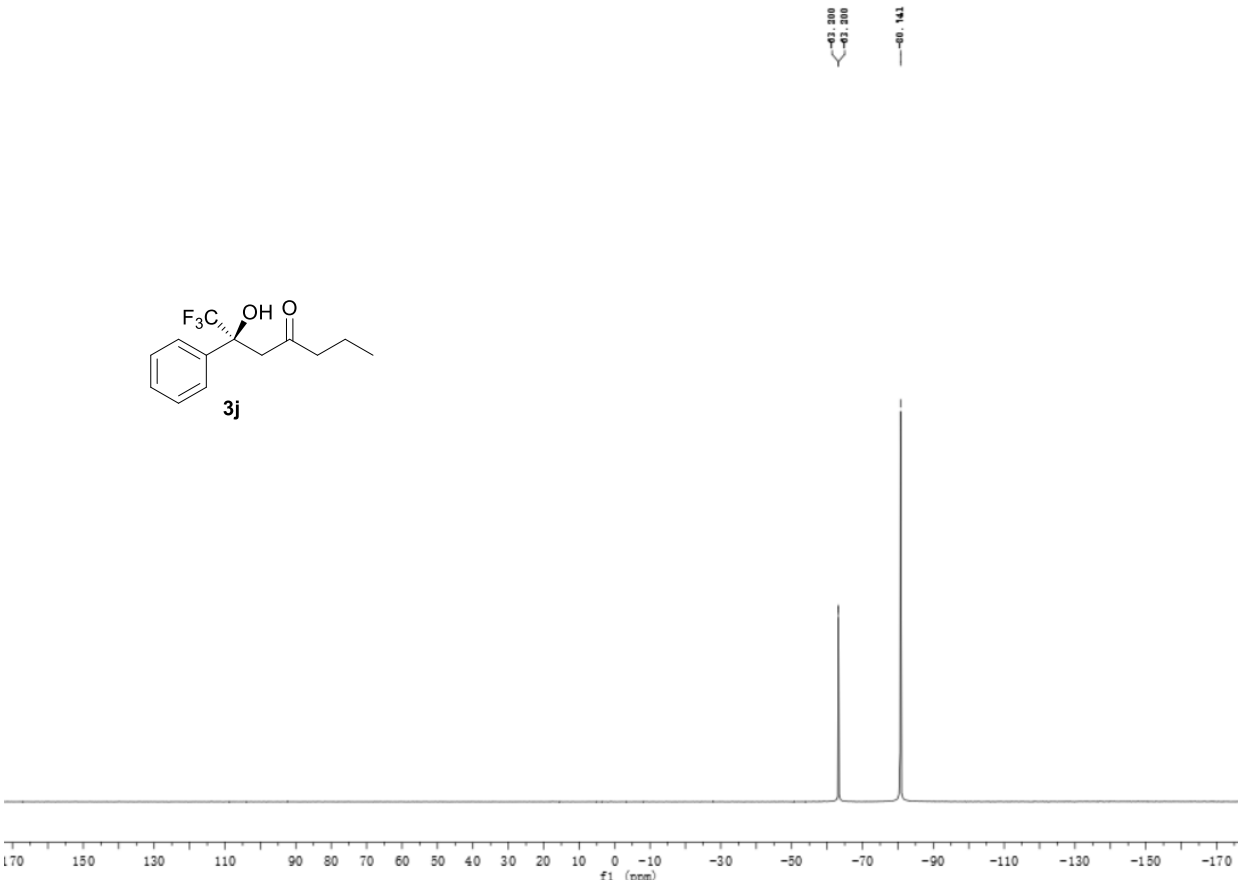

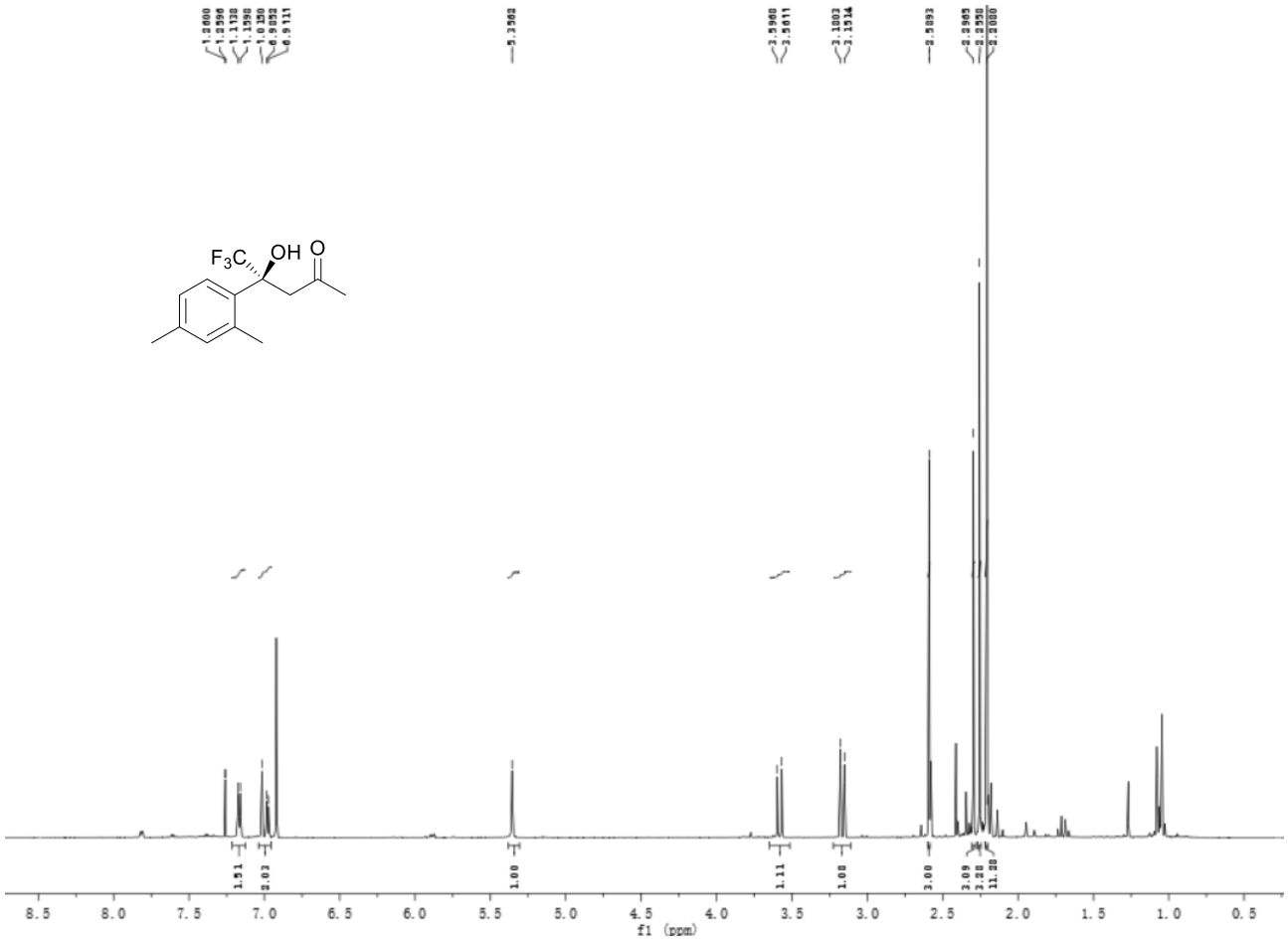

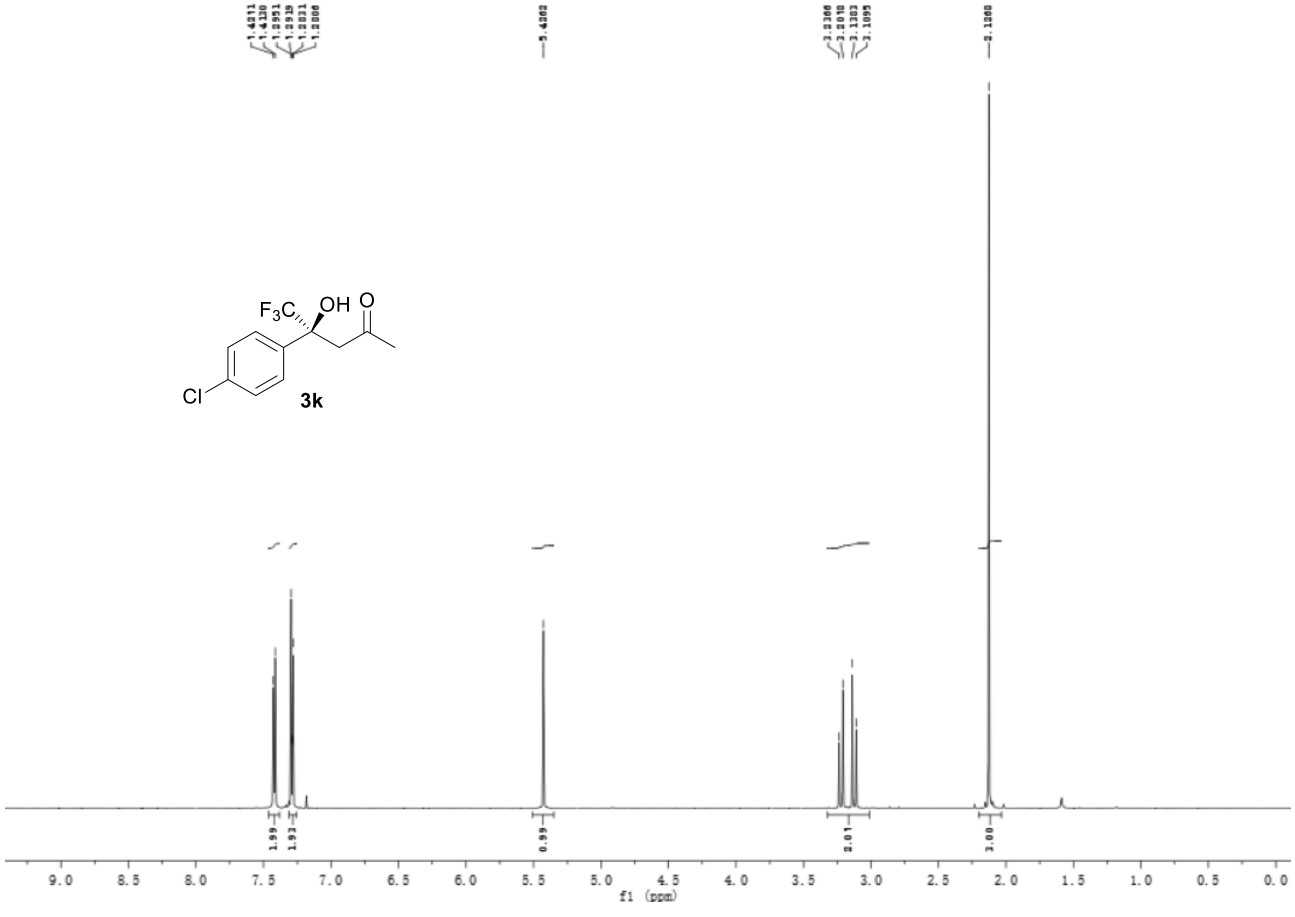

3k

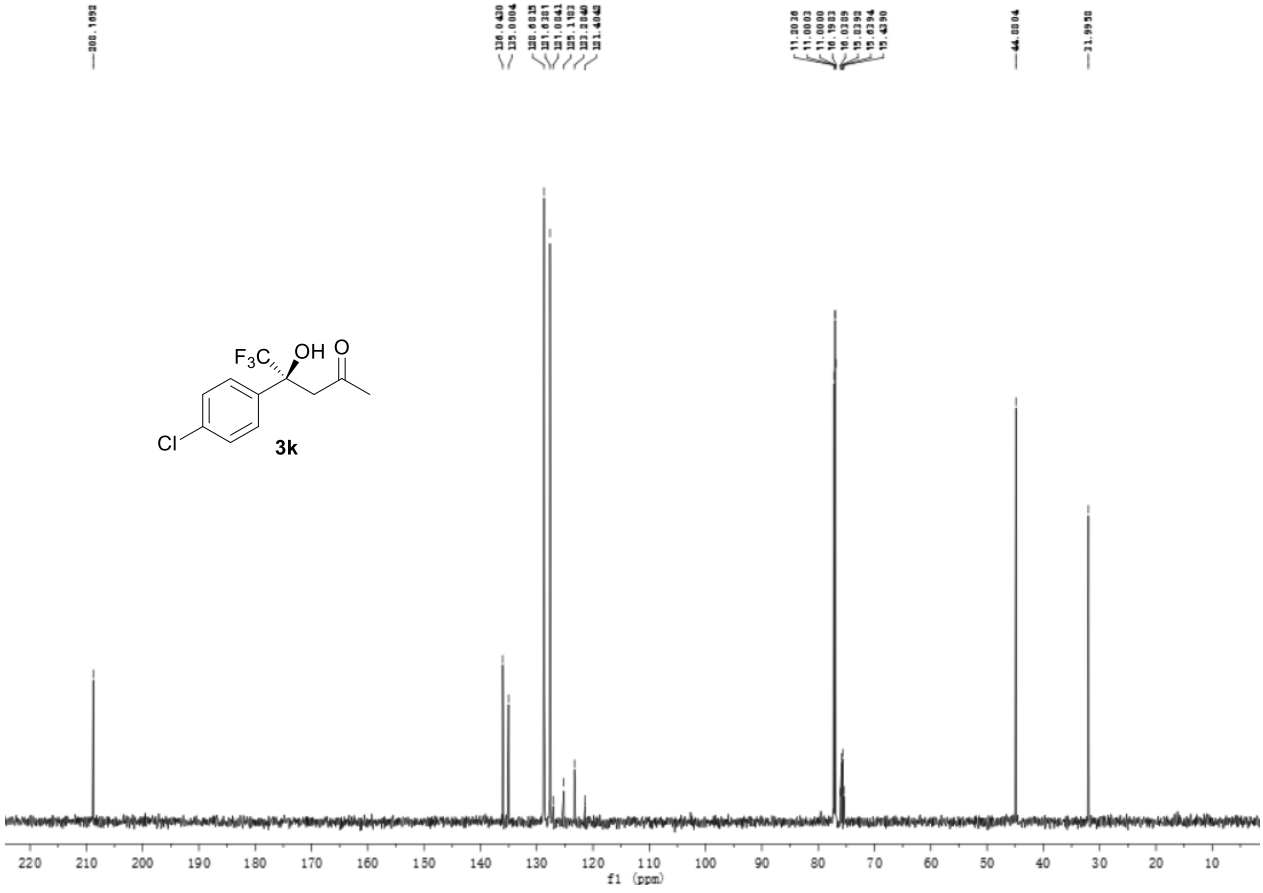

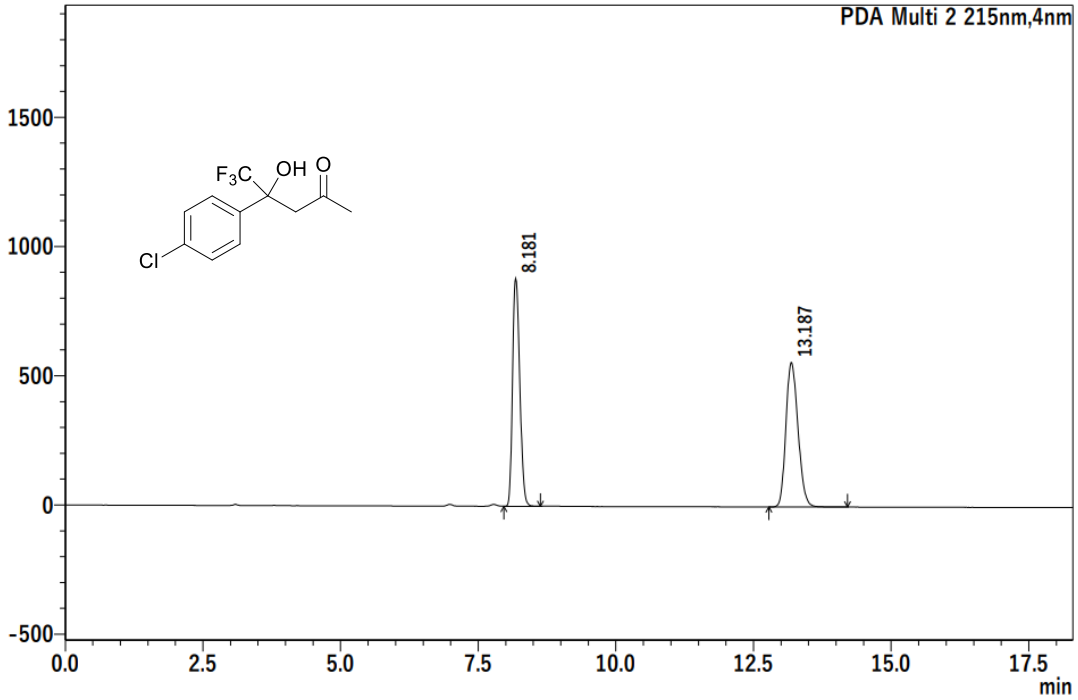

Peak Table

PDA Ch2 215nm

Peak#	Ret. Time	Area	Height	Area%
1	8.181	8047590	881706	48.440
2	13.187	8565988	558917	51.560
‡Œv		16613577	1440624	100.000

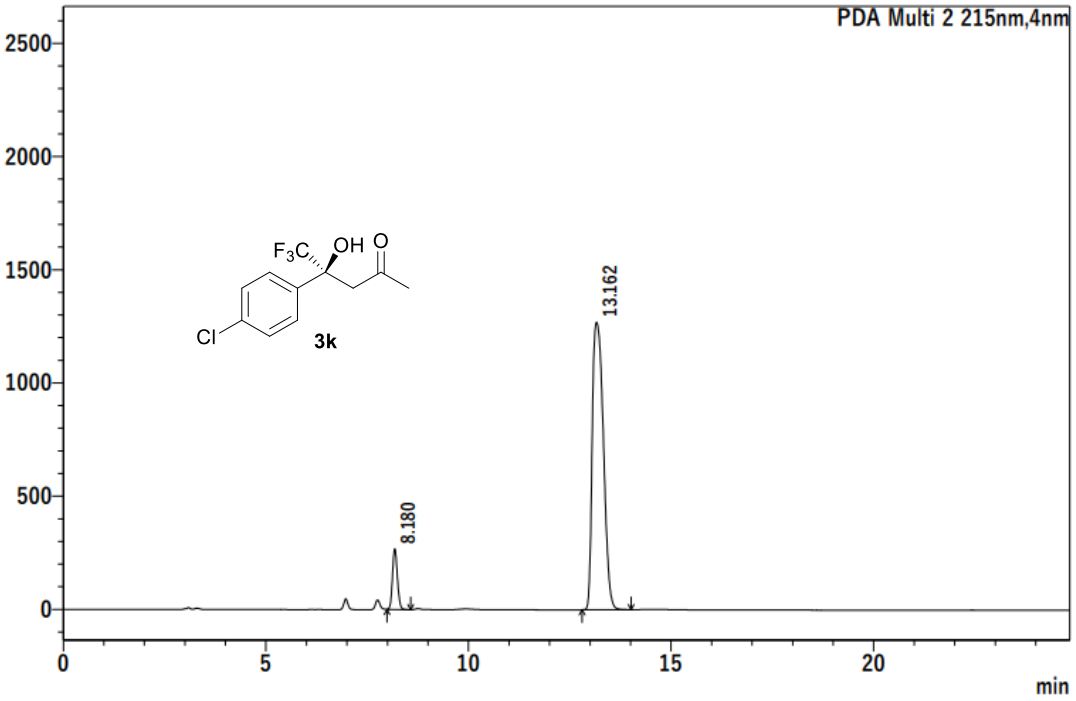

Peak Table

PDA Ch2 215nm

Peak#	Ret. Time	Area	Height	Area%
1	8.180	2249750	267055	8.502
2	13.162	24212248	1269765	91.498
‡Œv		26461998	1536820	100.000

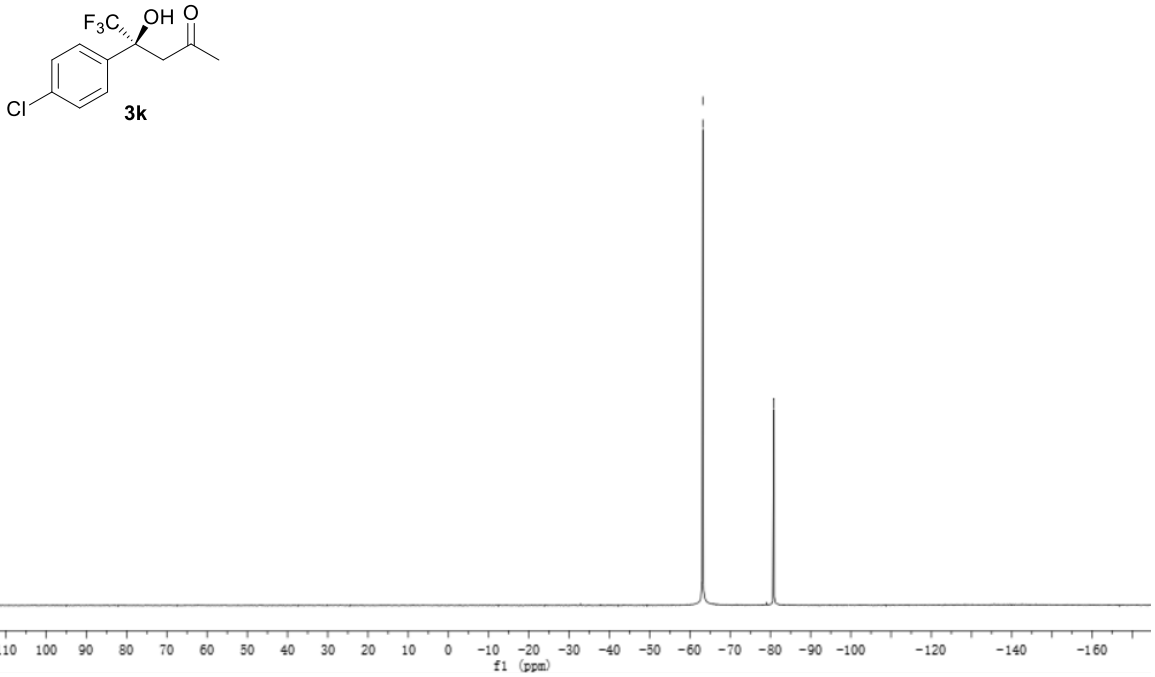

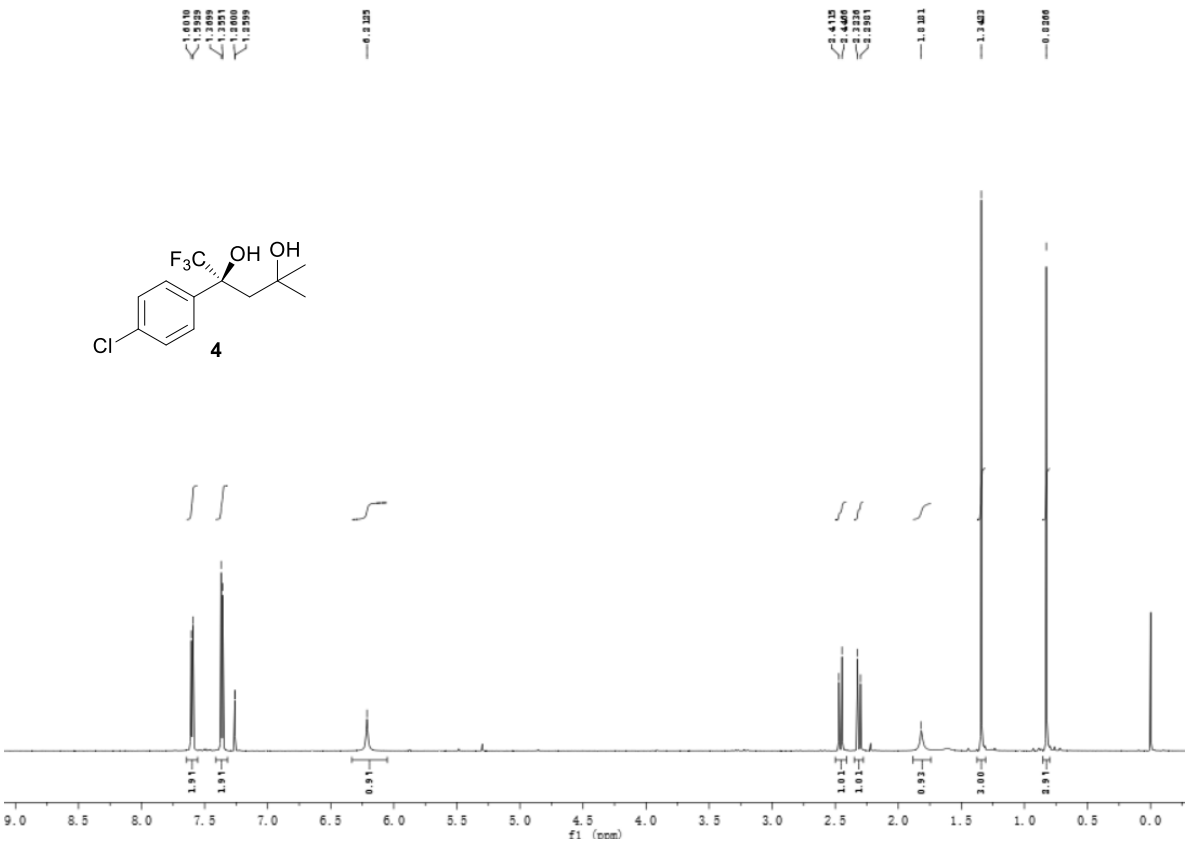
F3C
OH
OH
Cl
4
f1 (ppm)

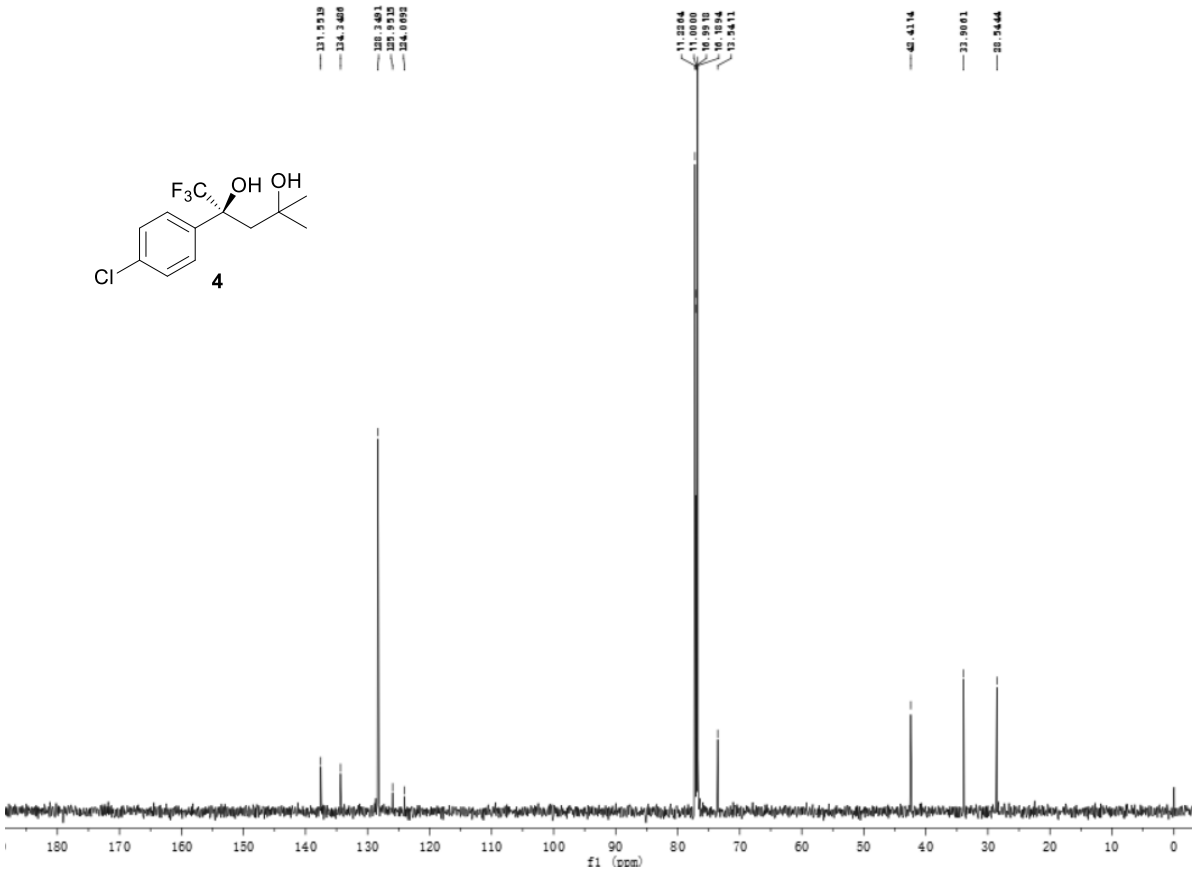
F3C
OH
OH
Cl
4
f1 (ppm)

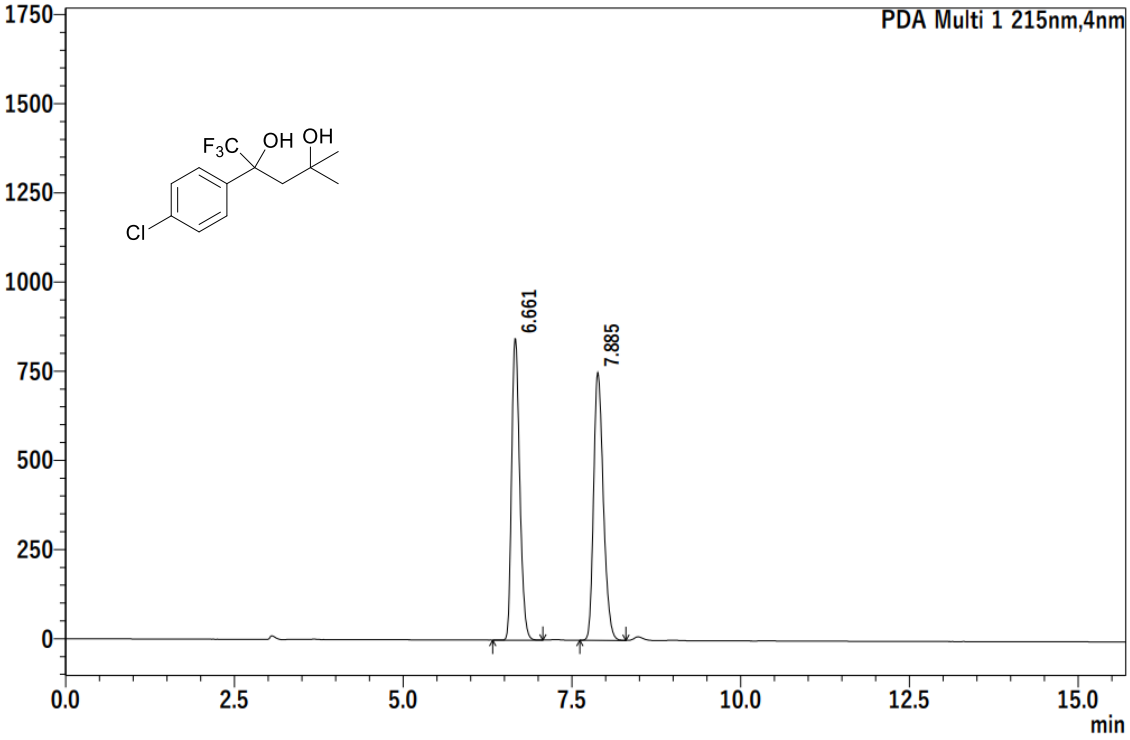

Peak Table

PDA Ch1 215nm

Peak#	Ret. Time	Area	Height	Area%
1	6.661	7083604	845382	48.351
2	7.885	7566833	750596	51.649
‡Œv		14650437	1595977	100.000

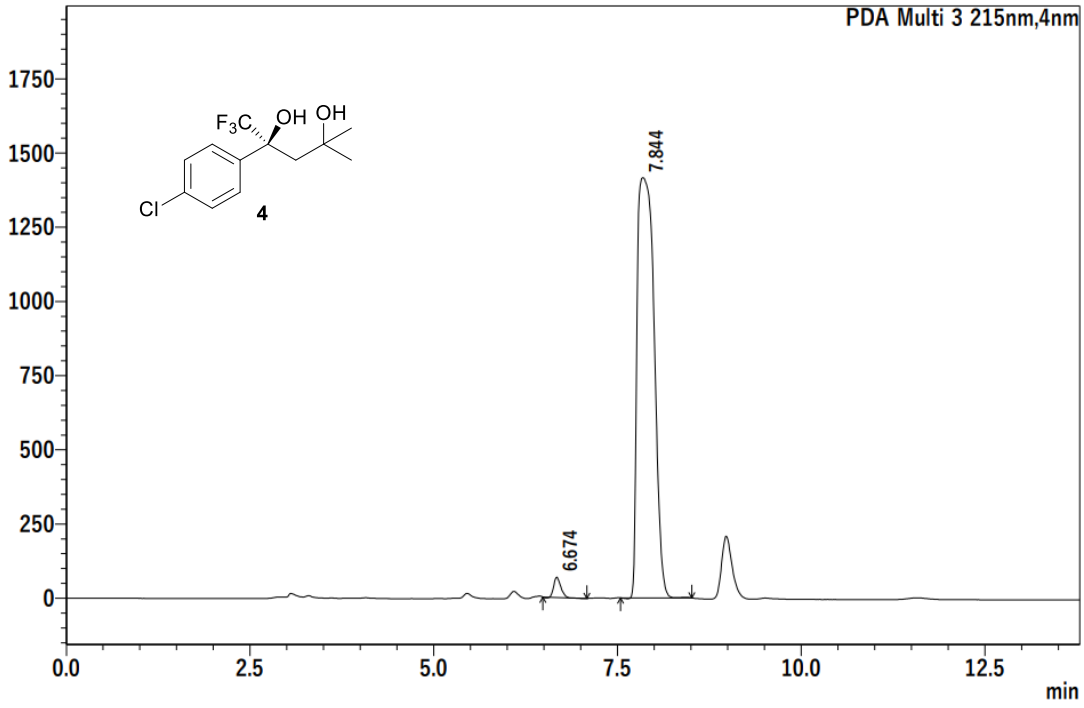

Peak Table

PDA Ch3 215nm

Peak#	Ret. Time	Area	Height	Area%
1	6.674	446581	68125	1.929
2	7.844	22698384	1416033	98.071
‡Œv		23144964	1484159	100.000

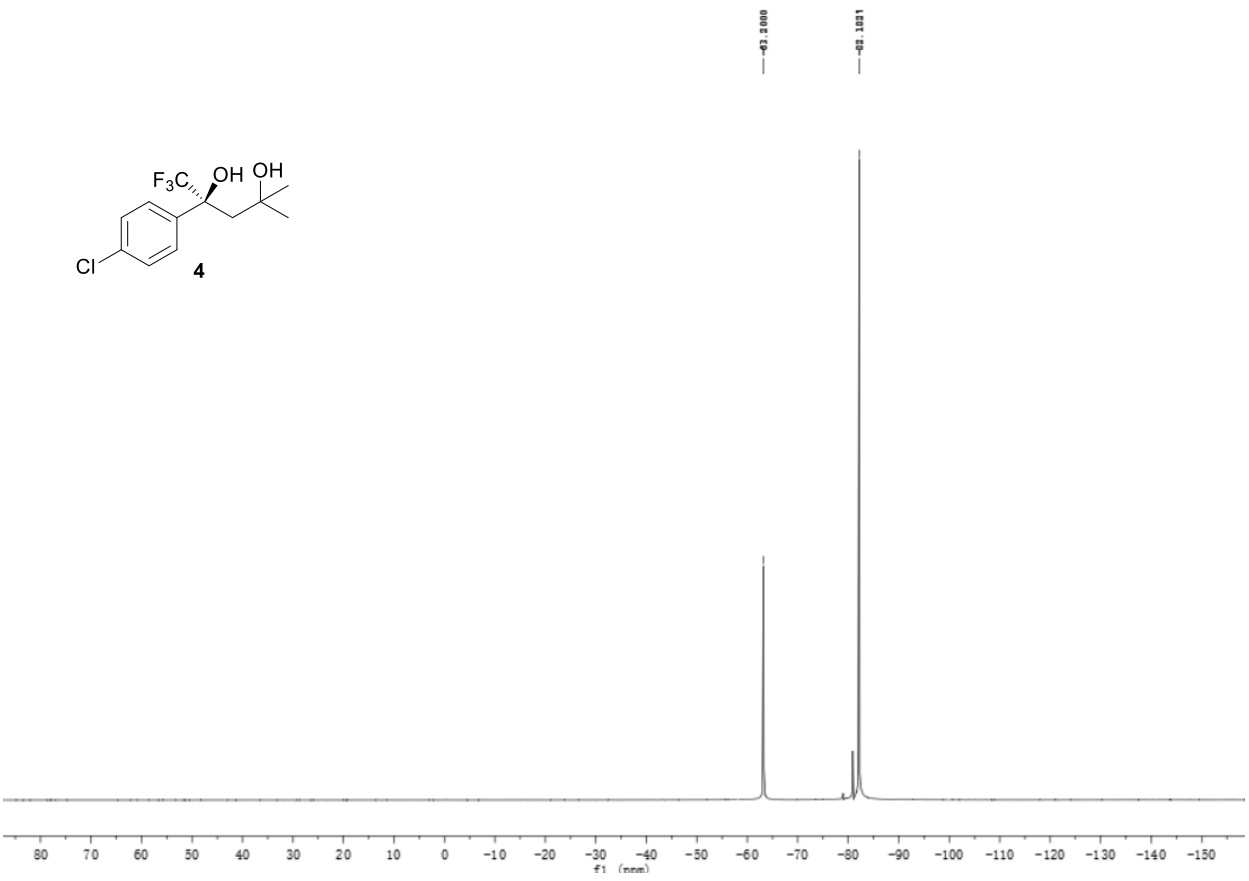

References

1 H. Miyamura, G. C. Y. Choo, T. Yasukawa, W.-J. Yoo and S. Kobayashi, *Chem. Commun.*, 2013, **49**, 9917.
2 A. Berkessel, W. Harnying, N. Duangdee, J. M. Neudörfl, H. Gröger, *Org. Process Res. Dev.*, 2012, **16**, 123.
3 Z. An, Y. Guo, L. Zhao, Z. Li and J. He, *ACS Catal.*, 2014, **4**, 2566.
4 X. Xu, Q. Q. Min, N. Li and F. Liu, *Chem. Commun.*, 2018, **54**, 11017.
5 N. Duangdee, W. Harnying, G. Rulli, J. M. Neudorfl, H. Groger, A. Berkessel, *J. Am. Chem. Soc.*, 2012, **134**, 11196.
6 (a) C. G. Kokotos, *J. Org. Chem.*, 2012, **77**, 1131; (b) S. Zhang, L. Li, Y. Hu, Y. Li, Y. Yang, Z. Zha and Z. Wang, *Org. Lett.*, 2015, **17**, 5036; (c) I. Vlasserou, M. Sfetsa, D. T. Gerokonstantis, C. G. Kokotos and P. Mountevelis-Minakakis, *Tetrahedron*, 2018, **74**, 2338.
7 H. Zong, H. Y. Huang, G. L. Bian and L. Song, *J. Org. Chem.*, 2014, **79**, 11768.
8 (a) Z. Tang, F. Jiang, L. T. Yu, X. Cui, L. Z. Gong, A. Q. Mi, Y. Z. Jiang, Y. D. Wu, *J. Am. Chem. Soc.*, 2003, **125**, 5262; (b) Z. Tang, F. Jiang, X. Cui, L. Z. Gong, A. Q. Mi, Y. Z. Jiang, Y. D. Wu, *Proc. Natl. Acad. Sci. U.S.A.*, 2004, **101**, 5755; (c) C. Allemann, J. M. Um, K. N. Houk, *J. Mol. Catal A Chem.*, 2010, **324**, 31.
9 The phenyl group is effectively a smaller group than the trifluoromethyl group. The order of relative sizes for trihalomethyl and phenyl group are CCl_3 > CF_3 > Ph: (a) E. J. Corey, X. M. Cheng, K. A. Cimprich, S. Sarshar, *Tetrahedron Lett.*, 1991, **32**, 6835; (b) P. V. Ramachandran, A. V. Teodorovic, H. C. Brown, *Tetrahedron* 1993, **49**, 1725; (c) N. Hara, R. Tamura, Y. Funahashi, S. Nakamura, *Org. Lett.*, 2011, **13**, 1662